Settlement Behaviour of Heinenoordtunnel — A numerical study

By

K.T. Kwok

in partial fulfilment of the requirements for the degree of

Master of Science
in Geo Engineering

at the Delft University of Technology,
to be defended publicly on Tuesday August 30, 2022 at 14:00 PM

Supervisor:	Dr.Ir W. Broere
Thesis committee:	Dr.Ing M.Voorendt,
	Ir. X.H Zhang,

TU Delft

Abstract

The 1st Heinenoordtunnel is an immersed tube which has been open for service in the Netherlands since 1969. Over the past 50 years, a large and increasing settlement has been measured along the tunnel alignment. The greatest value of settlement (65 mm) occurs in tunnel element 1 from 1978 to 2018. The maximum differential settlement has reached 30 mm between element 1 and 2 which causes a potential threat to the tunnel serviceability. In addition, Distributed Optical Fiber Sensors (DOFS) was used to measure daily joint deformation of immersed tunnel. The result of DOFS has shown a periodic settlement under tide.

The aim of this thesis is to investigate the long-term and daily settlement behavior of Heinenoordtunnel. The study starts with the geological information investigation, followed by settlement analysis using 2D Finite Element Modeling. Both long-term settlement and daily cyclic settlement are simulated and compared with the monitoring data.

In long term settlement analysis, the results show that the consolidation settlement of tunnel element is trivial (<0.5mm) over the 50 years operation. The calculated result does not match with the monitoring data under a constant load assumption over the operational period. Therefore, three additional factors are considered which can be the possible causes of the excessive settlement. Those factors are the growth of traffic volume, fluvial deposition on riverbed and secondary compaction on the foundation. The main results are summarized as follows:

(1) The settlement due to extreme traffic growth is between 10 and 20 mm which increases gradually from 1979 to 2018.

(2) The fluvial deposition causes an average settlement of 1.68 mm over the past 40 years of operation.

(3) The secondary compaction result is in between 5.30 and 10.70 mm, while the exact value depends on the selection of creep parameter.

(4) The combined settlement is in between 18.27 and 30.62 mm that is significantly less than the monitoring data.

Based on the above findings, the combination of those three factors cannot provide a sound explanation on monitoring data. Hence, a sensitivity analysis will be conducted in the final stage of the research.

In the daily settlement response simulation, a coupled flow simulation is applied on both traverse and longitudinal direction under tidal fluctuation. The summary of results is indicated as below:

(1) A phase delay of excess pore water pressure occurs for soil under the low permeable layer. This causes periodic rebound and settlement on the tunnel element

(2) The amplitude of tunnel cyclic settlement is in between 0.143 and 0.215 mm

(3) The deformation of intermediate immersion joint is under 0.059 mm

Since the difference between calculation and monitoring results is over 0.2 mm in joint 6, it is important to conduct sensitivity analysis on the Plaxis model.

To verify the importance of soil variability, the sensitivity analysis is conducted by reducing the stiffness parameter with two standard deviation value in long term settlement analysis and one standard deviation value in daily settlement analysis. The long-term settlement become twice as the initial value after the parameter adjustment. The difference between monitoring data and Finite Element result reduces by 30 to 192 percent of the original value. On the other hand, the daily settlement of tunnel reduces by 4 to 17 percent under the one standard deviation increment. The daily response of tunnel is closer to the monitoring data after parameter adjustment.

In conclusion, the three factors considered in this research causes a significant change on the total settlement of immersed tunnel. The periodic response of tunnel settlement is verified from the coupled flow mode. Finally, some recommendations are made for future study.

Preface

This thesis, “Impact of Tidal Fluctuation on Heinenoord Tunnel” is written to fulfill the graduation requirement of MSc Civil Engineering, specializing in Geo-Engineering, at the Delft University of Technology. I was involved in this project from June 2021 to May 2022.

I am glad to mark an end of my three years study as a master student with this research. Tunneling is my greatest interest in geotechnical engineering. Implementation of optical fiber is an innovative idea on the monitoring of immersed tunnel. Although problems are usually encountered, it is rewarding when the result matches with the initial prediction. Through the process of trial and error, I have activated the knowledge obtained from the lectures and further revised the unclear concepts on geotechnics.

This thesis is an impossible task without the help and support from my supervisors and people around me. First of all, I would like to thank Dr. Ir W. Broere for his guidance and flexibility. I am appreciated your valuable feedback and suggestions on the critical parts of the thesis. I would also thank Dr. Ing M. Voorendt for his comments on the research and thesis. The report becomes more concise under your guidance. Moreover, I would like to thank Ir. X, Zhang, my daily supervisor, for all the support and patience over the past 14 months. The new ideas from Zhang have inspire me to work on a correct direction.

Also, I would like to thank my family for their unconditional support on my entire life. Life is not always a smooth sailing, hardships and challenges are often encountered. They are the excellent listeners whom I can share my thoughts and setbacks in life. Year 2021 is the toughest year to me and my family, because one of the members has passed away. I hope that everyone in the family can stay optimistic and look forward to the future.

All in all, studying as master student is an amazing journey in TU Delft. Learning is a lifelong process which requires persistence and humble attitude towards new ideas. Therefore, I would like to summarize my studying experience with the following quote:

“The more you learn, the more you know. The more you know, the more you forget. The more you forget, the less you know. So why bother to learn.” ***Stephen Hawking***

Table of Content

List of Figures

List of Tables

List of Symbol

a	Tip area ratio in CPT
c	Cohesion in Mohr Coulomb Failure Criteria
$C_{\alpha\varepsilon}$	The coefficient of secondary compaction
C_{qc}	Cone resistance correction factor
E_{50}	Secant modulus
E_{oed}	Odometer Stiffness Parameter
E_{oed}^{ref}	Odometer stiffness parameter under the reference level of 100kPa
E_{ur}	Unloading reloading stiffness
E_{ur}^{ref}	Unloading/Reloading stiffness parameter under the reference level of 100kPa
f_s	Sleeve resistance in the Cone Penetration Test
G	Shear modulus of soil
I_c	Soil behavior type index
k	Permeability constant
K'	Bulk modulus of water
p	Pore pressure of soil
p_{ref}	Isotropic stress level (100kPa)
P_{atm}	Atmospheric Pressure
q_c	Measured cone resistance
$q_{c,table}$	Modified cone resistance value under 100kPa of effective stress.
q_t	Modified cone resistance
Q_t	Normalized non-dimensional value of top resistance
Q_{tn}	Friction angle
R_f	Cone friction ratio
t_i	Time starts for the creeping under a reference value
u_2	Pore water pressure at the shoulder position of penetrometer
v	Poisson ratio
σ_o'	Effective stress at the tip of penetrometer.
σ_n	Normal stress of soil in Mohr Coulomb Failure Criteria
σ_{vo}	Total vertical stress of soil

σ'_{vo}	Effective vertical stress of soil
Φ_p	Friction angle in the Mohr Coulomb Failure Criteria
τ	Applied shear stress
γ	Saturated unit weight of water

Chapter 1 Introduction

This chapter introduces the thesis background, objectives, research questions, methodology and report outline in a sequential order. It aims to describe the research motivation and how the result can be achieved.

1.1 General Description on Immersed Tunnel

Immersed tunnel is mostly built underwater (rivers, harbors or sea) since it requires water as a medium to transport and submerge prefabricated elements. Comparing with bored tunnel, the burial depth of immersed tunnel is relatively shallow which results in a shorter burial length (usually, a further reduced project cost). Over the past century, more than 150 immersed tunnels have been built and in use worldwide. More than 50 immersed tunnels are built in Europe and two third of them locate in Netherlands. Since Netherlands locates at the delta region of the European continent, canals and rivers are commonly found across the country. Waterway provides a good condition for the transportation and submersion of tunnel element (Gursoy,1995; Lunniss and Baber,2013).

An immersed tunnel generally consists of several elements (with each about 100m long) that are connected under water, while the joint between is referred to as immersion joint. The long element usually comprises of several short segments (with each about 20m long) as it improves the condition of concreting and reduces the risk of thermal concrete cracking. The joint between segments is called dilation joint. The construction process of immersed tunnel often involved several steps: to begin with, the segment is concreted and combined in the dry-dock to form a tunnel element; next, a trench is excavated along the tunnel alignment under riverbed; then the tunnel element is towed to the immersion site by tugboat, submerged and connected under water; finally, the tunnel element is backfilled on two sides and top (Lunniss and Baber, 2013). The immersion joint between tunnel elements generally have a lower stiffness and enable some local movement of the tunnel in the service period (Wang, 2020), which helps reduce the possible adverse internal forces due to uneven settlement.

However, many immersed tunnels with an operation period of several decade years have shown signs of deterioration. Some serviceability problems are encountered in the maintenance survey which causes a potential risk to tunnel operation. Several most common serviceability issues are indicated as below:

(1) Large differential settlement usually occurs unexpectedly during the operational period, and may cause excessive joint deformation and cracks on the tunnel element.

(2) Excessive deformation on immersion and dilation joint, which cause leakage problems on the immersed tunnel. It increases the risk of rusting on steel reinforcement which reduces the structural stability.

For safety maintenance, the settlement behavior of immersed tunnel should be monitored and analyzed during the whole service period, and remedial actions shall be taken when deterioration issue occurs.

1.2 Motivation of the Research

(1) Heinenoordtunnel

The 1st Heinenoordtunnel is an immersed tube built under the Oude Maas River in the Netherlands, which was open to traffic in year 1969. The whole burial length of Heinenoordtunnel is 754 m and the immersed tube section is about 574 m. There are 5 elements with each about 115 m long, while the GINA and OMEGA gaskets are used to seal the immersion joint and prevent water from entering inner tube. Each element is further divided into 6 segments with dilation joints. Figure 1.1 shows the side and top views of Heinenoordtunnel. It is noted that the closure joint between tunnel element 4 and 5 is formed by on-site concreting inside the tunnel.

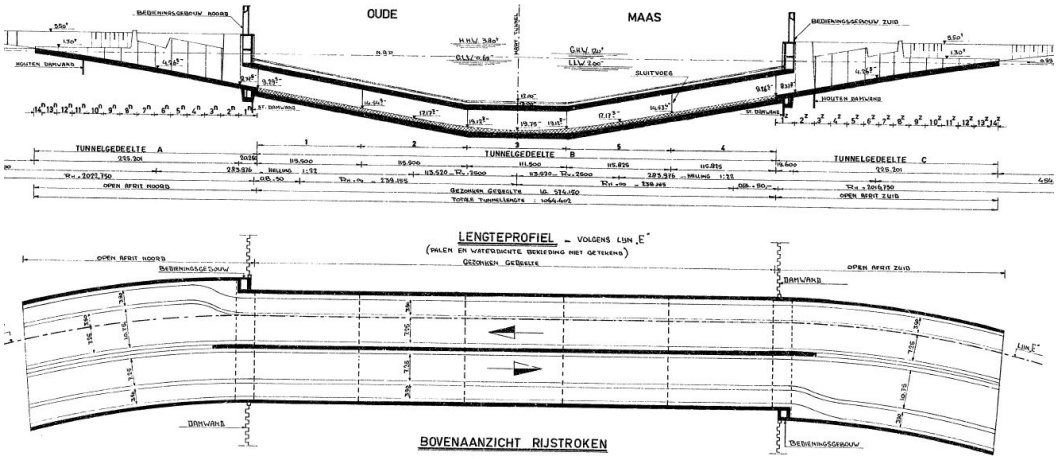

Figure 1.1: Longitudinal tunnel profile of Heinenoordtunnel

(2) Long-term Settlement of Heinenoordtunnel

Considering the unloading effects in trench excavation, the overburden pressure induced by tunnel installation and sand backfill is relatively small. Hence, the settlement of tunnel element is expected to be insignificant. However, it is reported that many immersed tunnels exhibit an excessive settlement (Wang, 2020), while the Heinenoordtunnel is one of the examples.

The long-term settlement of Heinenoordtunnel was measured by manual leveling along the longitudinal direction since 1979. The measured tunnel settlement is relative to the reference point on approach ramps. An increasing tendency of tunnel settlement is measured along the tunnel alignment. Figure 1.2 has shown the monitoring data in the west tube of Heinenoordtunnel from 1979 to 2018 . The greatest value of settlement has reached about 65 mm in tunnel Element 1, while the minimum value of settlement is 40 mm in tunnel Element 3. This settlement is unexpectedly significant and has caused some serviceability problems such as joint leakage and concrete cracking (Rijkswaterstaat. 2008). It is important to investigate the potential reason behind the large settlement of Heinenoordtunnel for safety maintenance. These potential factors may include changes of loading condition, geological response of foundation soil, et al.

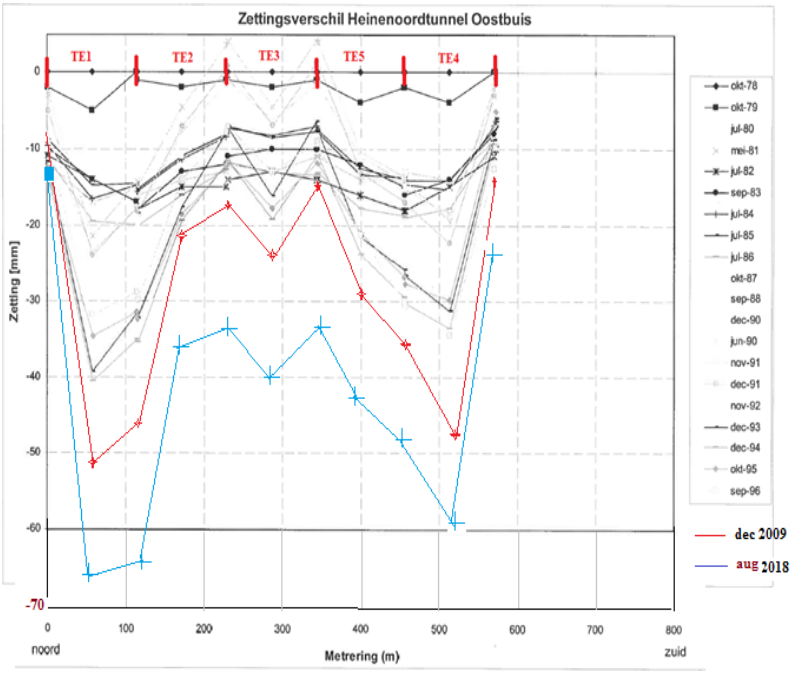

Figure 1.2: The settlement of Henenoordtunnel (West tube) across 40 years of operation

(3) Daily cyclic settlement of Heinenoordtunnel under tide impact

Besides long-term settlement monitoring (at yearly interval), Distributed Optical Fiber Sensor (DOFS) is applied to measure the immersion and dilation joint deformation (a total of 30 joints). DOFS is a sensitive sensor which measures the distributed strain and temperature along the optical fiber axis, while the working principle can be found from the journal published by López-Higuera et al., (2011) and Motil et al., (2016).

In Heinenoordtunnel, DOFS is aligned as extensometers at joints, which measures both joint openings and uneven settlement (of the two sides of joint) under a sub-hour interval (Zhang and Wout, 2022). Figure 1.3 has shown a typical setup of optical fiber sensor at dilation joint of the Heinenoordtunnel. The optical fiber is installed along the horizontal and diagonal direction that is fixed by 3 points along the joint. The horizontal optical fiber (FL1) measures the joint opening deformation that is the uneven settlement between two joint sides. It can be determined by combining the change of stain of both fiber lines FL1 and FL2.

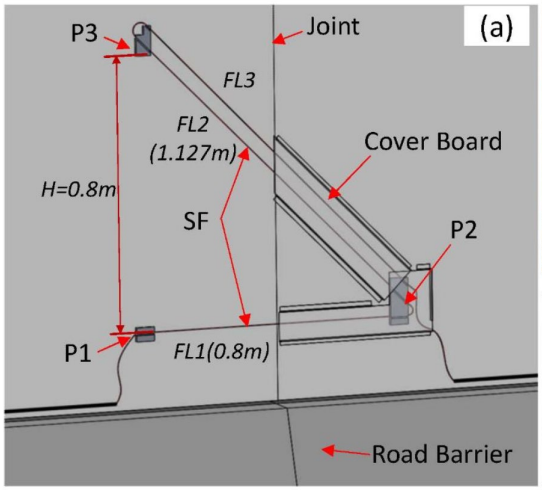

Figure1.3: DOFS sensor at dilation joint in Heinenoordtunnel (Zhang and Wout, 2022)

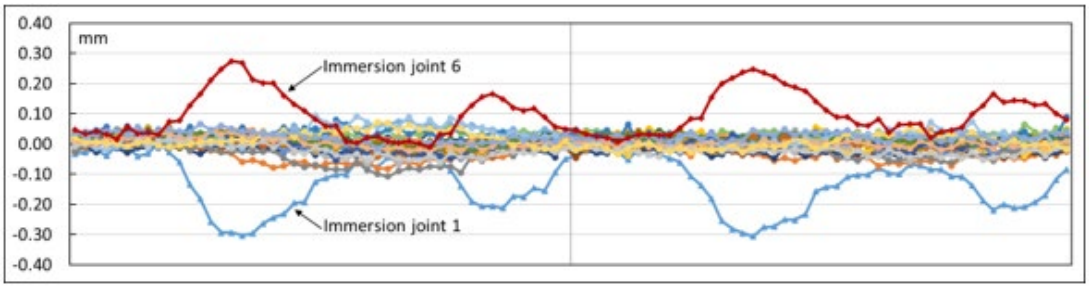

Figure 1.4: Daily uneven settlement behavior of immersion and dilation joint

Figure 1.4 has shown the joint deformation result by uneven settlement from 14 to 15 June 2021 (Zhang and Wout, 2022). As shown in figure 1.4, joint 1 and 6 experienced much larger vertical joint deformation than the remaining joints. The deformation curve of joint 1 and 6 has shown an apparent cyclic behavior (with a half-day period), which follows the tidal variation along the Oude Maas River. The measured periodic joint deformation amplitude is about 0.30 mm at Joint 1. The immersion tunnel section and approaching structure is connected by immersion joints 1 and 6. As the approach structure is supported on piles, the settlement of approaching structure due to tide is insignificant, comparing with the sand foundation supported tunnel element. Therefore, the data from the DOFS in Figure 1.4 implies that the entire immersed tunnel alignment settles (under high tide) and floats (at low tide level) periodically with tide. The settlement behavior of immersed tunnel under tide is shown as figure 1.5.

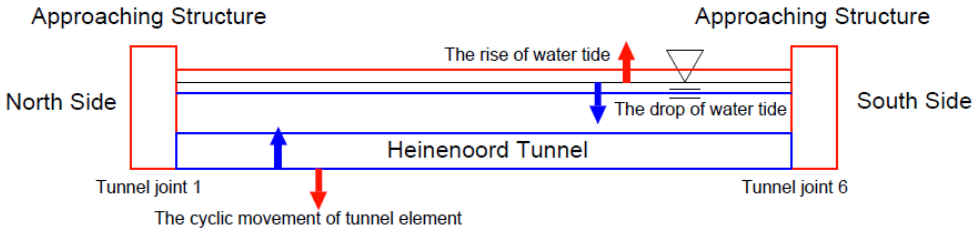

Figure 1.5: The cyclic movement of Heinenoordtunnel to tide variation

However, the mechanism of the cyclic behavior of immersed tunnel is still not known. To understand the behavior of Heinenoordtunnel under tide, further investigation is required. The hydraulic and settlement response of soil under tide is the focus of this research.

1.3 Main Research Question

The main objective of this research is to provide a sufficient explanation on the response of Heinenoordtunnel from the monitoring data. The main question is raised as below:

- *What are the accountable reasons to the settlement behavior of Heinenoordtunnel shown by the measurement data?*

Specifically, this research is divided into two main parts. The first part is the explanation of the increasing long-term settlement of immersed tunnel throughout the operation period. The second one

is the analysis of daily periodic settlement under tidal fluctuation.

For the first part work on the explanation of long-term settlement, several sub questions are investigated as below:

- *Will there be an increasing load applied on the immersed tunnel throughout the operation period?*
- *What are the changes of calculated settlement if the increasing load is considered in the Finite Element Model?*
- *Would sensitivity of geological unit play an important role on the calculation result?*

The second part of work is the explanation of cyclic settlement under tidal fluctuation, the below sub questions are examined:

- *Can the existing soil mechanics and geo hydrology theory determine excess pore water pressure of soil from tidal fluctuation?*
- *How will the calculated result changes if the impact of tidal fluctuation is included in the analysis stage?*
- *Does the tidal fluctuation cause a significant impact on water tightness of the immersed tunnel?*

To provide an answer all those research questions, numerical simulation methodology is adopted, while part of the work is based on theoretical analysis.

1.4 Thesis Outline

The thesis outline section gives a clear structure of the report and indicates how the research questions can be answered. The entire thesis report consists of 8 chapters which are summarized below:

Chapter 1 introduces the thesis background, objectives, research questions and methodology. It explains the initiative of this research and gives a logical flow on solving the problem.

Chapter 2 conducts a literature review. The following topics are reviewed such as the long-term settlement behavior of immersed tunnel, settlement mitigation, tidal impact on tunnel response. This indicates that the excessive long term and periodic daily settlement of Heinenoordtunnel is not an isolated case. It happens on other immersed tunnel projects with similar geological condition across the world.

Chapter 3 focuses on the interpretation of geological parameter for subsequent modelling stages. It starts with the soil profile classification from Cone Penetration Test (CPT) and bored hole sample. Robertson's method is then used to calculate the soil strength parameters. Since hardening soil model and consolidation mode are used in the numerical analysis stage, the permeability constant and stiffness parameter shall be determined empirically from tip resistance value (qc) and Ic value.

Chapter 4 simulates the long-term settlement of Heinenoordtunnel based on the traverse cross-section model, using 2D FEM in PLAXIS. The tunnel consolidation settlement over the 50 years

operation is analyzed. Further analyses are performed to investigate the three likely causes of excessive settlement, namely increasing traffic load, riverbed sedimentation and secondary compaction. The comparison between monitoring data and numerical result is done after adding up all three impacts in the Finite Element Model.

Chapter 5 simulates the periodic settlement behavior of Heinenoordtunnel under tide variation, based on the traverse cross-section model in PLAXIS. A coupled flow and consolidation model is used to simulate the deformation of foundation soil under tide. The simulation results are then compared to the monitoring data from the Finite Element result.

Chapter 6 studies both the long term and daily settlement behavior of Heinenoordtunnel along the longitudinal direction in PLAXIS. The longitudinal analysis is done to check the consistency of the calculation result. Then, Finite Element results are further compared with both the DOFS and leveling result for tunnel behavior analysis.

Chapter 7 conducts a sensitivity analysis in both settlement history and tidal response calculation. The stiffness parameters are altered to investigate how significant the calculation result will change. The altered Finite Element result and monitoring data is then compared. Finally, the significance of soil variability is quantified on the tunnel settlement analysis.

Chapter 8 summarized the results and findings of this research. Limitations exist in the numerical simulation, while some suggestions are made on the further investigation. Also, the impact of tidal fluctuation can be considered in the design process of immersed tunnel.

Chapter 2 Literature Review

This section reviews the general information of immersed tunnel, long-term settlement and tidal impacts on tunnels. At each sub-section a summary of literature review is provided.

2.1 General information of Immersed tunnel

(1) Immersed tunnel construction process

The first immersed tunnel was built in Boston, United State in 1893 (Grantz, 2003). It is a 100m long sewer that transport wastewater underneath the river. The entire tunnel is made up brick and concrete. Water can penetrate through the cracks between bricks into the inner lining. Hence, the watertightness and serviceability are the issues to the sewer.

With improvement of construction technology, immersed tunnel was implemented on public transportation in the early 20th century. In 1910, the Michigan Central Railway Tunnel, was built to transport passenger across the Detroit River. After 3 decades, Maas Tunnel, the first immersed tunnel in Europe, was built in Rotterdam. Due to the success of the Maas Tunnel construction, immersed tunnel become widely used in Netherlands. In the year 2013, 31 immersed tunnels have been built in Netherlands that is two third of the total number in Europe (Gavin, 2020).

Comparing with bored tunnel, the construction time and cost of immersed tunnel is relatively low. It is because the burial depth of immersed tunnel is significantly lower than the bored tunnel, which reduces the construction length. The construction impact of submerged tunnels is relatively less to dykes and the existing structure. Hence, immersed tunnel is an alternative solution if the construction cost is the great concern.

Some issues are found in the construction of immersed tunnel. Immersed tunnels are sensitive to differential settlement. Several centimeters of differential settlement can cause cracks and leakage of element and segment joint. Leakage of water occurs, when the applied load exceeds the design value (Liang, 2017). Hence, the immersion and dilation joints are under a good condition.

(2) Dilation and Immersion Joint of Immersion Tunnel

Watertightness is an important issue in immersed tunnel construction. The differences of temperature from cementation cause cracks (Chen, 2017). Making the entire tunnel element in several segment can reduce the thermal impact on cementation. To ensure the water tightness between tunnel segment, the dilation joint is built that the local and global section is shown as the figure 2.1.

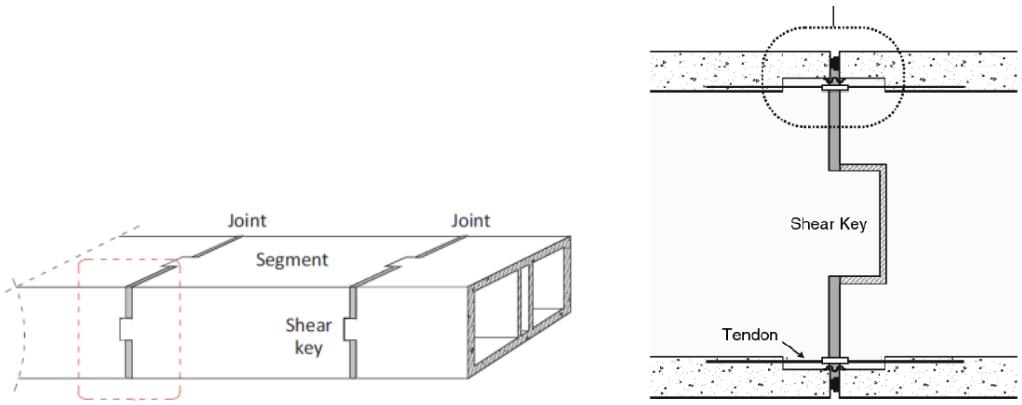

Figure 2.1: The detailing of segment joint in the global and local view

The shear key restrains the deformation of segment and element joint along the shear direction. Figure 2.1 has shown a typical cross section of segment joint. The tendon is connected between the segments that allows the expansion and contraction of concrete segment.

The immersion joint has a similar function as the dilation joint, but the structural detail is different. The watertightness condition is achieved by gina gasket and omega ring. This allows the deformation of immersion joint. Figure 2.2 shows the details of immersion joint and the gina gasket.

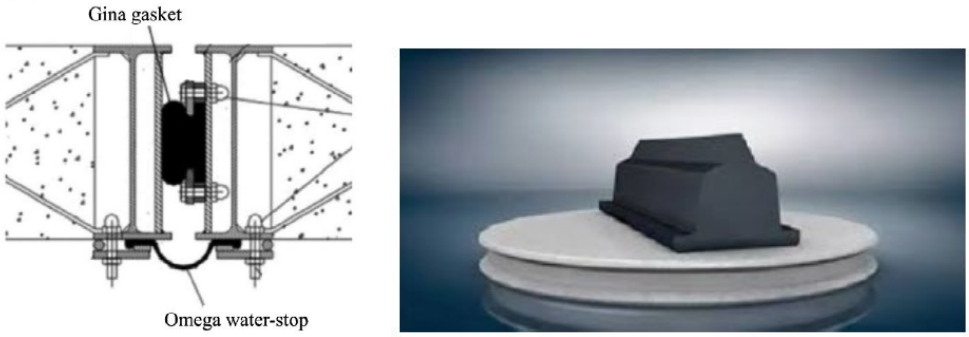

Figure 2.2: The detailing of immersion joint and the diagram of gina gasket

2.2 Long term settlement of immersed tunnel

(1) Case study on the long-term settlement

The high and increasing settlement of Heinenoord tunnel is not a unique case. It is commonly found in various projects, especially under soft soil condition. More than 10 cases of excessive tunnel settlement are investigated in Japan, Europe and America (Grantz, 2001). 2 typical cases are discussed in this literature review because they share similar geological conditions as Heinenoord tunnel. The value of long-term settlement after construction is in between 10 to 75mm (Grantz, 2001). It is important to summarize the accountable factors on the high value of tunnel settlement during the operational period.

Antwerp, Belgium: Scheldt tunnel (1966-1969)

The 510m long immersed tunnel was built across the Scheldt river between 1966 and 1969. The entire tunnel alignment consists of 5 tunnel elements. Four box sections are under the dimension of 99.0 X 47.9 X 10.1m, while the remaining one is 11.5 X 47.9X10.1m (Havno, 1969). The 47.9m wide section

provides 6 lanes for railway and vehicle traffic.

Immersed tunnel settlement is measured at the end and after 11 years of construction. The value of settlement is in the range between 17 to 53 mm over the service period. Over a third of total settlement is contributed by the long-term response of the tunnel element. Hence, settlement over the service period is under consideration in the calculation.

Schelde Tunnel settlements

Element number	North	1	2	3	4	5	South
Until end of construction		66 96	141 156	74 61	57 55	48 132	
After 11 years of construction		53 39	38 30	35 25	21 17	19 30	
Totals		119 125	179 186	109 86	78 72	67 162	

Table 2.1: The long-term settlement of Scheldt Tunnel

Aalborg, Denmark: Limfjord Tunnel (1966-1969)

Limfjord tunnel was built along the river in Aalborg, Denmark. The burial length of immersed tunnel is 510m that consists of five 102 X 27.4 X 8.5m concrete elements. 6 lanes are constructed in the 27.4m width of tunnel for heavy and light vehicles to cross the Limfjord river.

Research is done along the geological profile of Limfjord Tunnel. The geological condition is totally different between the north and south sides of the immersed tunnel (COWI, 2019). Along the southern direction, a thick layer of chalk is found under the tunnel alignment. Chalk is the porous, carbonate rock which has a greater stiffness than soil. The rock head of chalk layer drops from the south to north of Limfjord tunnel. At the north end, the chalk layer is found 60m below the mean sea level. The 30m glacial sand and clay are found above the rock head, while soft mud and silt are on top of the glacial soil. To minimize the joint deformation along the northern end, the whole layer of soft mud and silt are dredged and replaced with sand back fill. In addition, 3 m of sand is applied above the tunnel subgrade which further consolidate the glacial soil. Figure 2.4 indicates the geological profile and the alignment of Limjford Tunnel.

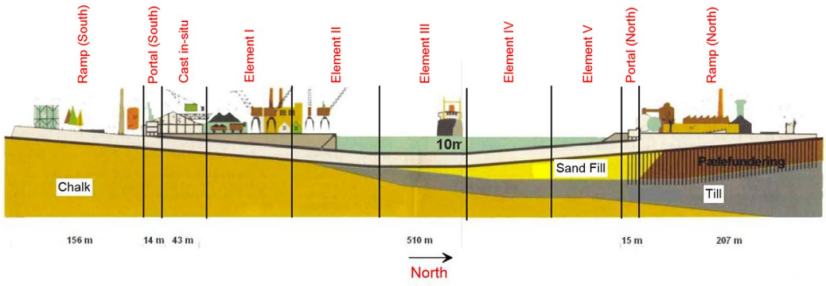

Figure 2.3: Geological profile of Limjford Tunnel

Monitoring is done along the tunnel alignment during the 50 years of tunnel operation. According to the monitoring result in 2017, the measured settlement is under 25 mm at the south side, while the value is about 130 mm along the east side. The chalk layer gives greater support to the tunnel elements than glacial till at along the north. The settlement at the south is only 20% of that in the north. Although the soft soil are excavated under the tunnel element, the clay along the excavated surface are consolidated by the sand backfill. Lateral movement of sand subgrade causes the settlement of Limfjord Tunnel.

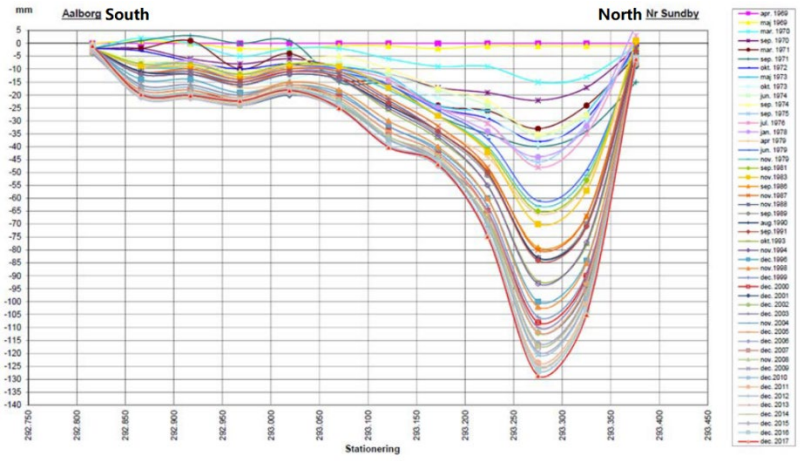

Figure 2.4: Long term Settlement of Limjford Tunnel

From the case history, surcharge and subsoil condition are the influential factors on the long-term settlement of immersed tunnel. The surcharge is caused by fluvial deposition and vehicles. The normally consolidated soil is more sensitive to tunnel construction than glacial soil or rock. Therefore, the choice of suitable foundation is an important strategy to maintain the differential settlement in an acceptable level.

(2) Possible factors on long term settlement

Immersed tunnels are constructed as a permanent underwater crossing in many countries. The long-term settlement response becomes a prominent consideration in tunnel design (Lotysz, 2010). In the construction project of immersed tunnel, 100 years of service period is usually included in the contract. (Liu, 2014).

Uneven settlement can be a potential threat to the structural safety of immersed tunnel, but it is often neglected by consulting engineers (Shi, 2016). Tidal effects, riverbed siltation, scouring and dynamic load from vehicle are the long-term factors which cause differential settlement on the tunnel alignment (Zhang, 2016). Since Netherlands locates at the delta region, tidal effects and riverbed siltation are the possible factors on the long-term settlement. Both factors are discussed in this section.

Siltation on the excavated surface and sand foundation causes severe problem on the immersed tunnel (Grantz, 2001). Although the highly compressible clay can be excavated in the trench construction process, sedimentation occurs when water flows slowly along the river. Mixture of silt and clay particles deposit on the trench and sand foundation which forms thin geological layer with uneven thickness. Since the newly formed layer is unconsolidated, the compaction of silt contributes to the long-term differential settlement of immersed tunnel. Siltation under the tunnel element is restricted and monitored carefully in the immersed tunnel projects. In the construction process of Oresund Tunnel, for example, the impact of siltation is minimized under the tunnel element (Marshall, 1999). Therefore, sounding on the excavation level is conducted and the newly formed sediment layer is dredged several hours before the installation of tunnel element and sand foundation.

Large tidal variation cause compaction of sand foundation over the service period. Since sand is highly permeable, water flow into and out of sand quickly under the change of hydraulic boundary condition. When the water level rise, pore water pressure increases simultaneously in sand layer. On the other hand, the pore water pressure drops in the low tidal conditions. The consistence change of

pore water pressure causes gradual compaction on the sand layer. Therefore, densely compacted sand is found in the North Sea where heavy wave applied on the seabed continuously (Jardine, 1998). Under normal circumstances, pore water pressure of sand foundation layers oscillates for more than 30000 times after 60 years of service period. Settlement of immersed tunnel is developed gradually under the impact of tide over service period (Zhou,2021).

(3) Long term settlement reduction method

In most geological conditions, the immersed tunnel can be constructed with sand foundation. Soft soil is removed and replaced with sand in the process of trench excavation. However, the limitation of sand foundation exists when thick alluvial layer is found underneath the seabed. Hong Kong – Zhuhai – Macao immersed tunnel, for example, up to 40 m thick of normally consolidated clay is found in along the alignment (Bai, 2019). Dredging is not an economical and effective solution in this scenario, because large volume of normally consolidated soil is excavated. Long term settlement on immersed tunnel is encountered when clay layer is consolidated along the slope (Grantz, 2001). Further improvement of geological condition and foundation is essential to reduce the settlement of immersed tunnel.

Deep cement mixed (DCM) is the construction method which increases the stiffness of foundation soil. By mixing the cement with normally consolidated clay, the bond between soil particles increases due to cementation (Yapage,2014). The artificial soil layer has greater bearing capacity and stiffness than soft soil, which reduces the long-term settlement of immersed tunnel. Comparing with trench excavation under great depth (ie.>40m), the construction time and cost of the DCM is relatively less. Therefore, deep cement mixed is an economical approach for embankment and immersed tunnel construction (Lai, 2006). In South Korea, DCM was implemented on the Busan – Geoje Fixed Link, where a 60 m of marine clay is found under the seabed (Lee, 2012). Figure 2.5 has shown a typical cross section of immersed tunnel which is supported by the deep cement mixed.

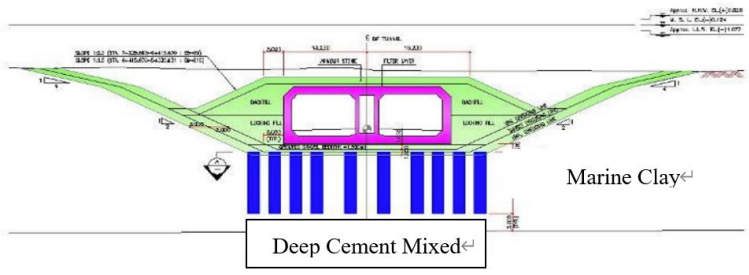

Figure 2.5: Cross Section of DCM in the ground treatment of immersed tunnel

Although the long-term settlement of immersed tunnel is reduced by DCM installation, detailed design verification is required. Laboratory analysis and elasto-plastic simulation are conducted on the cement mixed soil sample. The triaxial result shows that the stiffness and strength of cement mixed soil increases, but it becomes more dilative (Liyanapathirana,2012). The bond between soil particles breaks when yielding occurs. Residual strength of cement mixed soil is the same as the normally consolidated clay. Therefore, conservative load determination is required to ensure that the settlement of immersed tunnel is under elastic range.

Apart from Deep Cement Mixed, pile foundation can be an alternative measure to reduce the long-term settlement of immersed tunnel. Stiff bearing piles support the tunnel element when stiffer

layer is found under the seabed, for example bed rock (Oslen, 2022). Bearing pile are widely implemented in different countries where rock head is closed to the foundation level. Figure 2.6 has indicated a typical immersed tunnel section which is supported by the end bearing pile.

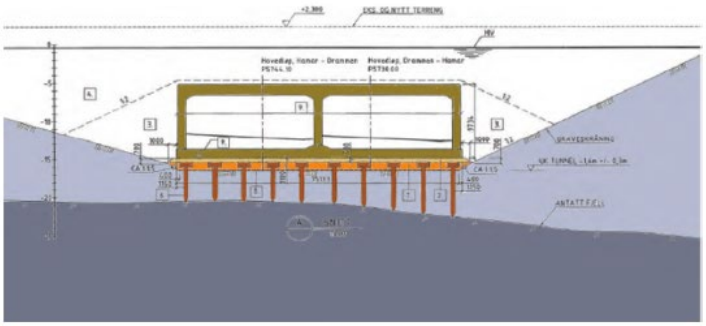

Figure 2.6: Cross Section of immersed tunnel that is supported by end bearing pile

(4) Comparison between foundation treatment methods

To select a suitable foundation treatment method in real project, it is important to quantify and compare the long-term settlement of immersed tunnel under Deep Cement Mixed, end bearing piles and sand foundation. Figure 2.7 shows the settlement response of immersed tunnel under different geological conditions and construction methods.

project	Outer Ring Tunnel	Changhong Tunnel	Yongjiang Tunnel	Zhujiang Tunnel
purchasing method	D&B	D&B	traditional	traditional
construction duration	4 years	2 years	8 years	3 years
hydrogeology	serious siltation and soft ground	serious siltation and soft ground	serious siltation and soft ground	intermediary weathered rock ground
foundation type	sand flow	pile	grouting	sand flow
accumulative settlement	23 cm	2 cm	8.84 cm	3 cm

Table 2.2: Settlement of immersed tunnel under different construction method

Sand flow foundation works well on rock profile (settlement = 3 cm), but induced long term settlement is more than 20 cm under soft soil ground condition (Wang.2020). End bearing pile foundation causes the least amount of settlement among all construction methods, that is 2cm. Deep cement mixed (DCM) reduces the long term settlement of immersed tunnel, but the value is 80mm which can be a potential threat on the watertightness. Hence, monitoring and condition survey is essential to maintain the immersed tunnel in good condition, when DCM is applied to tunnel construction.

2.3 Tidal impact on immersed tunnel

(1) Background on daily settlement of tunnel

To understand the tidal impact on immersed tunnel in depth, further literature study is required. Case study can give a rough idea on short term response of immersed tunnel. This section is subdivided into two parts. They are the daily settlement and the structural deformation of tunnel under the variation of water table. Tidal oscillation causes changes of hydrostatic pressure on the immersed tunnel. In terms of the short-term settlement response, no high frequency monitoring research is done on immersed tunnel. However, few papers determine the settlement of bored tunnel under tidal fluctuation. It can be useful to predict the result on immersed tunnel. Leveling is conducted hourly along the Liefkenshoek Rail Tunnel, Belgium. A 10mm oscillation of vertical displacement is

measured at the tunnel segment between high and low tidal condition (Schotte, 2016). It is important to identify the possible cause on the short-term settlement on Heinenoord tunnel.

(2) Case history on the daily settlement on Liefkenshoek link

Liefkenshoek link is a twin bored tunnel which connects the port of Antwerp by passing through the River Scheldt (Van Bogaert, 2008). The entire length of the tunnel is 6km, while the crosssection diameter is 7m. Soil investigation is done along the tunnel alignment. Sand backfills and Quaternary clay layers are found above the tunnel element (Bogaert, 2009), while an average thickness of 80m boom clay laid under tunnel alignment. Boom clay has low hydraulic permeability, with the magnitude of 10^{-12} m/s (Delahaye, 2002). Hence, the pore water pressure in boom clay may not follows the tidal level fluctuation. Figure 2.8 indicates the longitudinal profile of Liefkenshoek tunnel under different geological unit.

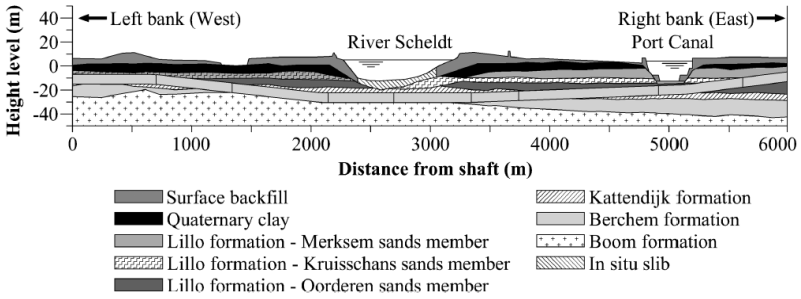

Figure 2.7: The longitudinal profile of Liefkenshoek tunnel under different geological unit

Before finding out the short-term response of tunnel under tide, it is important to determine the influence zone of tide on the geological profile. A uniform rise and fall of water level is measured along the river Scheldt. The variation of water level is between 6 and -0.5m TAW (the Belgium Water Level Reference). The impact of tide reduces sharply outside the boundary of river. The water head becomes constant along the excavation shaft 07 and 08. To illustrate the impact of tide, the chainage of Liefkenshoek tunnel and the excavation shaft is shown as figure 2.9 below.

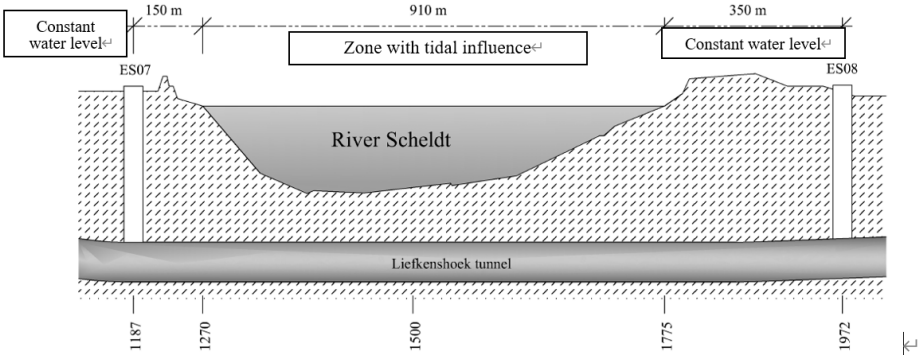

Figure 2.8: The chainage of Liefkenshoek tunnel under River Scheldt

8 consecutive leveling measurements were conducted from 9:45 am to 5:30 pm along the Liefkenshoek tunnel. The measurement starts from the chainage 1100 to 1500 that covers the position of riverbank and under the Scheldt River. The level of the tunnel section is stable at the excavation shaft 07, but the level oscillates across time at the riverbank, that is between the chainage 1250 to 1300. From chainage 1350 to the center of the river (1500), the leveling difference between high and low tide is constant and equal to 10mm. The entire tunnel element rises and fall in the same phase

with the tidal level fluctuation. Figure 3.10 has shown the variation of tunnel level across the day.

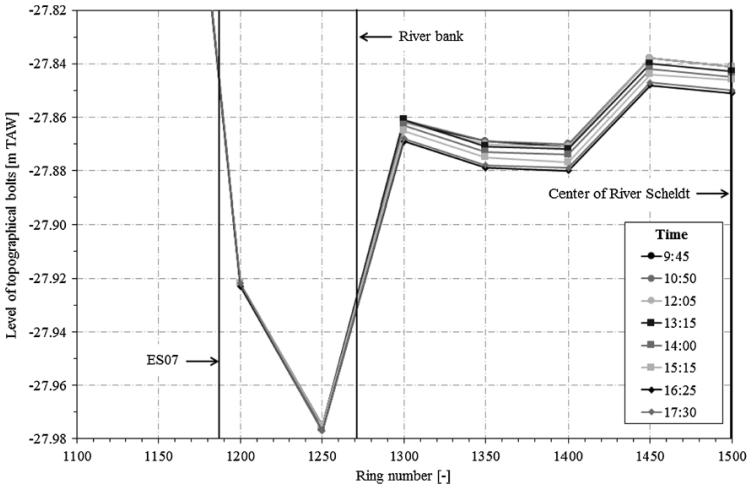

Figure 2.9: Leveling of Lifkenshoek tunnel across the day

The monitoring result has shown that the level variation of Liefkenshoek tunnel is related to tide in River Scheldt. The 10mm of settlement variation is a geotechnical behavior rather than a structural response, because the entire tunnel segment settles under the Scheldt River. The high tide increases the external load applied on the boom clay that causes elastic compaction, while load tide reduced the applied load and causes soil rebound. Further investigation is needed to understand the impact of tide on soil.

(3) Section deformation of bored tunnel under tide

Apart from the settlement of tunnel alignment, tide also induces structural deformation along the concrete section. The tunnel section can be subjected up to 5 - 8m of tidal level variation (Grantz, 2002). In high tidal condition, the load increment is equal to 50 - 80kPa, that is 5-10% of the total stress across the tunnel section (Schotte, 2016). It can cause structural damage, inflow of water and other serviceability issue on immersed tunnel. Figure 3.11 illustrate the hydrostatic stress applied on the bored tunnel under low and high tidal conditions.

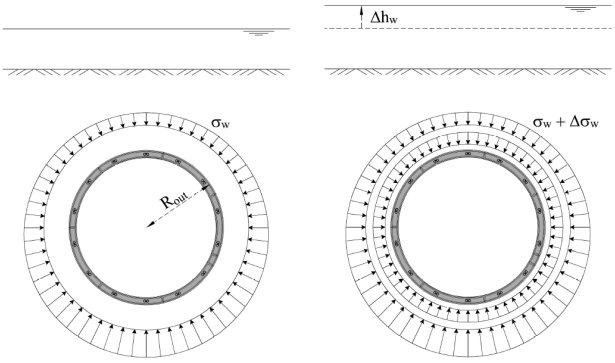

Figure 2.10 Tide induces hydrostatic stress on tunnel lining

Research is done on measuring the strain of concrete lining under tide. The strain sensor is installed around ZhaoShan immersed tunnel that is under 5m of tidal fluctuation. A sinusoidal pattern of strain is measured with the amplitude of 3.5με (Wei, 2017). The period of strain pattern is 12 hour and in phase with the tidal variation. Figure 3.12 shows the monitoring equipment setup and data.

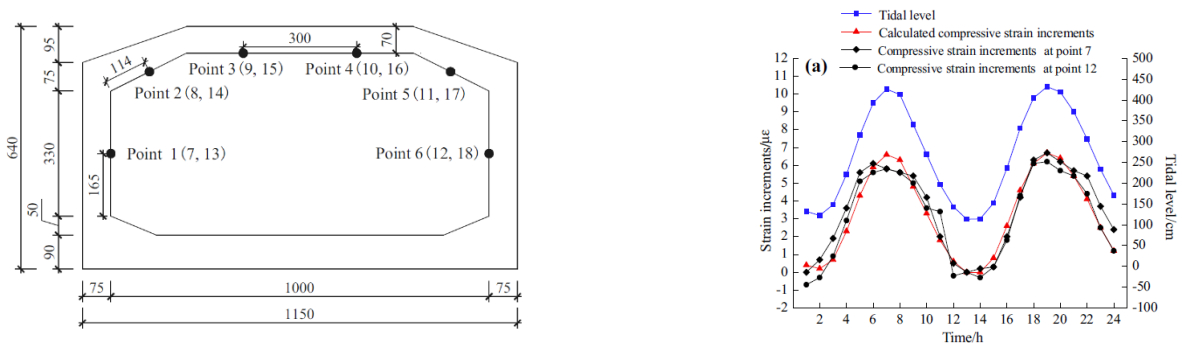

Figure 2.11: Monitoring setup (left) and result (right) of immersed tunnel section under tide

2.4 Summary of the Literature Review

Immersed tunnel can be an economical solution for vehicles to cross the canals under water. Tunnel segments and elements are connected by joint which is sensitive to differential settlement and angular rotation. A few centimeters of joint deformation can cause joint leakage and cracks on the shear keys. Therefore, it is important to figure out the possible causes of the long- and short-term settlement of immersed tunnel.

Previous literature review has summarized possible factors that contribute to the long-term settlement of immersed tunnel. Among all factors mentioned in the previous section, siltation and consolidation of soft soil have the most significant long-term impact on the immersed tunnel. Siltation induces addition load and weaken the sand foundation of the tunnel, while compression of soft soil causes more than 50 mm settlement in long term. Heinenoord tunnel locates at the delta region of Waal and Maas River. The low flow rate of the rivers causes significant siltation in the sand foundation and on top of the riverbed. However, the exact rate of siltation and geological condition of Heinenoord tunnel are not known that requires further investigation. In addition, the volume of traffic increases over the service period, but the exact value is not known. Traffic load determination can give a more precise calculation on the long-term tunnel settlement. Siltation and increasing of traffic load are considered in Finite Element Simulation.

Considering the short-term tunnel response, the variation of total load is applied on the tunnel alignment across the day. Due to the impact of tide, water table rises and falls twice a day that causes a change of total load on the tunnel alignment. Researchers measure the level along the Liefkenshoek link, a Belgian bored tunnel in Antwerp across the day. The highest rebound of tunnel occurs under the trough of tide, while the greatest settlement of tunnel occurs when the water level reaches the peak value. However, it is not sufficient to draw any conclusion on the short-term settlement of immersed tunnel because the construction methods and stress path are different in the bored tunnel excavation.

Based on the above reasons, Finite Element model is built to determine both the long- and short-term response of Heinenoord tunnel in the next section. The Finite Element result is then compared with the monitoring data. This can verify the importance of tide and siltation on the settlement of Heinenoord tunnel.

Chapter 3: Geological Condition Analysis

This chapter focuses on the soil layer classification and parameter interpretation. The geological profile is classified by bored hole data and CPT information, while the soil parameter is determined from NEN table and Robertson's method. Finally, a discussion on assumption and limitation of CPT data interpretation is added at the end of this chapter.

3.1 Geological Soil Parameter Determination

3.1.1 Available data sources

The Heinenoordtunnel was open to use since 1969, and there is quite limited geological information facilitating the soil parameter determination beneath the immersed tunnel structure. However, very close to the 1st heinenoordtunnel, a bored tunnel was constructed in 1990, namely the 2nd Heinenoordtunnel, which locates about 100m from the immersed tunnel, as show in figure 3.1.

Since the geology of the riverbed is formed by sedimentation, the horizontal scale of fluctuation is larger than the distance between two tunnels. The variation of geological profile is not significant within the distance of 100m. In this thesis, the geological information from the 2nd Heineordtunel was used. The Centrum Ondergrond Bouwen (COB) website has provided a longitudinal and traverse geological section, see (https://www.cob.nl/kennisbank/?searchwp=Heinenoord%20Tunne).

Figure 3.1: The location of Heinenoord 1st and 2nd Tunnel

To implement the data on this research, the immersed tunnel profile is drawn on the geological section diagram. The profile is shown as the figure 3.2 below:

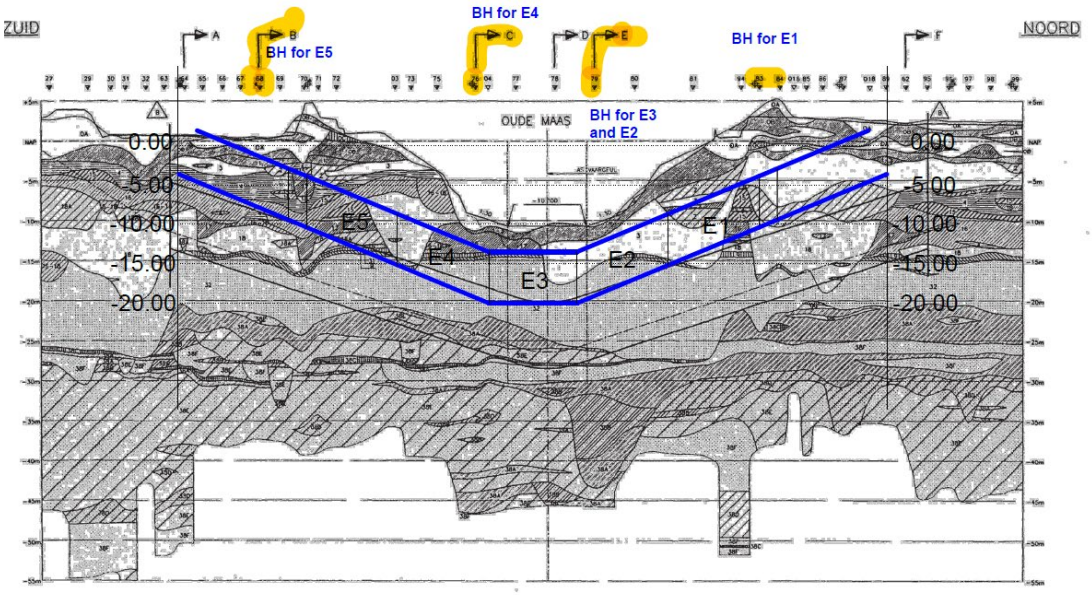

Figure 3.2. The longitudinal profile and bore hole location of Heinenoordtunnel

The above geological profile indicates the location of CPT and bored holes along the Heinenoord tunnel. To calculate tunnel settlement precisely, the geological condition of each element is represented by a single bored hole. As no bored hole data is found on Element 1, the closest one (BH68) is selected. Also, Element 3 and 4 share the same bored hole which locates at the immersion joint of these two elements. The table 3.1 below has shown the CPT and Bored hole used in this research.

Table 3.1: The selection of CPT and bored hole under the tunnel element

	Tunnel Element				
	E1	E2	E3	E4	E5
CPT Number	84	53	53	49	68
Bored Hole Number	83	53	53	49	68

The Ic parameter obtained from CPT is used to verify the soil classification from bored hole data. The geological profile of each element is determined in the next section.

3.1.2 Geological Profile

The geological profile along the transverse tunnel section is shown in the figure 3.4 below:

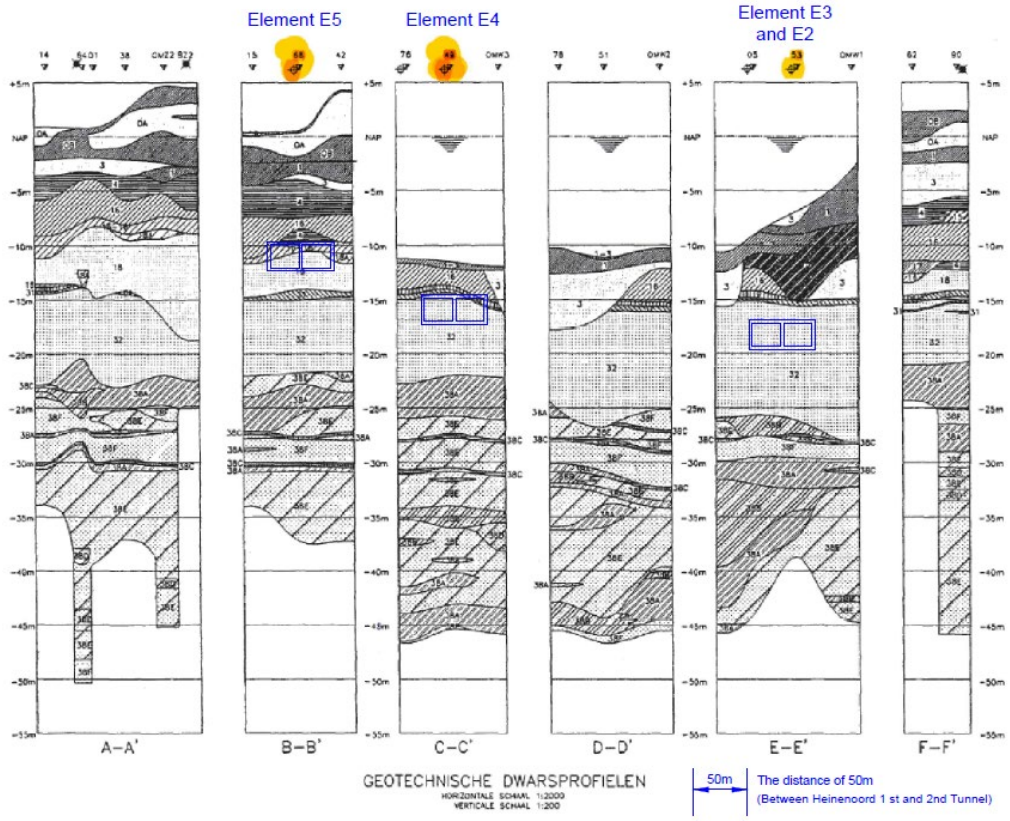

Figure 3.3: The location of bored hole and traverse tunnel section

The geological profile is almost homogenous along the horizontal direction. However, a significant variation of soil profile is found under the tunnel element 2 and 3. It is hence necessary to take an average on the thickness of clay layer in the numerical simulation stage.

Special attention should be paid on normally consolidated clay and peat layer because the compressibility generally higher than pre consolidated soil. Soft soil contributes more on the total settlement than coarse sand from tidal fluctuation, given that the thickness of geological unit is the same. Before performing the simulation, it is vital to figure out the most load sensitive geological unit in the soil domain.

Due to the heterogenous nature of soil, geological unit can be a mixture of sand, clay and even organic content. The proportion of soil component will greatly affect the compressibility and hydraulic conductivity. Cone resistance and sleeve friction are obtained from the cone penetration test, the soil can only be classified by empirical formula. It is not sufficient to carry out an accurate soil classification. Further interpretation from bored hole is required to find out the component of soil mixture precisely.

Apart from the classification of geological unit, several assumptions are made on the estimation of soil condition underneath immersed tunnel element. The slope of tunnel alignment is under the gradient of 1 to 20. The level difference between the ends of element is 5 meters or even more. Thus, the geological profile varies under the tunnel element. In the traverse direction analysis, it is assumed that the entire tunnel element is placed horizontally. The base of the tunnel element is represented by

its center position.

3.1.3 Soil Layer Interpretation

(1) Element 1

The table 3.5 below indicates the geological profile at tunnel element 1. The soil interpretation result from CPT is coherent with the bore hole record. Further investigation is required to figure out minor components of soil such as shells and plant debris.

Table 3.2. The Soil Interpretation in Element 1

Depth (NAP)	Legend	Geological Time Description	Geological unit classification based on Robertson's method
-2.25 to -10m	3	Holocene Sand	Sand mixed with single layer of clay
-10 to -15m	18	Holocene Sand	Moderate Dense Clean Sand
-15 to -16 m	1	Holocene Silty Clay	Silty Clay
-16 to -21 m	32	Holocene Sand	Moderate Dense Clean Sand
-21 to -23m	38A	Pleistocene Clay	Moderate Dense Clay
-23 to -24m	38B	Pleistocene Clay	Clay
-24 to- 29m	38D	Pleistocene Sand mixed with clay	Silty Clay (Overconsolidated)
-29 to -38m	38E	Pleistocene Sand	Moderately Dense Sand (With few clay layer in Between)

The foundation level of tunnel element 1 locates at the center of dense sand layer NAP -12.5m. Due to the low compressibility of sand, the settlement is expected to be less than normally consolidated clay and peat. Although thin clay layers and peat track were found in this layer, the measured qc value is as much as the pure sand from NEN table. It is logical to consider that the geological unit is solely sand in the Finite Element Simulation.

From NAP -15.0 m to -16.0 m, some plant debris and other organic content are found in the clay layer, which can significantly reduce the compressibility. The tip resistance value is around 2 MPa that is under 163.4 kPa of effective stress. It is considered as a highly compressive soil and contribute most to the settlement under tidal fluctuation. However, the thickness is only 1 meter that cause less settlement than the other 4 tunnel elements.

(2) Element 2 and 3

According to site investigation data from COB, only bored hole number 53 was found at the location of immersion joint between Element 2 and 3. The contract drawing has shown a uniform geological profile from the base of the immersed tunnel to NAP -27.5m. To check for the consistency of geological unit, the calculated result of settlement should be compared with monitoring data in the later section. The soil interpretation result is shown as the table below:

Table 3.3 The Soil Interpretation in Element 2 and 3

Depth (NAP)	Legend	Geological Time Description	Geological unit classification based on Robertson's method
0 to -6.5m	N/A	N/A	water
-7.5 to -8.0m	3	Holocene Sand	Sand
-8.0 to -9.0m	16	Holocene Clay	Clay
-9.0 to -12.0m	16-18	Holocene Clay	Very Clayey Sand
-12.0 to -16.0m	18	Holocene Sand	Moderate Dense Sand
-16.0 to -26.0m	32	Pleistocene Sand	Dense Sand
-26.0 to -30.0m	38E	Pleistocene Sand	Dense Sand
-30.0 to -31.0m	38D	Pleistocene Sand	Little Silty Sand
-31.0 to -32.0m	38F	Pleistocene Sand	Sandy Silt
-32.0 to -36.0m	38A	Pleistocene Clay	Stiff Clay
-36.0 to -39.0m	38E	Pleistocene Sand	Dense Sand

The construction drawing has shown that the foundation level of tunnel element 3 and 2 are NAP -20m and NAP -17.5 m respectively. Both elements lay on the dense sand layer under a high stiffness value. The deformation of dense sand layer is relatively less compared with organic clay and peat.

From NAP -26.0 to -28.0 m, a clay layer was found which contains small portion of fine sand. Although the compressibility is much higher than the upper sand layer, the settlement is relatively less compared with the previous result. It is because the thickness of clay layer under Element 3 and 2 is only half of that in Element 5 and 4. Even though the geological unit and strain are the same, the thin clay layer from Element 3 and 4 causes less settlement than the other two cases.

(3) Element 4

The soil classification result under tunnel element 4 is shown at the table below. Some remarks are given on the geological unit that potentially causes a crucial impact on the joint deformation.

Table 3.4. The Soil Interpretation in Element 4

Depth (NAP)	Legend	Geological Time Description	Geological unit classification based on Robertson's method
0.00 to -11.25m	N/A	N/A	Water
-11.25 to -14.0m	16	Holocene Sand	Clay mixed with Sand
-14.0 to -15.0m	38C	Pleistocene Peat	Humic Clay
-15.0 to -23.0m	32	Pleistocene Sand	Sand
-23.0 to -26.0m	38A	Pleistocene Clay	Clay mixed with Sand
-26.0 to -28.0m	38E	Pleistocene Sand	Sand
-28.0 to -30.5m	38F	Pleistocene Sand	Medium Dense Sand
-30.5 to -34.0m	38E	Pleistocene Sand	Medium Dense Sand
-34.0 to -35.5m	38D	Pleistocene Sand	Highly Sandy Clay
-35.5 to -37.5m	38E	Pleistocene Sand	Slightly Clayey Sand
-37.5 to -39.5m	38E	Pleistocene Sand	Slightly Clayey Sand
-39.5 to -41.5m	38E	Pleistocene Sand	Moderate Dense Sand
-41.5 to -43.5m	38A	Pleistocene Sand	Slightly Clayey Sand

From NAP -11.25 to -15.00 m, the normally consolidated soft clay is found under the river. According to the bored hole sampling result, some plant debris is found and the soil sample is black in color. Organic content in soil increases the compressibility. The construction drawing has shown that the base level of immersed tunnel Element 4 is -15NAP. The top layer of soil is excavated. Tunnel element is then sunk to -15NAP. Hence, less impact is done on the settlement of immersed tunnel this layer of soil.

From NAP -15.00 to -23.00 m, a sand layer is determined underneath the soft clay. Coarse grain gravel and some shells are found from bored hole sample. In general, coarse grain soil has a greater hydraulic conductivity than cohesive soil. The excess pore pressure dissipates quickly than clay. Due to the high stiffness of sand particle, contribution of total settlement from this layer will be less than normally consolidated clay.

From NAP -23.00 to -26.00 m, a sandy clay layer is found from CPT data. Due to the low permeability of clay, it is expected that the pore water pressure changes slow with the variation of water table. A more detailed numerical simulation is required to figure out how the cohesive soil behaves under tidal variation.

(4) Element 5

The geological result underneath tunnel element 5 is indicated at the table below. Both CPT and bored hole data have shown a coherent result on soil characterization. Special attention is taken on the geological unit which potentially causes greater settlement from tidal fluctuation.

Table 3.5. The Soil Interpretation in Element 5

Depth (NAP)	Legend	Geological Time Description	Geological unit classification based on Robertson's method
0.5 to -2.0m	OA	Holocene Sand	Sand mixed with small proportion of clay
-2.0 to -4.0m	1	Holocene Clay	Sandy Clay
-4.0 to -10.5m	4	Holocene Peat	Peat
-10.5 to -13.5m	3	Holocene Sand	Moderate Dense Sand
-13.5 to -15m	4	Holocene Peat	Soft Clay
-15 to -21.5m	32	Pleistocene Sand	Moderate Dense Sand
-21.5 to -26m	38A	Pleistocene Clay	Sandy Clay
-26 to -28m	38E	Pleistocene Sand	Medium to Dense sand
-28 to -30m	38E	Pleistocene Sand	Moderate Dense Sand
-30 to -31m	38A	Pleistocene Clay	Clay
-31 to -37m	38E	Pleistocene Sand	Sand

From NAP 0.5 to -10.5m, the table has shown a clay and peat layers that deformed greatly under the tidal fluctuation. The bored hole data indicated that organic content is not only found in peat, but also in both clay and sand. But the foundation level of immersed tunnel is around NAP -12.5m. The soil on top is excavated before installation of tunnel element and fill with sand. The surrounding peat and clay (above the tunnel foundation level) have done a neglectable impact to the tunnel settlement.

From NAP -13.5 to -15m, an organic soft clay was found from the bored hole data. It has a low stiffness and hydraulic conductivity that undergo a significant elastic deformation from time dependent load. Since the clay layer is close to the base of immersed tunnel (NAP -12.5m), it has a great contribution on the total settlement under the load increment.

From NAP -21.5 to -26m, a thick sandy clay layer was found. The bored hole data has shown that soil layer is densely packed. Since tide is a periodic phenomenon, the stress path is repetitive under the yield contour. Hence, the sandy clay is deformed under elastic range and contribute less on the total settlement from tidal load.

3.1.4 Soil parameter determination

(1) Constitutive parameter

Two methods are widely used to convert the cone resistance and skin friction from CPT into strength and stiffness parameters. They are the NEN 9997-1 table and Roberson's method. The implementation of those two methods is shown in the paragraphs below.

Method 1: NEN table

Comparing with the Roberson's method, NEN table only require the qc value from the cone penetration test. The parameter result from NEN is less precise but more conservative than the Roberson's method. Before interpreting the parameter from NEN table, qc value is converted with respected to isotropic reference stress at 100kPa. The conversion is written as follows:

$$C_{qc} = (\frac{100}{\sigma_0'})^{0.67} \tag{3.1}$$

Where C_{qc} is the cone resistance correction factor and σ_0' is the effect stress at the tip of penetrometer.

$$q_{c,table} = C_{qc}(q_c) \tag{3.2}$$

Where $q_{c,table}$ is the modified cone resistance value under 100kPa of effective stress. q_c is the measured cone resistance and C_{qc} is the cone resistance correction factor.

For sand, the cohesion is conceptually equal to zero. However, zero cohesion can cause a calculation error in Finite Element Software. It is more convenient to tentatively input cohesion as 1kPa in sand layer. The soil is classified by the Ic value of from the CPT result, while the cohesion and friction angle can be obtained from interpolation of modified qc value at the NEN table.

Method 2: Robertson method

Robertson (2015) determines friction angle from the CPT result. Unlike the method from NEN, Roberson has made an additional modification of qc value base on the pore water pressure and the tip area ratio that is shown as below:

$$q_t = q_c + u_2(1-a) \tag{3.3}$$

Where q_t is the modified cone resistance, qc is the measured cone resistance, u_2 is the pore water pressure at the shoulder position of penetrometer and a is the tip area ratio.

For sand, no correction of qc is required. However, modification is vital in clay, especially in soft soil. The resistance ratio is then calculated base and sleeve resistance.

$$R_f = \frac{f_s}{q_t} \times 100\% \tag{3.4}$$

Where f_s is the sleeve resistance, q_t is the modified tip resistance and R_f is the friction ratio.

The value of measured cone resistance qc is greatly affected by the compression from the surcharge. To reduce the impact of effective stress on the tip resistance qt, a normalized non-dimensional value of Qt is calculated from the formula below:

$$Q_{tn} = \left(\frac{q_t - \sigma_{v0}}{P_{atm}}\right)\left(\frac{P_{atm}}{\sigma'_{v0}}\right)^n \quad (3.5)$$

Where n = 1 for Clay, 0.75 for Silt and 0.5 for Sand when the stress reference level Patm = 100 kPa. σ_{vo} and σ_{vo}' is the total stress and effective stress respectively. P_{atm} is the value of atmospheric pressure.

After determining the value of Q_{tn}, the friction angle Φ_p can be determined with the use of the formula below:

$$\phi_p = 17.6 + 11\log Q_{tn} \quad (3.6)$$

(2) Consolidation coefficient

Although the pore water pressure is formed differently between clay and sand, the input parameters are the same in both cases. The consolidation parameter Cv governs the rate of consolidation under transient differential equation.

Odometer Stiffness Determination

Several researchers tried to correlate the odometer stiffness with the in-situ cone resistance from the CPT test. Different empirical formulas are used to determine parameters of geological unit. Lunne and Christoffersen (1972), has found out the empirical relationship of compressibility of clay with a given qc value. The formulas are shown as the table below:

Table 3.6. Determination Odometer Stiffness in Clay from Tip Resistance

Source	Correlation between Eoed and tip resistance in clay
Lunne and Christoffersen	E_{oed} = 4(qc)
Trofimenkov	E_{oed} = 7(qc)
Meigh and Corbet	E_{oed} = (5 to 8)qc

To make a concise judgement, method provided by Lunne and Christiffersen (Add Citation)is first adopted in this research. If the determined result does not match with monitoring data, further adjustment is required.

Apart from the odometer stiffness of clay, Lunne and Christoffersen has also done extensive research on both loose and dense sand. The relationship is interpreted as follows:

Table 3.7. Determination Odometer Stiffness in Loose Sand from Tip Resistance

Emprical formula of Eoed in loose sand	
Emprical formula	Tip resistance value
Eoed = 4.qc	for qc < 10 MPa
Eoed = 2.qc + 20 (MPa)	for 10 MPa < qc<50 MPa
Eoed = 120 Mpa	for qc > 50 MPa

Table 3.8. Determination Odometer Stiffness in Dense Sand from Tip Resistance

Emprical formula of Eoed in dense sand	
Eoed = 5.qc	for qc < 50 MPa
Eoed = 250.qc	for qc > 50 MPa

Permeability Constant Determination

From previous section on Roberson method, the normalized cone tip resistance Qt and skin friction ratio Fr is determined from the raw data of CPT. Soil can be a mixture of both sand and clay particle. The value of Ic is obtained that can classify different geological unit. The formula of Ic can be expressed by the formula below:

$$I_c = \sqrt{(3.74 - \log Q_{tn})^2 + (\log F_r + 1.22)^2} \tag{3.7}$$

The Ic value can also be used to determine the permeability of soil. It can be classified through interpolating the Ic value with the table 3.8:

Table 3.9. The Interpretation of Permeability Constant from the Value of Ic

SBT Zone	SBT	Range of k (m/s)	SBT_n I_c
1	Sensitive fine-grained	$3x10^{-10}$ to $3x10^{-8}$	*NA*
2	Organic soils - clay	$1x10^{-10}$ to $1x10^{-8}$	$I_c > 3.60$
3	Clay	$1x10^{-10}$ to $1x10^{-9}$	$2.95 < I_c < 3.60$
4	Silt mixture	$3x10^{-9}$ to $1x10^{-7}$	$2.60 < I_c < 2.95$
5	Sand mixture	$1x10^{-7}$ to $1x10^{-5}$	$2.05 < I_c < 2.60$
6	Sand	$1x10^{-5}$ to $1x10^{-3}$	$1.31 < I_c < 2.05$
7	Dense sand to gravelly sand	$1x10^{-3}$ to 1	$I_c < 1.31$
8	*Very dense/ stiff soil	$1x10^{-8}$ to $1x10^{-3}$	*NA*
9	*Very stiff fine-grained soil	$1x10^{-9}$ to $1x10^{-7}$	*NA*

**Overconsolidated and/or cemented*

3.2 Soil parameters determination results

As mentioned in the previous section, the strength, stiffness and permeability of geological unit can be determined from CPT result and empirical formula. In opposite to immersed tunnel design, it is not necessary to make a conservative parameter selection in this research. But a precise selection of soil parameter is required to calculate the exact joint deformation under tide and compare it with the monitoring data. The result of soil parameter is shown in this section, while other intermediate terms, for example, Qt, Ic, are attached in the appendix of this report.

Table 3.10. Strength and Siffness Parameter of Soil under Element 1

Depth (NAP)	Legend	Geological Unit	Dry Unit Weight (kN/m^2)	Saturated Unit Weight (kN/m^2)	ϕ From CPT	c	E50 (Mpa)	Eoed, (Mpa)	Eur (Mpa)	Permeability Constant (ms^{-1})
-2.25 to -10m	3	Sand mixed with single layer of clay	19	21	37.8	0	28	28	140	2.47E-05
-10 to -15m	18	Moderate Dense Clean Sand	19	21	41.1	0	22.3	22.3	111.9	5.85E-04
-15 to -16 m	1	Clay	19	21	28.3	17.51	10.6	5.3	53	9.03E-10
-16 to -21 m	32	Moderate Dense Clean Sand	19	21	40.5	0	77	77	385	5.18E-04
-21 to -23m	38A	Moderate Dense Clay	19	21	26.8	13.39	8.2	4.1	40.8	6.48E-10
-23 to -24m	38F	Clay	19	21	25.9	10	13.9	6.9	69.7	3.08E-10
-24 to- 29m	38D	Silty Clay (Overconsolidated)	19	21	31.1	30	42.3	21.16	211.7	1.00E-09
-29 to -38m	38E	Moderately Dense Sand	19	21	38.4	0	30	30	152	7.69E-05

Table 3.11. Strength and Siffness Parameter of Soil under Element 2 and 3

Depth (NAP)	Legend	Geological Unit	Dry Unit Weight (kN/m^3)	Saturated Unit Weight (kN/m^3)	ϕ From CPT	c	E50 (Mpa)	Eoed, (Mpa)	Eur (Mpa)	Permeability Constant (ms^{-1})
0 to -6.5m	N/A	Water	-	-	-	-	-	-	-	-
-7.5 to -8.0m	3	Sand	19	21	35.64	0	107	107	535	2.55E-06
-8.0 to -9.0m	16	Clay	19	21	32.05	10	69.98	34.98	350	8.92E-08
-9.0 to -12.0m	16-18	Very Clayey Sand	19	21	37.04	0	86	86	430	9.19E-06
-12.0 to -16.0m	18	Moderate Dense Sand	19	21	31.31	0	55.88	55.88	279.4	1.50E-02
-16.0 to -26.0m	32	Dense Sand	19	21	40.35	0	68	68	340	2.67E-04
-26.0 to -30.0m	38E	Dense Sand	19	21	42.94	0	82	82	410	4.94E-04
-30.0 to -31.0m	38B	Little Sandy Silt	19	21	30.30	2	14.2	7.11	71	7.15E-08
-31.0 to -32.0m	38F	Sandy Silt	19	21	30.30	2	17.16	8.58	85.8	7.23E-08
-32.0 to -36.0m	38A	Stiff Clay	19	21	30.30	75	23.24	11.62	116.2	9.70E-08
-36.0 to -39.0m	38E	Dense Sand	19	21	39.95	0	47.32	47.32	236.6	3.31E-04

Table 3.12. Strength and Stiffness Parameter of Soil under Element 4

Depth (NAP)	Legend	Geological Unit	Dry Unit Weight (kN/m^3)	Saturated Unit Weight (kN/m^3)	ϕ from CPT	c	E50 (Mpa)	Eoed, (Mpa)	Eur (Mpa)	Permeability Constant (ms^{-1})
0.00 to -11.25m	N/A	Water	-	-	-	-	-	-	-	-
-11.25 to -14.0m	16	Clay mixed with Sand	19	21	33.54	19.15	13.8	6.59	65.9	7.45E-08
-14.0 to -15.0m	38C	Humic Clay	19	21	31.4	2	16.33	16.33	81.67	1.30E-08
-15.0 to -23.0m	32	Sand	19	21	41.17	0	49.8	49.8	248	5.85E-04
-23.0 to -26.0m	38A	Clay mixed with Sand	19	21	32.93	27.5	10	10	50	7.76E-08
26.0 to -28.5m	38E	Sand	19	21	39.83	0	39	39	198.3	2.19E-04
-28.5 to -30.5m	38F	Medium Dense Sand	19	21	43.24	0	60	60	301.7	7.95E-04
-30.5 to -34.0m	38E	Medium Dense Sand	19	21	41.15	0	44	44	220	5.92E-04
-34.0 to -35.5m	38D	Highly Sandy Clay	19	21	25	2	7	3.5	35	9.63E-10
-35.5 to -39.5m	38E	Slightly Clayley Sand	19	21	38.74	0	26	26	133.3	8.56E-06
-39.5 to -41.5m	38E	Moderate Dense Sand	19	21	39.7	0	31	34	171	3.11E-04
-41.5 to -43.5m	38A	Slightly Clayley Sand	19	21	38.575	0	35	35	176	9.19E-06

Table 3.13. Strength and Stiffness Parameter of Soil under Element 5

Depth (NAP)	Legend	Geological Unit	Dry Unit Weight (kN/m^3)	Saturated Unit Weight (kN/m^3)	ϕ from CPT	c	E50 (Mpa)	Eoed, (Mpa)	Eur (Mpa)	Permeability Constant
0.5 to -2.0m	OA	Sand mixed with small proportion of clay	19	21	36.73	0	36.24	36.24	180	6.89E-06
-2.0 to -4.0m	1	Sandy Clay	19	21	33.36	20	14.86	7.43	74.33	1.14E-06
-4.0 to -10.5m	4	Peat	19	21	25.74	2	10.36	5.18	51.83	6.40E-10
-10.5 to -13.5m	3	Moderate Dense Sand	19	21	40.79	0	57.7	57.7	288.3	5.55E-04
-13.5 to -15m	4	Soft Clay	19	21	27.5	10	10.51	5.26	52.56	9.78E-10
-15 to -21.5m	32	Moderate Dense Sand	19	21	39.805	0	41.90	41.90	209.5	4.65E-04
-21.5 to -26m	38A	Sandy Clay	19	21	31.25	20	31.12	15.56	155.6	9.00E-08
-26 to -28m	38E	Medium to Dense sand	19	21	43.22	0	62.63	62.63	310	7.94E-04

-28 to -30m	38E	Moderate Dense Sand	19	21	40.96	0	54.6	54.6	270.3	2.49E-04
-30 to -31m	38A	Clay	19	21	31.25	28	36	18	180	6.79E-08

3.3 Summary

This section has shown the method of soil classification and parameter determination. However, several assumptions are made which can possibly reduce the accuracy of the result. For example, the soil variability does not exist, while the empirical formula can make a precise parameter determination. This can be the source of errors on the numerical simulation stage.

In the tunnel simulation, PLAXIS 2D finite element software, is used to calculate the tunnel settlement and pore water pressure distribution on soil profile. Both traverse and longitudinal direction models are made, but the uncertainty exists on geological profile and parameter selection. To verify impact of uncertainty, a sensitivity analysis is conducted, while the results are indicated at the final stage of the report.

Chapter 4: Long-term Settlement Simulation

This chapter focus on the long-term settlement simulation which incorporates both construction activities and operation of Heinenoordtunnel. A transverse cross-section Finite Element Model is built based on the loading and geological condition of tunnel element. The simulation result is then compared with the monitoring data. Some suggestions are given to explain the discrepancy between monitoring data and FEM result.

4.1 PLAXIS software information

Plaxis is a commercial software which performs finite element calculation on the stability and deformation of geological structure. Both time dependent and non-linear behavior of geological unit is simulated under advance constitutive model. Plaxis offers a wide range of applications, including immersed tunnel, deep excavation and embankment stability analysis. In this research, Plaxis is used to simulate the settlement behavior and pore water pressure on immersed tunnel.

The construction projects of immersed tunnel usually last for more than one and a half years. It is not clear to distinguish whether the clay layer is drain or not under the given time of construction. To solve this scenario, the consolidation mode from Plaxis is selected. The long-term settlement and excess pore pressure is determined, while the detailed procedures are written in this chapter.

4.2 FEM model information

4.2.1 Selection of constitutive model

Before the construction of Finite Element Model, it is important to choose a suitable stress- strain relationship of soil under construction load and tide. Tunnel construction involves unloading of soil from trench excavation and reloading from installation of tunnel element. Under the above loading condition, hardening soil model is used to simulate the pore water pressure and settlement response of soil underneath the immersed tunnel.

(1) Failure criteria of HS model

Hardening soil is an elastic – plastic constitutive model. The failure contour is based on Mohr Coulomb criteria that cannot capture the dilatancy of soil. Due to the buoyancy effect, the submerged weight of soil and immersed tunnel element is less than its dry weight. It does not cause an issue to the ultimate bearing capacity of foundation soil. Hence, Mohr Coulomb failure contour is sufficient in the tunnel element analysis. The failure criteria is indicated as follow:

$$\tau = \sigma_{\mathrm{n}} \tan\phi + c \tag{4.1}$$

Where σ_{n} and τ are the normal stress and shear stress applied along the shear failure surface. Two input parameters can be figured out from CPT data, they are the internal friction angle ϕ and the cohesion c.

(2) Stress – strain relationship of HS model

In terms of serviceability, three stiffness parameters are used to simulate the response of soil under different loading condition (Celik, 2017). A great difference is found between primary loading and unloading/reloading response of soil. This can provide a more precise settlement analysis of immersed tunnel. Figure 4.1 indicates the deviatoric stress strain response of linear elastic and hardening soil model.

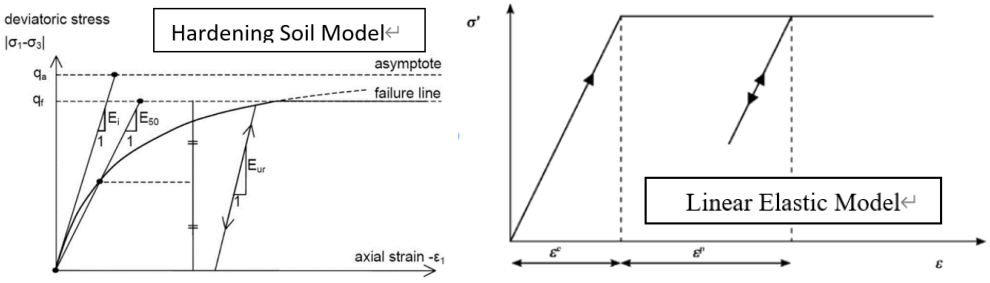

Figure 4.1: The stress and strain relationship of hardening soil and linear-elastic model

(3) Yield surfaces of the HS model

Hardening soil model is usually considered as the double hardening model. There are two yield contours in this constitutive model, they are shear and cap hardening line. The expansion of when the stress path moves beyond the initial one. The elastic-plastic deformation when the expansion of yield contour. The evolve of yield contour and development of the shear and cap hardening is indicated as figure 4.2 below.

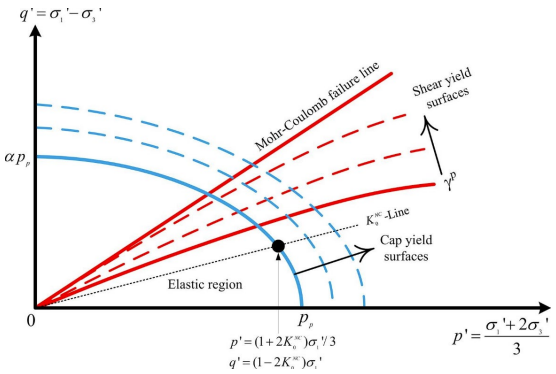

Figure 4.2: Double hardening yield contour of HS model

(4) Stiffness parameters determination

Code of practice NEN9997 provided an empirical relationship which correlates the cone resistance value with both stiffness and strength parameter. The value of E100 can be determined from the NEN9997 table. Three stiffness parameters are included in the hardening soil model, they are Eoed, Eur and E50. The stiffness parameter is isotropic stress dependent in the hardening soil mode (Celik, 2017). The value of Eoed is first transformed to the odometer stiffness with 100kPa of isotropic reference stress. Then, the remaining 2 parameter are then calculated from the Eoed value. The relationship between Eoed and its reference level is indicated as follows:

$$E_{oed} = E_{oed}^{ref}\left(\frac{c\cot\phi' - \sigma_1'}{c\cot\phi' - p'^{ref}}\right)^m \tag{4.2}$$

Where E_{oed}^{ref} is the odometer stiffness under 100kPa of isotropic stress, c and Φ are the cohesion and friction angle of the soil respectively, pref is the isotropic stress level (100kPa).

For pure sand layer, the value of m is equal to 0.5. The value of E50 is roughly the same as the odometer stiffness Eoed (Schanz, 1988). The unloading/reloading stiffness is roughly 3 to 5 times as much as the reference value of E50. That is shown as the equation below:

$$E_{oed}^{ref} \approx E_{50}^{ref} \tag{4.3}$$

$$E_{ur}^{ref} = (3to5)E_{50}^{ref} \tag{4.4}$$

Where E_{50}^{ref} E_{ur}^{ref} is the secant and unloading/reloading modulus of soil under the reference stress level respectively (100kPa)

In the pure normally consolidated clay layer, the value of m is equal to 1. The value of E50 at the reference level is roughly twice as the value of Eoed. This is indicated as the equation below:

$$E_{oed}^{ref} \approx 0.5E_{50}^{ref} \tag{4.5}$$

$$E_{ur}^{ref} = (3to5)E_{50}^{ref} \tag{4.6}$$

Soil can be the mixture of both sand and clay in construction site. The composition of fine and coarse soil particles is determined from material index (Ic). The Eoed value can be determined from tip resistance of the cone penetration test. Then, the value of Eoed is converted to its reference value, ie. 100kPa. The other two stiffness parameters can then be determined by formula (4.3), (4.4), (4.5), (4.6).

4.2.2 Domain Information

Apart from choosing the suitable constitutive model, it is vital to determine the size and shape of domain. The tunnel element is 30m in width and the height is 9m, while the elevation is in between -12.5 to -20NAP. The bored hole information has shown the geological section with the depth between – 35 and – 40 NAP.

In trench construction, the excavation depth is approximately 10m, with the inclination of 14.5 degrees. The total width of trench and tunnel element is equal to 160m. Hence, the domain size is set as 240 m x 35 m to make sure that the zone of influence is included in the Finite Element simulation. The figure 4.3 has shown the size and shape of the domain in the Plaxis simulation.

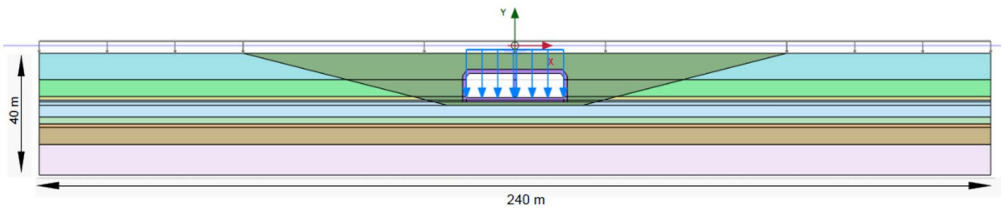

Figure 4.3: The input domain in the Plaxis model

4.2.3 Hydraulic boundary conditions

The Heinenoordtunnel locates at the Oude Maas river, in the south of Rotterdam. The soil domain has the width of 240 m that is a seventh of the straight part of the river. The location of immersed tunnel is indicated as the figure 4.4 below.

Figure 4.4: The plane view of Heinenoord tunnel

In the traverse direction, the water level is the same along the Maas River. The Maas River is straight for 1.5km, that is 7 times as the width of soil domain. Water flux can flow horizontally along the geological profile. Hence, the seepage boundary is input in the Plaxis model. A clay layer is found underneath the soil domain. Water is not permeable along the vertical direction, it is hence assumed that the water boundary is closed. The exact boundary condition is shown as the figure 4.5 below:

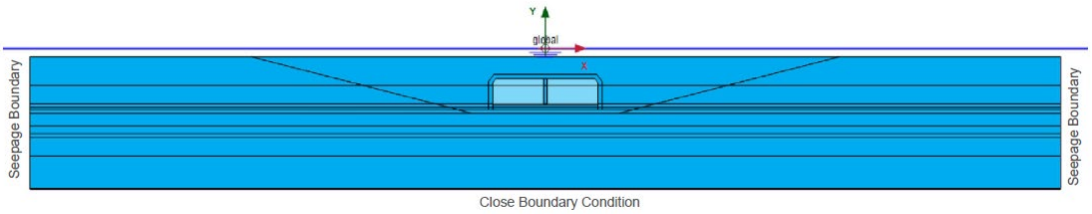

Figure 4.5: Hydraulic boundary conditions of tunnel element

4.2.4 Construction stages of Heinenoord tunnel

No record is found about the exact construction time and method used in tunnel construction. However, some approximations can be made based on the daily production rate of machine nowadays. It is assumed that the entire construction project is sub divided into 5 sections. 5 excavators are working simultaneously in trench excavation and sand backfill stage. The detailed calculation of construction time is attached in the appendix of the report. The construction time schedule is shown in the Figure 4.6:

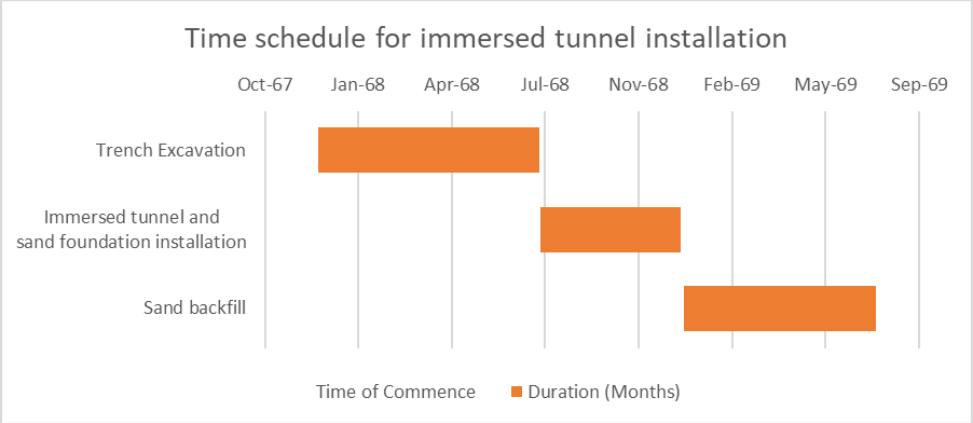

Figure 4.6: The time schedule of the immersed tunnel construction

The commencement of the Heinenoord tunnel is in the December 1968. The trench excavation time last for 7 months, while the duration of tunnel installation is 5 months. The installation of tunnel elements can be last for 6 months, when only a single element can be casted and tranport at the same time. The entire project lasts for 1.7 years that is comparable with the official data provided from ministry of infrastructure in Netherlands. The duration of construction activities is considered in the calculation steps from Plaxis. The calculation process in Plaxis model can be divided into two main stages. They are the construction phase and operation stage.

Comparing with operational phase, time of construction is relatively short, but it is sufficient to cause partial drainage condition in the clay and peat layer. Hence, it is more precise to use consolidation mode under a given construction time and hydraulic conductivity. The details of calculation stages and the time involved are indicated as below:

Table 4.1: Time schedule of Heinenoordtunnel Construction

Steps	Construction Activities	Time of Construction	Mode in Plaxis
1	Ko Initial Condition	---	---
2	Trench Excavation	7.5 months	Consolidation
3	Sand foundation + Immersed tunnel installation	6 months	Consolidation
4	Sand Backfill	7 months	Consolidation
5	Service period	50 Years	Consolidation

4.3 Simulation result analysis

4.3.1 Simulation result of element 1

The calculation result is based on the loading condition, construction steps and the parameter of soil. Traffic and sedimentation load is not considered in this stage. There are 5 immersed tunnel sections in total and the qualitative response of the soil domain is indicated in the section below:

Phase 2: Trench Excavation

Trench excavation stage is basically an unloading process, the soil underneath the trench is under a triaxial extension condition. A significant rebounding occurs, while the magnitude is controlled by

the unloading/reloading stiffness modulus Eur. The value of horizontal stress σ_3 reduces sharply and cause a minor settlement on the soil surrounding the trench. A typical settlement diagram of trench excavation is shown as the figure 5.2 below:

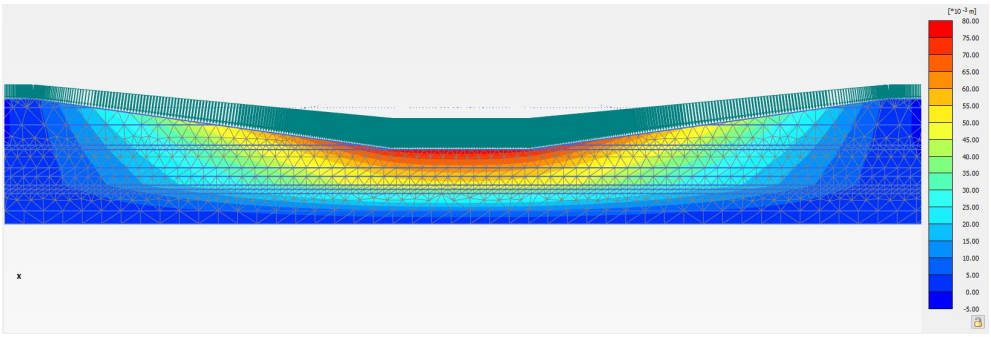

Figure 4.7: The unbounding result in the Plaxis model

The average depth of trench is equal to 10m. Therefore, the magnitude of unloading is approximately 200kPa. At the level of the excavation surface, the effective stress is 100kPa lower than the soil in Ko condition. This matches with the approximation on unloading.

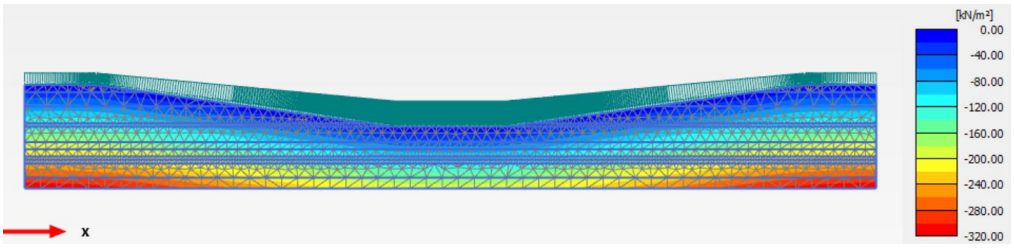

Figure 4.8: The effective stress of soil under trench excavation

The excess pore water pressure diagram is generated. The result shown that only 0.085 kPa excess pore water is found at the low permeable clay layer under the trench. Comparing with the magnitude of unloading, it can be considered as a completely drained response in the given time of construction.

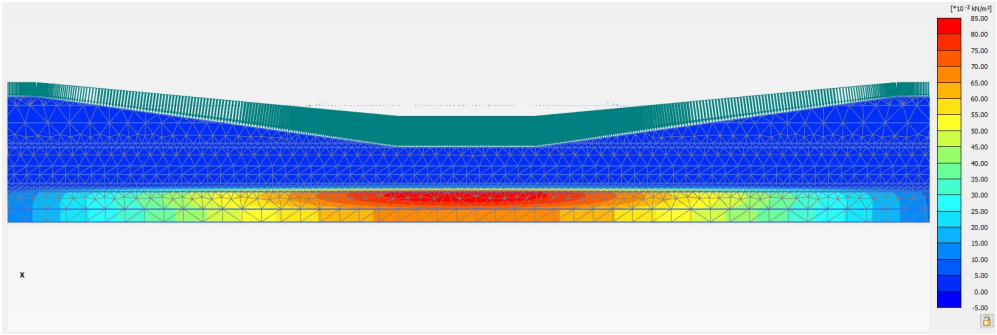

Figure 4.9: The excess pore water pressure distribution under trench excavation

Phase 3: Immersed tunnel and sand foundation installation

The settlement from immersed tunnel installation has a similar magnitude as that in trench excavation. Since weight of tunnel is balanced by the buoyancy force, the net pressure applied on the foundation soil is reduced. The unloading/reloading stiffness modulus applies in this scenario. The result of Plaxis model indicates that settlement value from tunnel installation is smaller than the unloading effect of soil due to excavation. The response is elastic rather than elastoplastic.

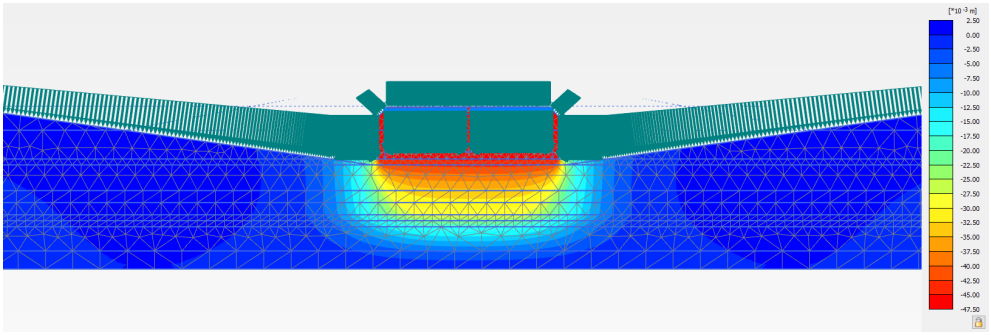

Figure 4.10: The settlement result from immersed tunnel construction

The excess pore water pressure distribution is indicated as the figure below. The maximum pore water pressure situation at the low permeability layer underneath the immersed tunnel. Comparing with the trench excavation, the distribution of excess pore water pressure is localized with the magnitude of 0.040kPa. The time of construction is sufficient to cause a drained response on the soil domain.

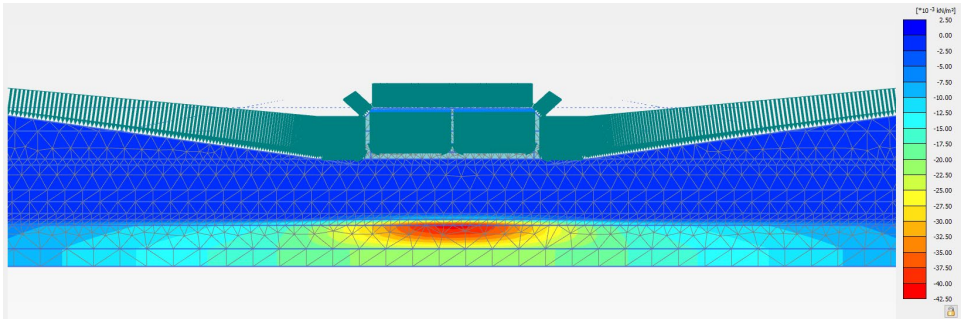

Figure 4.11: Excess pore water pressure under tunnel construction

Phase 4: Sand backfill stage

The greatest magnitude of settlement situated at the backfill next to the immersed tunnel element. The main reason is that the sand backfill is first deposited in the construction site. A cap hardening occurs because FEM model automatically considered the backfill as a loose sand. A high magnitude of settlement is encountered and the sand back deforms because of its weight.

The depth of sand backfill is not a constant value. The thickness of sand backfill is higher next to the tunnel element than right above it. The settlement value of immersed tunnel is relatively low comparing with the soil underneath the sand backfill. The distribution of settlement across the domain is shown as the figure 6.7 below.

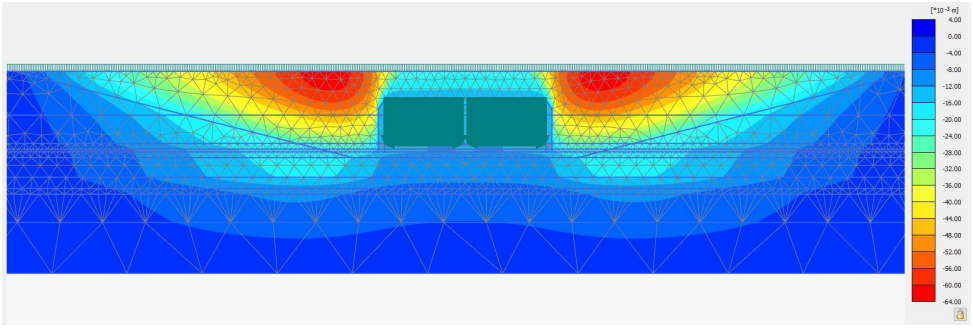

Figure 4.12: Settlement on sand backfill

After 202 days of sand backfill installation, the major proportion of excess pore water pressure

is dissipated effectively. There is only 0.046kPa of excess pore water remains in the soil domain. It is considered as a drained behavior of soil. It is predicted that the increment of settlement is insignificant when there is no additional load applied on the system in the operation stage. The result is shown in figure 5.8.

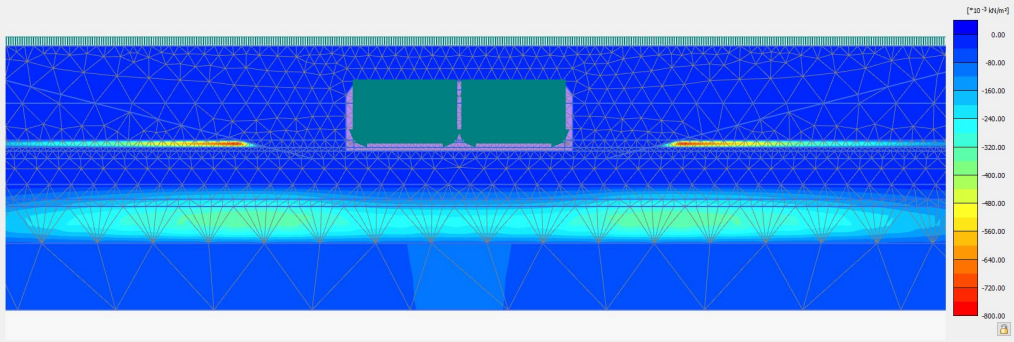

Figure 4.13: The excess pore water pressure during the sand backfill process

Phase 5: Tunnel operation stage for 50 years

The settlement distribution diagram of settlement is shown as below. The value of settlement is higher along the side of tunnel element, but the value is less underneath the tunnel. The settlement is caused by the loading from sand backfill. No additional load is applied on the immersed tunnel during the operation time. Comparing with the monitoring data over the operation period, the result varies linearly and does not match with the result in Plaxis. Hence, further investigation has to be done regarding the additional load applied on the immersed tunnel during the operation time.

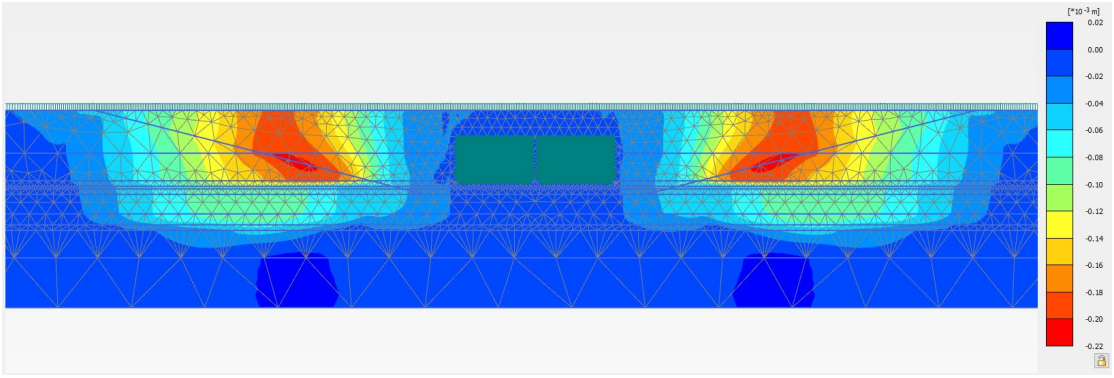

Figure 4.14: Settlement under the service period of 50 years

4.3.2 Settlement results of all tunnel elements

The response of soil under construction activities and tidal impacts are discussed qualitatively in the last chapter, but no exact calculation result is shown previously. Settlement data of immersed tunnel and possible explanations are included in this sub section.

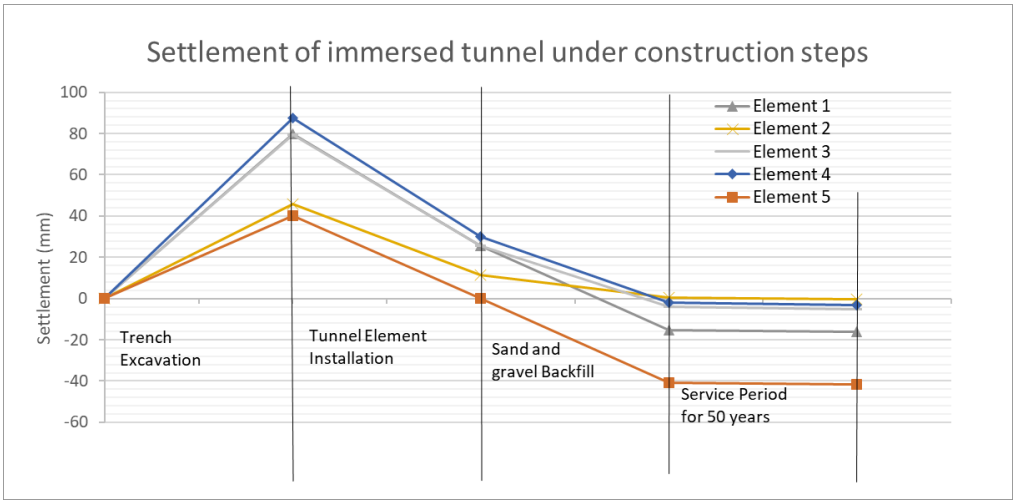

Figure 4.15: Settlement of immersed tunnel element under different time

Settlement results are similar among the 5 immersed tunnel elements. The greatest rebound occurs in the trench excavation process. The volume of soil being excavated and backfilled are different along all 5 tunnel sections. Hence, it is not feasible to make any conclusion on which geological profile has the greatest sensitivity towards the applied load.

The unloading and reloading modulus between sand and over-consolidated clay are similar. Even though the loading conditions are the same under immersed tunnel installation process, the magnitude of settlement is controlled by the elastic response of soil. The composition of soil does not cause a change on the settlement result in element installation.

There is a greater variation of odometer stiffness between sand and normally consolidation soil. Hence, the primary settlement from pre-loading of 10kN/m is closely related to the composition of soil. Among five elements of Heinenoord tunnel, element 3 has the lowest value of the settlement under the pre-loading stage. It is because the thickness of clay and peat layer is smallest among all 5 elements. The settlement is the greatest on the elements that connected with the approaching structure. A higher thickness of clay and peat layers are found in element 1 and 5 than element 2,3 and 4.

4.3.3 Difference between FEM and monitoring result

The long-term settlement analysis has shown that the excess pore water pressure is almost completely dissipated under the first 10 years of tunnel operation. This leads to a neglectable tunnel settlement during the service period. On the other hand, an increasing of settlement is measured over the 50 years of service period. Hence, there is high difference between the monitoring data and Finite Element result.

To illustrate the differences, figures 4.17 and 4.18 indicate the monitoring result along the tunnel alignment and the settlement comparison on tunnel element 1 respectively.

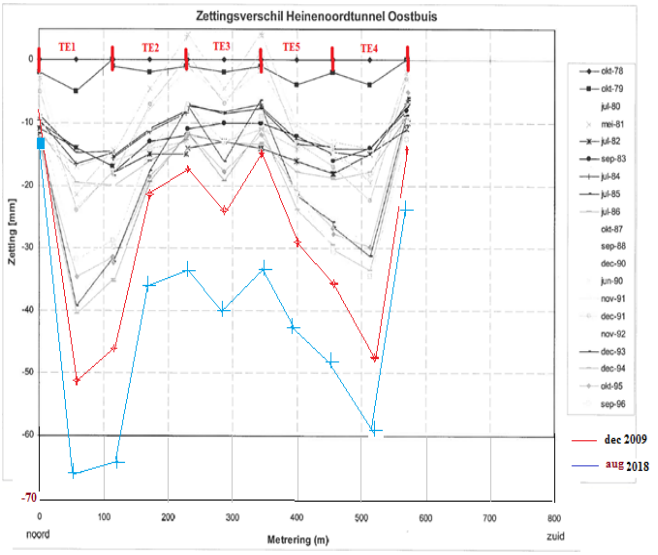

Figure 4.16: Monitoring result of Heinenoord tunnel from 1978 to 2018

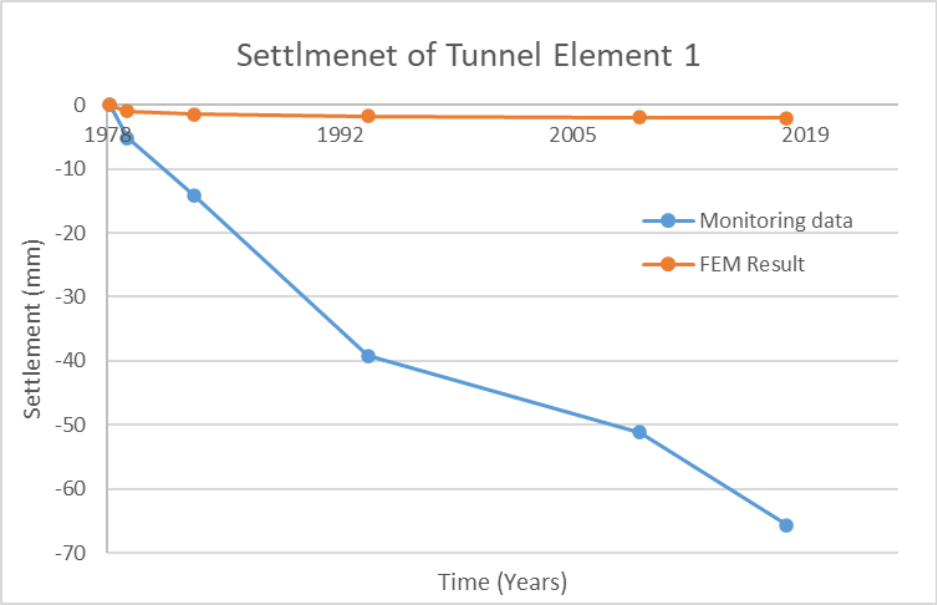

Figure 4.17: Comparison between monitoring data and FEM result

The difference between monitoring data and FEM result increases with time. 67mm settlement is measured in tunnel element 1 between 1979 and 2019, but the calculated result is only 2mm. The Finite Element Model output is inconsistent with the surveying result. Hence, questions arise on validity on loading condition in the modeling stage.

Several simplifications are made in the Plaxis model simulation. To begin with, it is assumed that the traffic load is constant over the service period. The weight of vehicles increases over the past 50 years to improve its performance. The number of cars passing through the Heinenoord tunnel also increase with time of operation. Therefore, the traffic load should be modified in the next section.

Apart from traffic load, the impact of fluvial deposition is not included in the Finite Element Model. The Heinenoord tunnel locates at the harbour of Rotterdam, where is the mouth of Oude Maas River. The slow flow rate enhances the sediment on the immersed tunnel. The Finite Element Model is closer to the actual scenario, when the impact of sedimentation is taken into account.

Finally, the effect of secondary compaction is not considered in the Plaxis simulation. The hardening soil (HS) model can simulation the deformation under unloading, reloading and also the primary compaction. The time dependent response of soil can be determined from consolidation mode. However, HS is unable to capture the secondary compaction. A rough estimation on creeping should be calculated in the next section.

All three factors are investigated on the next section of chapter 5. The impact of each factor is analyzed independently. The results are then compared to figure out which has the greatest influence on the tunnel settlement. Those three factors are applied simultaneously on the tunnel element. Hence, all three impacts are added up and compared with the monitoring data.

4.4 Effects of Traffic load on long-term settlement

4.4.1 Traffic loading estimation

(1) Traffic volume on Heinenoord tunnel

Heinenoord tunnel is one of the intermediate points of highway A29 which connects the north of Netherlands to the south and extended to Belgium. The construction works commenced in 1966 and the tunnel start operating since July 1969. The assumed annual traffic volume of the Heinenoord tunnel is 30,000 per day in design calculation. The traffic volume is 18,000 in 1969 and traffic load has reached the design value 4 years after the construction in 1973. The traffic volume grows linearly and reached 50,000 in 1980. In the year 2010, the number of cars that pass through the tunnel has turned to 125000. There is a 10 percent growth in the past 10 years. Since the traffic load exceeded the design value, a huge differential settlement occurs between tunnel elements and cause joint leakage on the immersion joint.

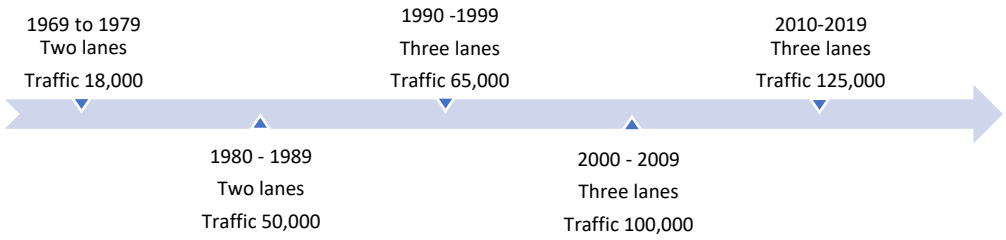

Figure 4.18: Traffic arrangement of Heinenoord tunnel during operation

(2) Traffic arrangement in year 1990

Due to the increasing demand of traffic, the infrastructure department allocated the number of lanes from 4 to 6 in the year 1990. Figure 4.20 has shown a cross section of Heinenoord tunnel before and after the traffic arrangement. The lanes are changed from 1 fast lane, 1 slow lane to 1 fast, 1 slow and 1 average lane.

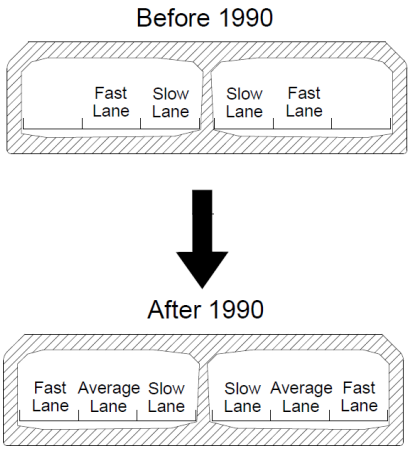

Figure 4.19: The change of traffic arrangement in Heinenoord tunnel

(3) Traffic load estimation

Euro code on traffic load estimation

Euro code EN 1991-2 has provided an approximation on traffic load under different conditions. Load Mode 1 (LM1) consist of the average traffic load of heavy lorries and cars globally. Load Mode 2 (LM2) consist of a specific axle load that act on the short structural member. A more precise approximation is done by Load Mode 1 on Heinenoord tunnel, because the traffic load is applied on the entire tunnel longitudinally rather than a small section. LM 1 comprises of two types of traffic loads. One is axle load on the Tandem System, another is the uniformly distributed load (UDL). The dimension of car and the tandem system is shown as the figure 4.21.

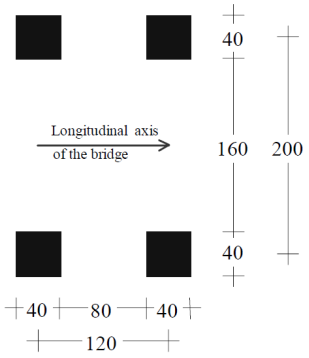

Figure 4.20: The tandem system on Load

The value axle load is different under different types of traffic. 3 main traffic loads are considered in the Tandem system. Notion lane n.1 to 3 represents loads from heavy, average, and normal vehicles respectively. The uniformly distributed load is also applied to the tunnel segment of the immersed tunnel. The load schedule is shown as the table 4.22 below:

Table 4.2: The traffic load schedule from Load Mode 1

Position	Tandem system - Axle load Qik [kN]	Uniformly distributed load qik [kN/m^2]
Notional lane n.1	300	9.0
Notional lane n.2	200	2.5
Notional lane n.3	100	2.5

Conversion of daily traffic volume into UDL

As mentioned in the previous sub section, the daily traffic volume has increased by 6 to 8 time since the first day of operation. The traffic volume cannot be implemented on Plaxis unless it is further converted into point load or uniformly distributed load. Two separate assumptions are made and discussed in this sub section.

Case 1: Traffic volume in peak hour

The traffic volume is not evenly distributed across the day. A huge difference of volume is found between the daytime and midnight. A higher volume of traffic is observed in peak hours. Traffic congestion is possible to occurs in Heinenoord tunnel recently. Cars are packed side by side and form a long queue. Under this extreme circumstance, it is assumed that vehicles are found every 2 meters in the tunnel segment. Figure 4.23 below illustrates the car distribution under traffic congestion.

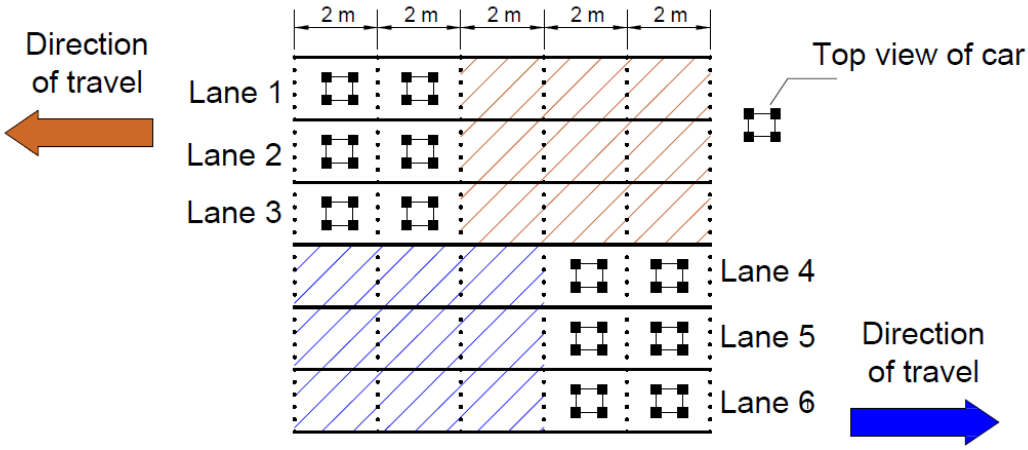

Figure 4.21: The traffic distributed under peak hour

The tandem load applies on the traffic lanes under Load Mode 1 from Eurocode. It is assumed that the point loads of vehicle are distributed uniformly across the entire lane segment ie (2x4.5m). The tandem system of Heinenoord tunnel is different before and after 1990. The lanes expanded from 2 to 3 in both the forward and backward direction. The Notional lanes changes from 1 and 2 to 1, 2, and 3 respectively. The calculation process of the uniformly distributed load is indicated in the Appendix section.

The summary of calculation result is shown as below.

For the two-lane scenario (in each direction):

The uniformly distributed load = 33.43kN/m

For the three-lane scenario (in each direction):

The uniformly distributed load = 48.67kN/m

Case 2: Average traffic volume

In the normal hours, the traffic volume of Heinenoord tunnel is less than peak hour. Traffic congestion is less likely to occur and the separation between cars drops significantly. It is assumed that 100,000 cars pass through the immersed tunnel daily. The distance between each car is approximately equal to 20 m. The figure 4.24 has shown the distribution of vehicles conceptually.

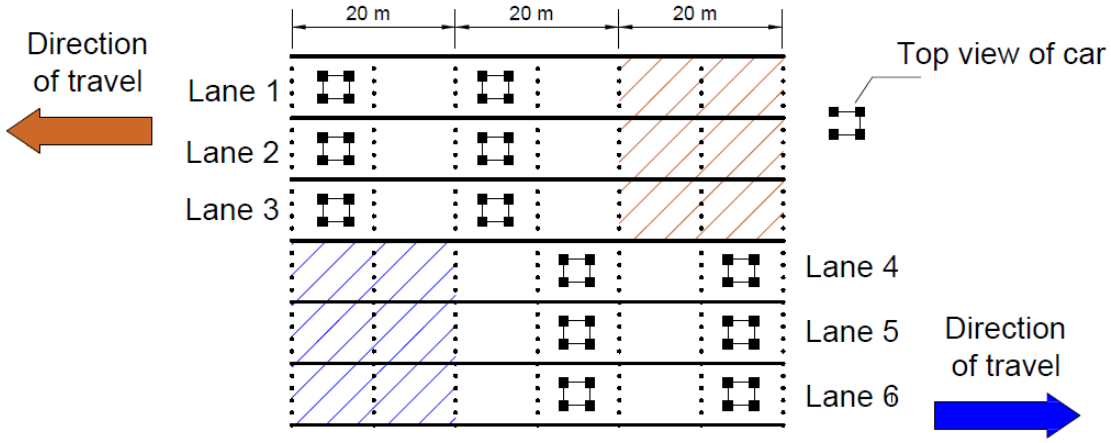

Figure 4.22: Traffic distribution under normal hours

Load mode 1 applied on the Heinenoord tunnel. An assumption is made that the 4-point loads of the vehicle are distributed evenly over the 20x4.5m of tunnel segment. Similar to case 1, the number of lanes expanded from 4 to 6 in the immersed to fulfill the increasing demand of traffic. The details calculation of uniformly distributed load from Tandem load are indicated in the appendix. The traffic load summary is shown as follows:

For the two-lane scenario (in each direction):

The uniformly distributed load = 6.79kN/m

For the three-lane scenario (in each direction):

The uniformly distributed load = 9.11kN/m

4.4.2 Input of traffic load in Plaxis

As mentioned in the previous section, the traffic volume has increased by 6 to 8 times during the operational period. On the other hand, the weight of heavy vehicles and regular cars rose because of the quality improvement. The live load increase with time of operation and cause leakage on the segment joint between Element 1 and 5.

It is assumed that the vehicle load increased by 10 percent per decade. The traffic loads from average and peak hours are analyzed separately in Plaxis. Intermediate calculation steps are taken under consolidation mode and the time interval is 10 years. The impact of changing of lanes in 1990s is also considered in the Finite Element calculation. The load schedule of heavy and average traffic conditions is shown in Table 4.25 below.

Table 4.3: Load schedule on the immersed tunnel

Years of operation	10 Years	20 Years	30 Years	40Years	50 Years
Load under heavy traffic (kN/m)	33.43	36.77	48.67	53.54	58.89
Load under average traffic (kN/m)	6.79	7.47	9.11	10.02	11.02

4.4.3 Traffic loading simulation result

Comparison between monitoring and Finite Element model result is shown as the figure 4.26. A large difference of settlement is determined between average and extreme traffic volume. The settlement under heavy traffic load is about 4 times under normal traffic. Settlement obtained from Plaxis model increases linearly. This matches with the input of the load schedule.

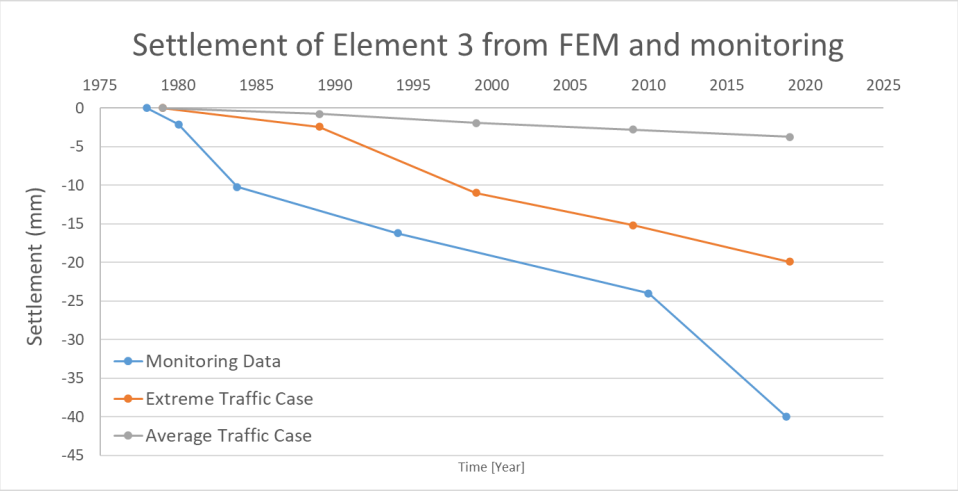

Figure 4.23: Settlement result comparison in Element 3

Monitoring of immersed tunnel started since 1979, that is 10 years after the tunnel is used. A linear relationship of monitoring data is obtained from 1979 to 2008, but the value increased sharply over the past 10 years. The calculated settlement of heavy traffic load matches with monitoring data, but variation become more significant from 2009 to 2019.

One of the possible reasons is that the estimation of loading in Plaxis is different from the exact loading on site. The construction drawing of Heinenoord tunnel only shows the traverse section of concrete element. The exact weight of ballast, pavement and utility is not included. The additional load is roughly approximated as 40kN/m in the Plaxis model. Due to the uncertainty on the applied load, it causes errors on the Finite Element Simulation.

The hardening soil model is controlled by the state parameter pc that is the pre – consolidation stress. The combined loading of tunnel element, transportation and sand backfill is greater than the unloading due to the removal of soil. The increase of pre overburden pressure cause elasto-plastic deformation. The Plaxis result indicated that cap hardening occurs since the sand backfill was applied. Therefore, the stress path is completely elasto-plastic during the 50 years of operation stages. On the other hand, the service load on Heinenoord tunnel cannot be identified. Therefore, the time of cap hardening can occur decades after the tunnel construction. It explains the sudden increase of monitoring settlement between 2010 to 2020. Figure 4.27 has shown the plastic integration point after

10 years of tunnel operation.

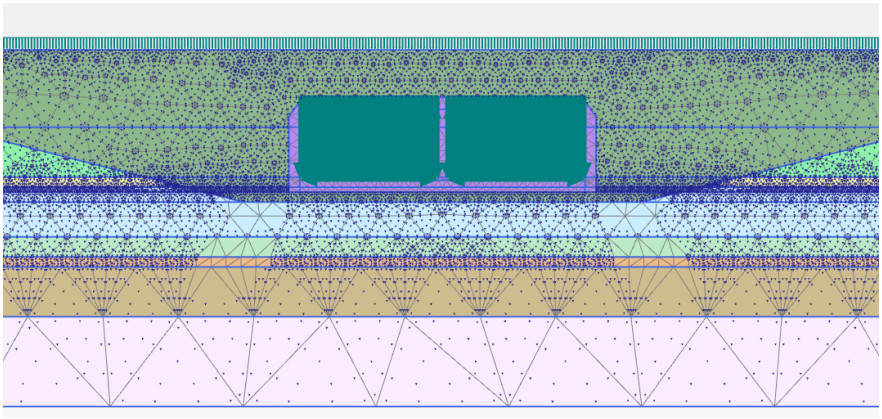

Figure 4.24: Plastic integration point after 10 years of tunnel operation

4.5 Effects of fluvial deposition on long-term settlement

4.5.1 Fluvial deposition loading estimation

Netherlands situated at the Rhine – Maas – Scheldt delta region. Fluvial deposition is significant because of the low flow rate at river downstream. Consistent dredging is required because cargo boat get strands when the river depth is less than water draft of the ship. This causes marine logistic problem in Netherlands.

Heinenoord tunnel located at the Oude Maas River that water flows from the branches of Maas and Rhine River. 11 and 21 percent of the total discharge from Maas and Rhine river flow into the Oude Maas River respectively. The location of the Heinenoord tunnel is shown as figure 4.28 below.

Figure 4.25: Location of the Oude Maas River and Heinenoord tunnel

An approximation is done on the value of sediment in the Rhine estuaries. Ten Brinke (2007) has estimated that the fluvial deposition is 2.5 x 10^9 kg/year in the harbour of Rotterdam. Depth of deposition in Rhine floodplain varies from 0.1 – 9 mm per years. The value of sediment depends on the exact location of the river. The Heinenoord tunnel locates near to the river mouth of the Oude

Maas River. The flow rate is less than the upstream of Waal and Maas River. Alluvium deposition rate is hence estimated as 9 mm per year on the riverbed of Heinenoord tunnel.

The alluvial deposition on Heinenoord tunnel is 9mm per year from the previous section. The total depth of surcharge is 45cm thick over the operational period under a constant value of alluvial deposition. The unit weight of deposition is 19kN/m^3, while the effective weight is 10kN/m^3. The total surcharge is taken as 4.5kN/m across the entire soil domain. To simulate a consistent alluvial deposition, the river deposition load is added gradually throughout the operation period. The load schedule is shown as the figure 4.29 below:

Table 4.4: Loading condition from alluvial deposition

Years of operation	10 Years	20 Years	30 Years	40Years	50 Years
Load from alluvial deposition (kN/m)	0.9	1.8	2.7	3.6	4.5

4.5.2 fluvial deposition simulation result

The increasing load applied on the immersed tunnel that simulates the fluvial deposition in the Oude Maas River. 5 intermediate steps are applied and under consolidation mode. Each step lasts for 10 years. Both calculation and monitoring result of element 3 is shown as the diagram 4.30 below.

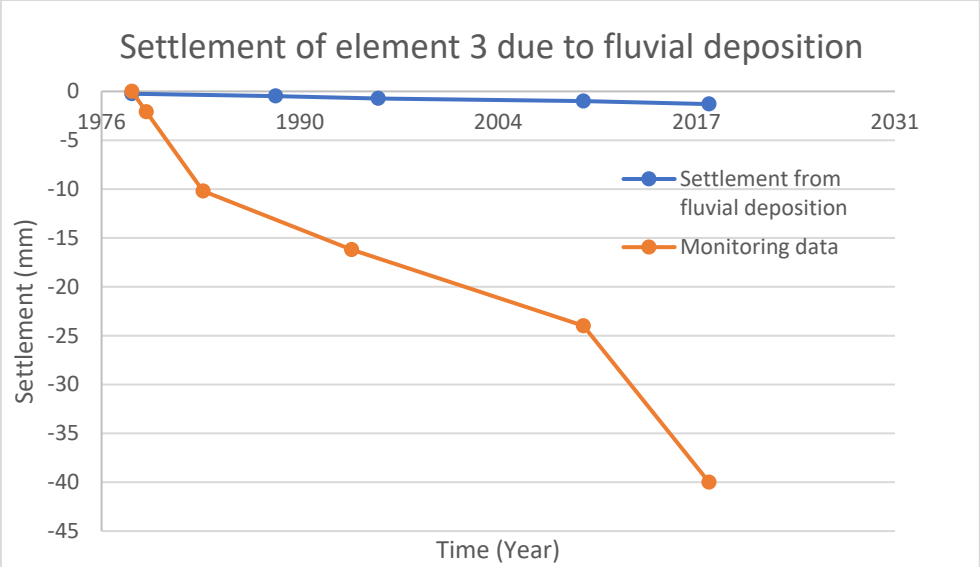

Figure 4.26: Result on settlement from fluvial depostion

Sediment deposition is a continuous process that the thickness increases with time. Fluvial deposition causes a Ko compression on the soil domain. Both monitoring data and Plaxis result has shown a linear relationship of settlement across time. However, the newly formed alluvium only contributed to a twentieth (1/20) of total settlement. It is hence concluded that sedimentation from river causes linear settlement on Heinenoord tunnel, but it is not a significant factor to the monitoring result. Table 4.31 has shown the settlement of element 3 under sedimentation along the Oude Maas River.

Table 4.5: Settlement of element 3 due to fluvial deposition

Years of operation	10 Years	20 Years	30 Years	40 Years	50 Years
Settlement of element 3 from alluvial deposition (mm)	-0.304	-0.626	-0.967	-1.319	-1.681

4.5.3 Conclusion

The estimation of fluvial deposition is conservative along the Oude Maas River. The actual thickness of sedimentation can be several times greater than the input form Plaxis model. However, increasing the deposition by 5 times only causes about 10mm of settlement in the Plaxis model. Hence, the adjustment on fluvial deposition is not sufficient to explain the monitoring result. To conclude, river deposition is not a significant factor to the tunnel settlement.

4.6 Effects of soil creep on long-term settlement

4.6.1 Time dependent behavior of cohesive soil

(1) Odometer result on cohesive soil

The time dependent behavior of cohesive soil is often considered as two types. They are the 1-dimension consolidation and secondary compaction.

In the odometer test, the primary compaction occurs on normally consolidated clay. The increment of load is first turned into increase of excess pore water pressure. Then, the excess pore pressure is dissipated through the drainage boundary of clay. The decrease of pore pressure is equal to the increase of effective stress. The clay sample is compacted until all the excess pore water is dissipated. The additional load induces consolidation settlement of clay.

After the end of primary consolidation (EOP), the secondary compaction begins. The secondary compaction is solely a time dependent behavior. Creep settlement occurs under a constant load. The compaction is due to the realignment of soil particles, rather than the shrinking of void. Figure 4.32 indicates the time dependent behavior of normally consolidated clay under odometer compaction.

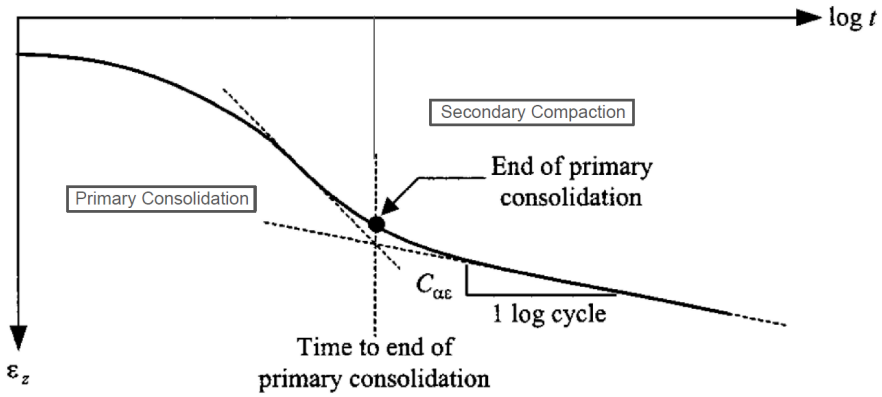

Figure 4.27: The time dependent behavior of NC clay under odometer compaction

(2) Empirical formula on secondary compaction

From the previous figure 5.25, an approximately linear relationship is obtained between the logarithmic time log[t] and vertical strain. The equation of secondary compaction is further written as the equation

$$\varepsilon_z = C_{\alpha\varepsilon} \log(1+\frac{t}{t_i}) \tag{4.7}$$

Where ε_z is the vertical strain of secondary compaction, $C_{\alpha\varepsilon}$ is the coefficient of secondary compaction with respect to axial strain, t_i is the starting time for creeping under a reference time value, t is the time taken since the end of primary compaction.

4.6.2 Estimation on secondary compaction

(1) Simplified geological profile of Heinenoord Tunnel

The geological profiles vary along the tunnel alignment, but an approximately 2m thick of cohesive soil are commonly found under all five elements. The clay layer which is closest to the element contribute most to the creep effect on element. To simplify geological profile, the creep settlement is considered as the secondary compaction of 2 m clay layer. Figure 4.33 illustrates the simplified geological profile on settlement calculation.

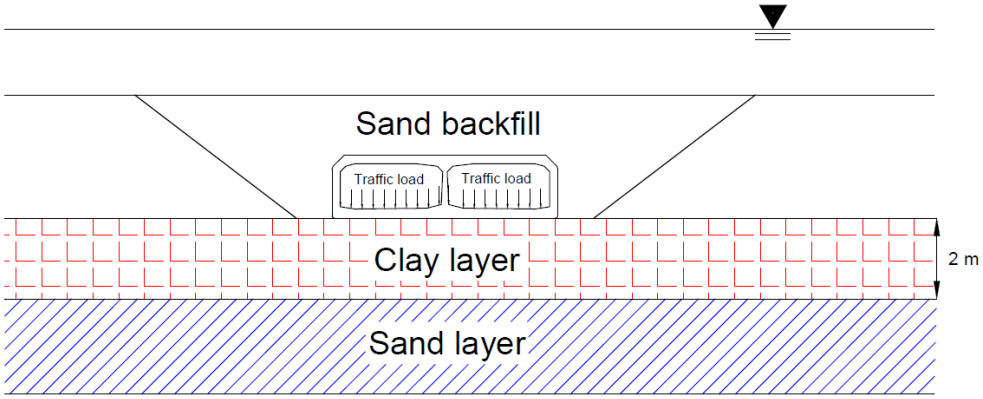

Figure 4.28: Simplified geological profile on creep settlement calculation

(2) Input of parameter in creep calculation

Before calculating the secondary compaction, it is important to determine the creep coefficient and the starting time. In the Heinenoord tunnel project, only field measurement (Cone Penetration Test) is found which cannot be used to determine the coefficient of secondary compaction. An alternative estimation can be done by finding the range of compaction coefficient from previous laboratory result. Research suggested that value of $C\alpha\varepsilon$ is in between 0.004 and 0.008 (Wang, 2020). The range of $C\alpha\varepsilon$ is considered in the calculation. The high, average and low value of $C\alpha\varepsilon$ is input as 0.004, 0.006 and 0.008 respectively.

The starting time of primary and secondary compaction is also considered in the creep calculation. As mentioned in the section 5.4.3, the construction involves unloading and reloading of surcharge. The installation of sand blanket and tunnel element is under the stress path of reloading, while the primary compaction occurs when the sand backfill is added on the trench. Hence, the start

of consolidation is estimated as the first day of sand backfill construction. After the 7 months of installation, nearly all the excess pore water pressure is dissipated which marked an end on primary compaction. Hence, the value t_i is equal to 150 days.

4.6.3 Result on creeping

Figure 4.34 indicate the result of creep settlement on Heinenoord tunnel under a range of . The secondary compaction is estimated in the range of 13 to 28 mm during the 50 years of tunnel operation. Since the monitoring data starts from 1978, the first 10 years of creep settlement is not considered in the result comparison. Creeping contributes between 5.3mm to 10.7mm of total settlement over the monitoring period. The value of creep settlement is still not sufficient to explain the long-term settlement result. Hence, further verification is required in the next section.

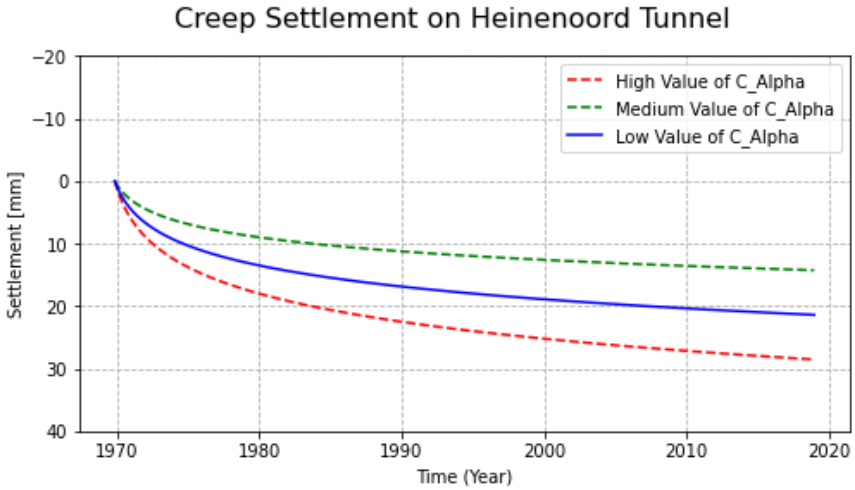

Figure 4.29: Creep settlement result on Heinenoord tunnel

4.7 Summary

The effects of creeping, rise of traffic volume and fluvial deposition are analyzed independently on the Plaxis model. Among all those factors, the rise of traffic volume influences the total settlement the most. The estimation of traffic load is divided into two parts: They are normal traffic volume and extreme traffic volume. The extreme traffic volume contributes 5 times of long-term settlement as the normal one. However, all three results are far less than the leveling result. It is not able to explain the settlement of Heinenoord tunnel on site.

In actual practice, fluvial deposition, increase in traffic load and creep response occurs simultaneously during the operation time. Adding up all three factors can make a more precise judgement on the long-term settlement response. The simulation is hence considered in two ways. The first one is the factor combination under normal traffic condition, another one is under extreme traffic conditions.

4.7.1 Settlement under normal traffic, sedimentation and creep

The impact of normal traffic load is added up with the sedimentation and creep response in this settlement analysis. To make an all-round judgement on the Heinenoord tunnel, the settlement of all 5 elements is analysis over the 50 years of service period. The result is shown as the table 4.35 below.

Table 4.6: The cumulative settlement under the alluvial deposition and normal traffic load

Settlement under normal traffic, secondary compaction and sedimentation					
Years of operation	Element 1	Element 2	Element 3	Element 4	Element 5
10 Years	-20.41	-19.29	-20.81	-20.90	-20.55
20 Years	-25.46	-24.48	-26.08	-26.19	-25.83
30 Years	-29.00	-27.79	-30.00	-30.11	-29.68
40 Years	-31.54	-30.53	-32.81	-32.95	-32.43
50 Years	-33.73	-32.84	-35.26	-35.41	-34.77
Settlement between 1979 – 2019	-13.32	-13.55	-14.46	-14.50	-14.22
Difference between FEM and monitoring data in 2019	44.49	22.75	25.54	32.60	51.38

The table above shows that the total settlement is between 13.32 and 14.50 mm since it open to service. Creeping of soil contributes most to the long-term settlement of Heinenoord tunnel. The impact of traffic and sedimentation only comprise approximately 20 percent of the total settlement. The FEM result is still not sufficient to explain the leveling data along the tunnel alignment. Hence, the extreme traffic condition have to be considered in the next part of the conclusion.

4.7.2 Settlement under extreme traffic, sedimentation and creep

The actual traffic condition lies between traffic jam and fast traffic in Heinenoord tunnel. The fast traffic Finite Element simulation may underestimate the impact of transportation in actual condition. To indicate the significance of traffic volume, Finite Element Model is built under the extreme traffic condition, sedimentation and creeping that is shown as figure 4.36 below.

Table 4.7: The cumulative settlement under the alluvial deposition and extreme traffic load

Extreme Traffic Load Combination + Fluvial + Secondary Compaction					
Years of operation	Element 1	Element 2	Element 3	Element 4	Element 5
10 Years	-31.30	-24.51	-34.67	-34.19	-32.67
20 Years	-38.98	-29.87	-41.60	-41.32	-38.64
30 Years	-38.23	-34.64	-52.93	-51.69	-46.81
40 Years	-55.08	-39.38	-59.07	-56.97	-50.96
50 Years	-61.44	-42.78	-65.29	-62.19	-54.97
Settlement between 1979 – 2019	30.14	18.27	30.62	28.00	22.30
Difference between FEM and monitoring data in 2019	33.58	18.03	9.38	12.00	43.30

The calculated value of settlement is closer to the monitoring data under extreme traffic condition, but the differences exist and is not neglectable in some location. Element 1 and 5, for example, the FEM result is 30 mm less than the monitoring data. The FEM result indicates that the impact of traffic load cannot fully explain the settlement of Heinenoord tunnel under observation method.

4.7.3 Possible reasons on the result difference

One of the possible reasons is the repeating unloading and reloading from tidal fluctuation. Tide is a periodic load that applied on the seabed and foundation soil. The magnitude settlement is the same between high and low tidal conditions under consecutive cycles. Response of soil under tide is elastic in a short period of time. More than 30 thousand cycles of unloading and reloading applied on the tunnel element during 50 years of operation. Increase of stiffness and accumulation of settlement occurs due to the repeating loading. This causes an underestimation on the settlement in model.

Also, stiffness parameter obtained from CPT is a rule of thumb rather than a precise calculation. Empirical formula is used to correlate the odometer stiffness parameter with the tip resistance in the CPT measurement. However, the formula varies under different research. For example, the range of odometer stiffness in clay is in between 4 and 8 times of the cone resistance value. Hence, the field test result cannot provide an accurate prediction on the stiffness parameters.

The variability of soil can also be a significant factor to the discrepancy. Soil is a spatially heterogenous material. The cone resistance value fluctuates along the depth. An average value is obtained by sketching the mean of trend over depth. The result is then converted to the stiffness parameter and input in Plaxis. Finite Element Model simulates the soil behavior as a homogenous material which cannot fully capture the scenario on site. Therefore, it is important to figure out the influence of soil stiffness parameter on the long-term settlement result on Heinenoord tunnel.

To figure out the influence of stiffness parameter, the sensitivity analysis is conducted based on the normal distribution at the last part of the thesis. The value of stiffness parameter is modified, and the settlement is calculated. Then, the settlement result is compared with the monitoring data. This checks whether the variability of soil causes a great difference between leveling and FEM result.

Chapter 5: Daily settlement of immersed tunnel under tidal fluctuation

In this chapter, the methodology and calculation of element settlement is discussed in depth. The coupled flow mode is implemented under a harmonic boundary condition in Plaxis. A further explanation of differential settlement between tunnel element and joint deformation is indicated in the next stage of this subsection. Finally, the comparison between analytical mode and monitoring result is written in this report.

5.1 Model description

5.1.1 Couple flow-deformation model

(1) Background of calculation modes in Plaxis

Plaxis perform Finite Element simulation on soil under different loading and hydraulic boundary conditions. Three calculation modes are used in this research, they are plastic, consolidation and coupled flow type. Before considering the calculation mode in tidal simulation, it is important to understand the purpose and application of each mode.

Both plastic and consolidation mode calculate the soil response under static load, but some differences exist. Plastic mode simulates the behavior of soil within a short construction period. Time is insufficient for cohesive soil to dissipate excess pore water pressure, but sand is under a completely drained response. It is commonly used in deep excavation and soft soil tunnel boring.

In some situations, the cohesive soil is under partially drained or drained over the construction period. For example, surcharge is applied to strengthen the normally consolidated clay in reclamation project. The duration is usually over 2 years that provide sufficient time for clay to dissipated excess pore water pressure. Plastic mode from Plaxis is unable to capture the change of pore pressure in clay under time. Thus, consolidation mode is required the above scenario with the given time and hydraulic conductivity of soil.

Deformation of soil is not only induced by external loads, but also caused by change of hydraulic boundary conditions. Tide causes periodic change of water head on the soil domain which causes compaction and rebound of soil. Plastic and consolidation mode cannot calculate the deformation triggered by water flux. It requires coupled flow and deformation model simulate this scenario, which the mechanism is discussed in the next section.

(2) Governing equation in tidal analysis

In the coupled flow mode, Plaxis solve the Biot's 2D consolidation theory under the change of hydraulic boundary conditions. The time steps are taken in the FEM, while the result of excess pore pressure and settlement is displayed under time. It is important to understand the governing equation before analysis stages are taken.

Biot 2-Dimensional consolidation theory considers two coupled responses of soil, that are the pore water flow in the soil domain and the mechanical response of soil skeleton under load.

In the water flow consideration, Biots combined the equations of continuity and Darcy's law which form a time dependent differential equation. The Hook's law of isotropic elasticity is used to describe the stress strain response of water under change of pressure. The governing equation of water flow is written as:

$$\frac{\mathrm{k}}{\gamma}\nabla^2 p = \frac{n}{K'}\frac{\partial p}{\partial t} + \frac{\partial \varepsilon}{\partial t} \tag{5.1}$$

Where k is the permeability of soil, n is the porosity, K' is the bulk modulus of water, γ is the saturated unit weight of water, p is the pore pressure of soil and ε is the volumetric strain of porous medium.

The formula of volumetric strain is equal to the sum of vertical and horizontal strain. This is shown as:

$$\varepsilon = \left[\frac{\partial u}{\partial x} + \frac{\partial w}{\partial z}\right] \tag{5.2}$$

u is the displacement of soil along x direction, while w is the displacement of soil along the z direction.

In the mechanical response, Hoek's law is the governing equation which simulates the constitutive behavior of soil skeleton. With the implementation of effective stress concept, the spatial dependent of differential equation is written as:

$$\frac{\partial p}{\partial x} = G\left[\nabla^2 u + \frac{1}{1-2v}\frac{\partial \varepsilon}{\partial x}\right] \tag{5.3}$$

$$\frac{\partial p}{\partial z} = G\left[\nabla^2 w + \frac{1}{1-2v}\frac{\partial \varepsilon}{\partial z}\right] \tag{5.4}$$

Where G is the shear modulus of soil, v is Poisson ratio. The relationship between shear and Young's modulus is written as,

$$G = \frac{E}{2(1+v)} \tag{5.5}$$

Plaxis solves the above two coupled equations under a given boundary condition. Pore water pressure and soil settlement is calculated and exported as the output of the Finite Element Model.

5.1.2 Tidal information

In theory, tide causes sinusoidal fluctuation of water level with time. The tidal period is approximately 12 hours, while its amplitude varies under different locations. The information of water level and the coordinates of monitoring point can also be obtained on Rijkwaterstaat website. In the case of Heinenoord tunnel, the closest piezometer locates 4km away from the tunnel alignment, which is shown in the figure 5.1 below.

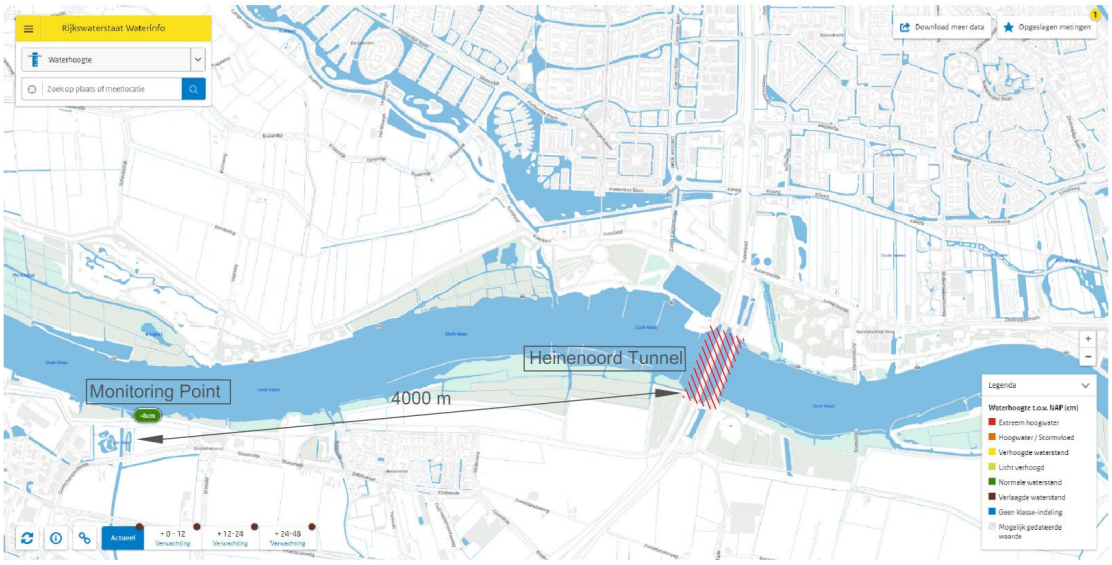

Figure 5.1: The location of Heinenoord tunnel and the monitoring point

Due to the time of concentration, the water level on Heinenoord tunnel is slightly different as the measurement from the piezometer. To simplify the input of hydraulic boundary condition, it is assumed that the water level on site is the same as the monitoring point. A complete set of water head is obtained across the day, while the time interval between each measurement is 30 minutes. Plaxis automatically interpolate the more water level data and generate the water head curve that is shown as figure 5.2 below.

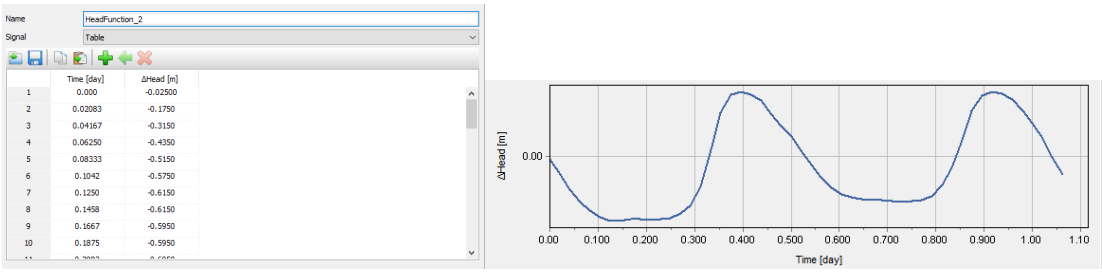

Figure 5.2: The input of water head (left) and the head function applied on Plaxis (right)

The water head data is not under a harmonic function, while the amplitude and period of tide is taken as 0.6m and 0.53 days respectively. The optical fiber sensor measures the immersion joint deformation between 13 and 14 of June 2021. To make a comparison between FEM and monitoring result, the water level of those two days is analyzed in Plaxis. The behavior of foundation soil is also investigated in the next section.

5.1.3 Calculation stages of tidal fluctuation in Plaxis

Tidal fluctuation can be considered as periodic unloading and reloading process on the soil domain. The stress path from tide is elastic and within the double hardening yield contour. In the hardening soil model, elasto - plastic strain occurs when the applied load is greater than the initial stress state of domain.

To simulate the elastic behavior of soil under tide, the additional pre-loading and unloading stage is established. Applying 10kN/m of uniformly distributed load causes a Ko compaction of the soil domain. This increases the initial stress state and causes elastic deformation under coupled flow simulation. Figure 5.3 has shown the traverse domain of tunnel element in the preloading stage.

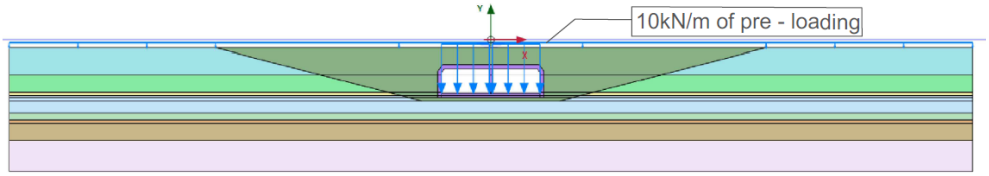

Figure 5.3: The pre-loading stage of soil domain

The pre-loading and unloading of 10kN/m are built under plastic mode. Although the cohesive soil is set as undrained, the condition can be selected as “ignoring the undrained (A) and (B) behavior”. Then, the preloading cause an increase in effective stress, while the excess pore water pressure is maintained as zero. Table 5.4 has shown the steps of tidal simulation in Plaxis 2D.

Table 5.1: The steps of tidal simulation in Plaxis 2D

Steps	Construction Activities	Simulation Mode
6	Pre-Loading of 10 kPa	Plastic (Ignore the Undrained A &B)
7	Unloading of 10 kPa	Plastic (Ignore the Undrained A &B)
8	Tidal Fluctuation Analysis	Coupled Flow

Since the amplitude of tide is around 0.6m, the 10kN/m is sufficient to keep the stress path under elastic contour.

5.1.4 Hydraulic boundary condition

Heinenoord tunnel locates at the Oude Maas River where the changing water level is applied on the riverbed. Therefore, the dynamic water boundary condition is applied on top of the soil domain. Cohesive soil is found beyond the bottom of the Plaxis domain. Water is not able to flow through the bottom boundary. The bottom boundary of soil domain is therefore set as close.

The vertical hydraulic boundary condition involves more complex procedures to determine. Figure 6.1 has shown that Heinenoord tunnel is situated at the straight segment of Oude Maas River. The horizontal length of the domain is about 250m that is a seventh of the straight river segment. Hence, the topography and water head beyond the domain is the same as that in the Plaxis model horizontally. To make judgement on the boundary condition, the excess pore water pressure of the soil domain have to be determined conceptually.

Tide is a periodic change of water level under the period of 0.5 days. Natural sand and backfill has a great hydraulic conductivity which the pore water pressure changes simultaneously with the tidal fluctuations. On the other hand, the permeability of cohesive soil can be 1000 times less than

sand. The period of tide is not sufficient for water to flow in and out of the whole layer of cohesive soil. The surface of cohesive soil is sensitive to tide, but the impact reduces drastically along the depth. There is no influence of tide on the bottom of the clay. Figure 5.5 illustrate the behavior of soil domain under high and low tidal level.

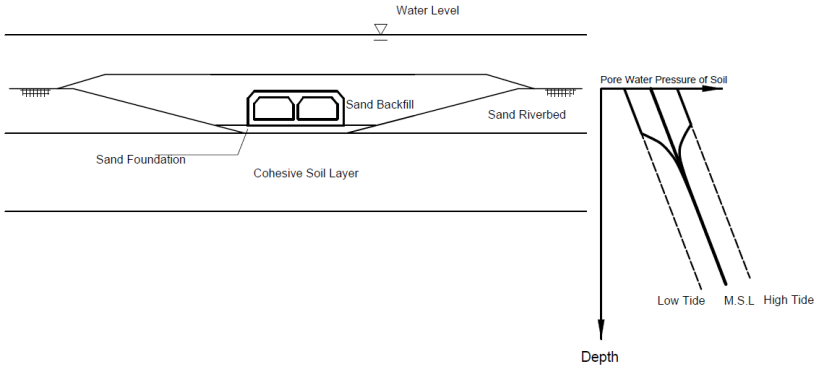

Figure 5.4: The pore water pressure along the soil domain under tide

The pore water pressure of backfill and riverbed follows the changes of water table from tide. Therefore, the water boundary condition of sand riverbed is set as the tidal fluctuation input. While the vertical boundary condition of cohesive soil and soil below is set as seepage. Figure 5.6 illustrates the exact hydraulic boundary condition in the tidal simulation.

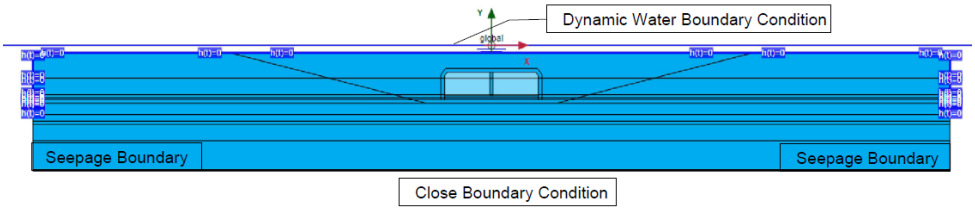

Figure 5.5: The hydraulic boundary condition of the soil domain

5.2 Element Settlement Result analysis

5.2.1 Phase 6: Pre-loading of 10kN/m on the settlement calculation

The uniformly distributed load of 10kN/m is applied to the soil domain. The characteristic of loading is similar to the load from the rise and fall of tide. The aim is manually increasing the cap and the pre-consolidation stress in the hardening soil model. It is also considered as the Ko compaction along the foundation soil. Hence, the settlement is the same throughout the entire domain of the immersed tunnel. The figure 5.7 shows the settlement of tunnel under 10kN/m of pre-loading.

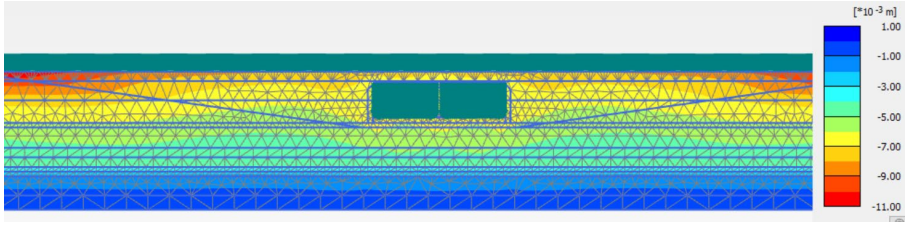

Figure 5.6: Settlement of immersed tunnel under pre-loading condition

Since all the geological unit is set as drained under the plastic mode, no excess pore water is established in the soil domain. The 10kN/m load increment increases the effective stress of every geological unit. However, it cannot conclude whether cap hardening occurs in the pre – loading stage. It can be achieved when the magnitude of rebound is determined from unloading.

5.2.2 Phase 7: Unloading on the 10kN/m on the settlement calculation

An unloading of 10kPa is applied after the preloading on the soil domain. The unloading settlement distribution is shown as the figure below. The magnitude of soil rebound is half of the pre-loading. It is because the unloading of soil is an elastic response, while both elastic and plastic strain occurs simultaneously in the pre-loading condition. Therefore, the initial stress state of the geological unit increases under the pre-loading step in Plaxis.

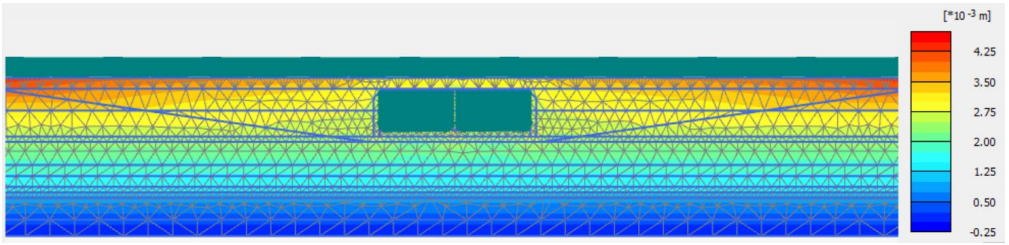

Figure 5.7: The rebounding of soil domain with 10kN/m unloading

Similar to the pre-loading stage, it is set as plastic and drained under the unloading stage. The excess pore water is zero throughout the soil domain. Cap hardening occurs when the pre-overburden stress exceed the initial stress state.

5.2.3 Phase 8: Tidal fluctuation simulation in Plaxis model

Three load cases of immersed tunnel from tide are considered in this section. Those cases are high tidal events, mean water level (0 NAP) and the low tidal events.

Low tidal case

In the low tidal events, a rebound of soil domain occurs in the Plaxis model. It is caused by the reduction of tidal load along the seabed. Due to the short tidal period, the change of pore water pressure in soil is not in phase with the variation of water head from tide. The effective stress is lowered and cause an upward rebound on the entire soil domain. The rebound condition is shown in the figure 5.9 below:

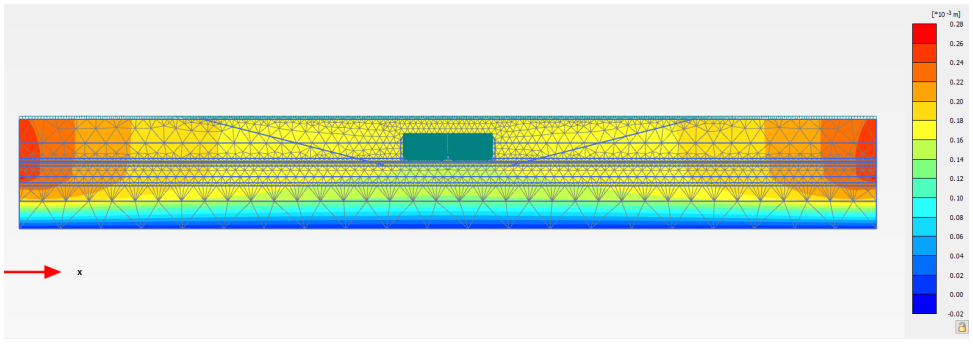

Figure 5.8: The rebound of soil under low tidal condition

The excess pore water distribution is indicated as figure 5.10. The most part of the domain is

under a drained condition except the low permeability layer from -34.0NAP to -38.5NAP. The low permeability zone under a gradual change of excess pore water pressure. Water flux flow out from the top of the low permeability layer (at -34.0NAP) due to the reduction of water level from tide. The flow of water continues. The remaining low permeability layer is under a partial drained condition. The excess pore water pressure at the bottom of low permeable layer is the same as the difference of head from tide (0.5m). This implies that the water flux cannot penetrate through the low permeability layer.

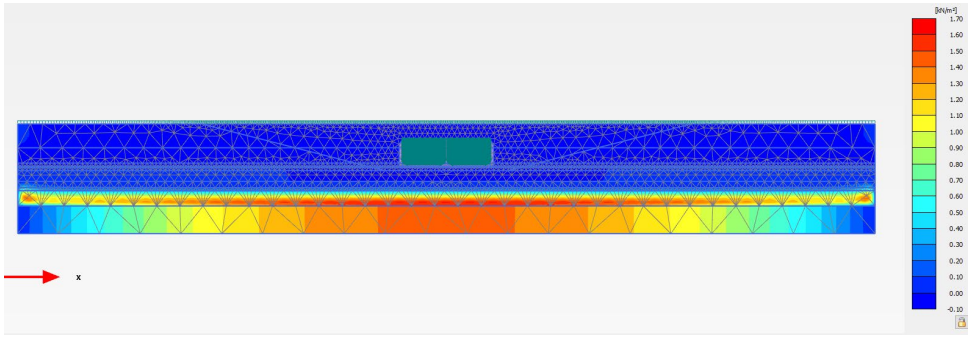

Figure 5.9: Excess pore water pressure due to reduce in tidal level

Average water level

The load applied under average water level condition is same as the operation phase (Phase 5) and unloading (Phase 7). The settlement and excess pore water pressure is zero in theory. Plaxis model revealed that small settlement occurs at the bottom of the immersed tunnel. Although the magnitude of settlement is neglectable comparing with the high tidal condition, it is considered as a source of error from Plaxis calculation.

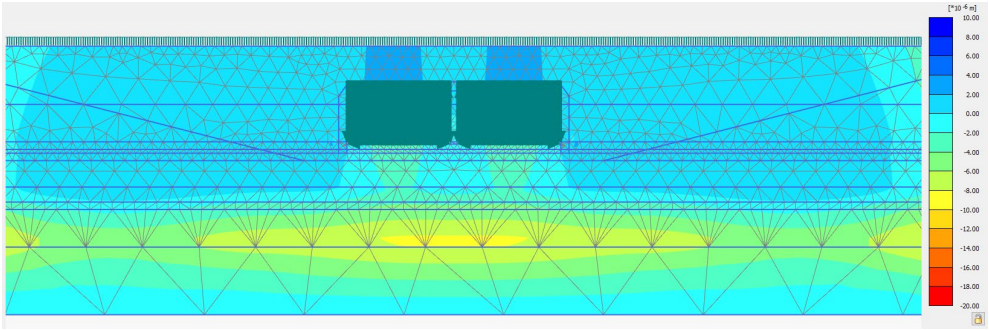

Figure 5.10: Settlement under average water level

The excess water pressure of the soil is shown as the diagram below. The partially drained zone is the same as the low tidal case, but the magnitude is relatively low. The value of excess pore water pressure is acceptable. The reason on the calculation error is indicated as the final part of this section.

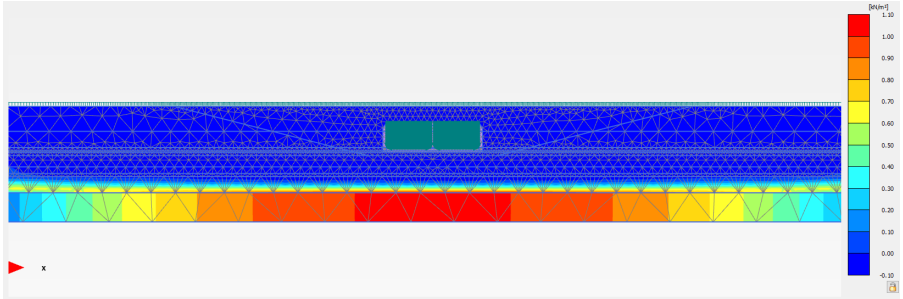

Figure 5.11: Excess pore water pressure under average water level

High tidal case

In the high tidal condition, settlement occurs in the domain and shown in the figure 6.12. The water level rise with a short period of time, the phase difference of excess pore water exists between seabed soil and the soil underneath. This causes settlement on the foundation soil. The loading of tide is considered as Ko condition, settlement occurs along the entire soil domain. The magnitude of settlement under the high tide condition is same as the rebound under low tide condition. This matches with the assumption of elastic response of soil under tidal fluctuation.

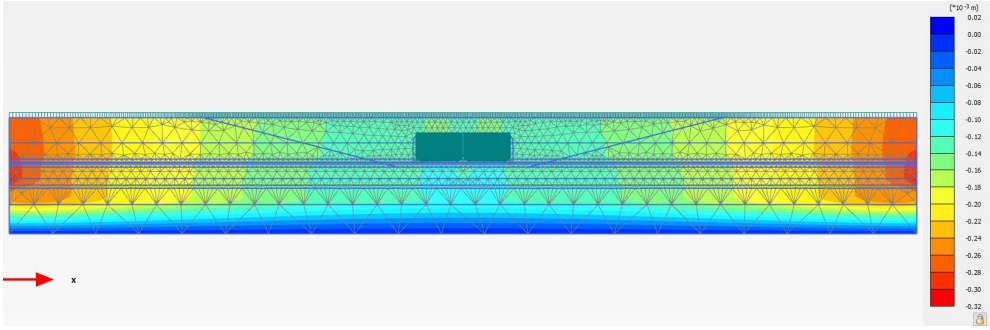

Figure 5.12: Settlement of immersed immersed tunnel under high tide

The result on excess pore water pressure is shown as figure 7.13. The distribution of excess pore water pressure is the same between high and low tidal condition. Under high tidal condition, a delay of excess pore water pressure occurs due to the low permeability of soil from -34.0 to -38.5NAP. The total load increases due to tide, but the water pressure is the same along the low permeability layer. Hence, the undrained compaction occurs. The soil settles due to the increase of effective stress.

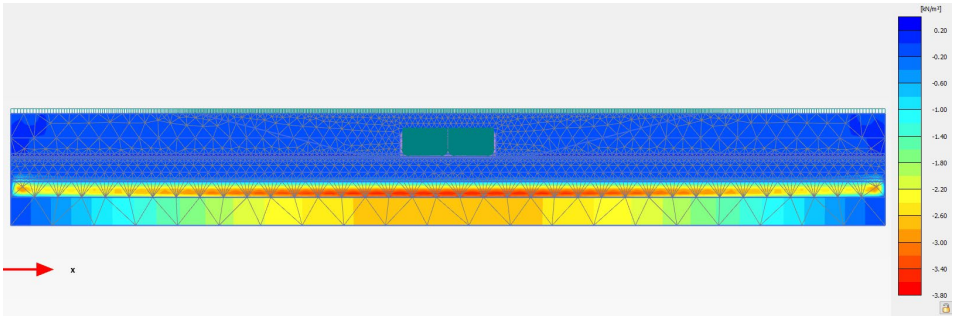

Figure 5.13: Excess pore water pressure of foundation soil under high tide

Behavior of soil under the peak tidal event

Previous section has shown the settlement and excess pore water pressure of soil domain under tidal fluctuations. However, it cannot clearly indicate the compaction of each geological unit and the distribution of pore pressure. To identify the behavior of soil under high tide, two cross sections are made and attached as the figure 6.15 below.

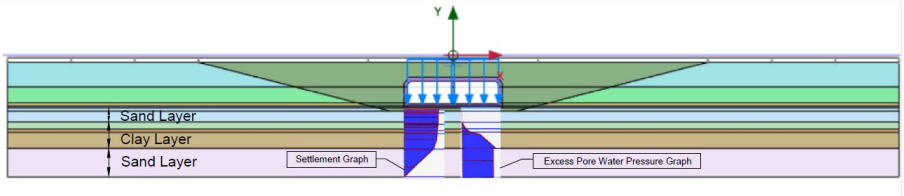

Figure 5.14: Behavior of soil under high tide condition

The above figure shows that the sand lay on top of the cohesive soil, while another sand layer situated underneath the clay layer. The pore water pressure of upper sand synchronizes with the increase water level. Therefore, the effective stress is the same and no compaction is observed on the top sand layer.

The cohesive soil layer has a lower hydraulic conductivity than sand. The cohesive soil layer comprises of three clay zones which act as a semi-impermeable layer under the tidal fluctuation. The top clay is the most sensitive layer to the increase in tide, because the time of concentration is smallest among all three layers. It takes more time for the water to flow into clay layer with greater depth. The water pressure cannot be built up for the cohesive soil under a greater depth. Due to the undrained condition, the net increase in effective stress causes the compaction along the cohesive soil layer.

Although bottom sand is highly permeable, the flow of water is blocked by the cohesive soil and it is considered as undrained condition. The pore pressure of bottom sand is lower that the hydrostatic value under the high-water events. Hence, the increase in overburden pressure causes the rise of effective stress. This causes the greatest value of compaction across the entire soil domain.

To conclude, the sections of excess pore water pressure and compaction have matched with the geo-hydrology response of soil. The greatest compaction occurs at the lowest sand layer which is under a completely undrained condition.

5.2.4 Settlement under a complete tide cycle

Previous section provided an in-depth investigation on the excess pore water of soil under tidal fluctuation. Settlement occurs in high tide condition due to the unsynchronized pore water pressure in soil and water head from tide. The settlement pattern of immersed tunnel under tide is also a concern in this research. The settlement of immersed tunnel across the time is shown as Figure 5.16.

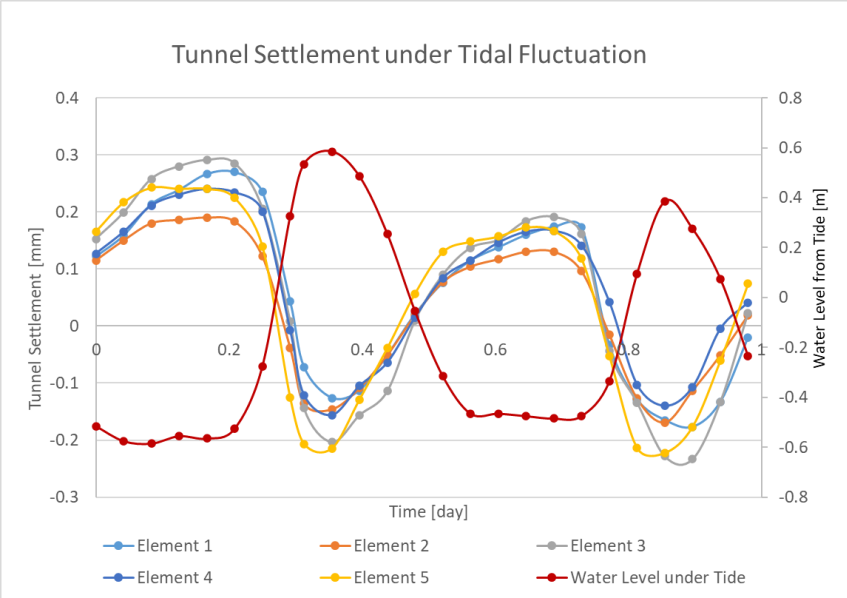

Figure 5.15: Settlement of immersed tunnel under two complete cycles of tide

The settlement of tunnel element is in the opposite phase with the variation of water head from tide. This is because of the low permeability of the cohesive layer. Time is not sufficient for the water to flow into or out of the soil domain.

In the high tidal condition, pore water pressure of cohesive soil and the soil underneath

maintained as the average value. Thus, both the total stress and effective stress increase which causes a settlement of soil domain and immersed tunnel element.

In the low tidal condition, the excess pore water pressure is maintained as average value. But the total stress and the effective stress of soil reduces that causes a rebound on the soil domain and the immersed tunnel.

5.3 Immersion joint deformation analysis

The Heinenoord tunnel consists of 5 elements and 6 immersion joints. There are two types of immersion joints. Figure 5.17 indicate the location along Heinenoord tunnel. The first one connects between the approaching structure and tunnel element (J1 and J6), while the second type connect between tunnel elements (J2 to J5). Since the response of elements and approaching structures behaves differently under tide, Joint 1 and 6 have to be analyzed separately from the remaining immersion joint.

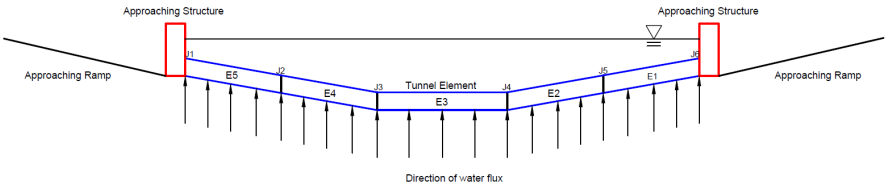

Figure 5.16: Location of immersion joint in Heinenoord tunnel

5.3.1 Joint deformation between elements

Although the tidal load is evenly distributed on the immersed tunnel, the geological response of tunnel elements is slightly different. It is because the composition of soil varies along the tunnel alignment. The difference of soil stiffness causes differential settlement which leads to joint deformation along Heinenoord tunnel.

In the 2-D finite element analysis, a homogenous soil domain is laid under the tunnel element. Tunnel alignment settles unevenly under changes of water table. The joint deformation is calculated as the differential settlement between two adjacent elements. Figure 7.18 illustrates the joint deformation across tunnel element 1 and 2.

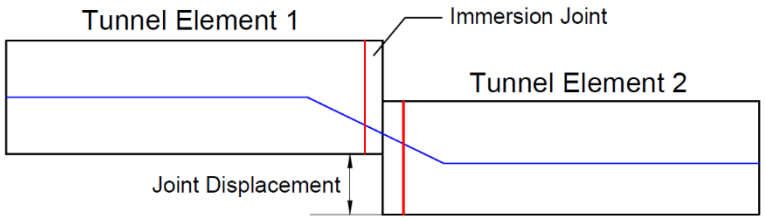

Figure 5.17: The differential settlement across tunnel element 1 and 2

In theory, tunnel elements rise and fall in the same phase under tide. The immersion joint deformation is caused by the differences in tunnel settlement. The greatest joint deformation occurs under the crest and trough of tidal variation. Table 6.19 has shown the peak joint deformation throughout the entire cycle of tide.

Table 5.2: Peak Joint Deformation in Tidal Cycles

Peak joint deformation in the tidal cycles				
Elements	1 to 2	2 to 3	3 to 4	4 to 5
Joint Deformation [mm]	0.113	0.084	0.051	0.061

The maximum joint deformation (0.113 mm) occurs between element 1 and 2 because of a great variation of soil stiffness under the immersed tunnel. The joint deformation between tunnel elements is not sufficient to cause serviceability issue under tidal fluctuations. The joint deformation is the same as relative displacement of elements and less than the settlement of tunnel element. Comparing the result of optical fiber sensor, both the calculated and monitoring has shown an irregular joint deformation under tide. The optical fiber sensor result is in between 0.051 to 0.113 mm which is comparable to the numerical result.

5.3.2 Joint deformation along the end of tunnel

The first and the last tunnel elements are connected to the approaching structure. The approaching structure has a high resistance on loads because it is well supported by piles. On the other hand, the tunnel element situates on the artificial sand foundation which has a weaker support comparing to approaching structure. Hence, tunnel elements are more sensitive to tide than approaching structure. Figure 5.20 illustrates a typical longitudinal section of immersed tunnel.

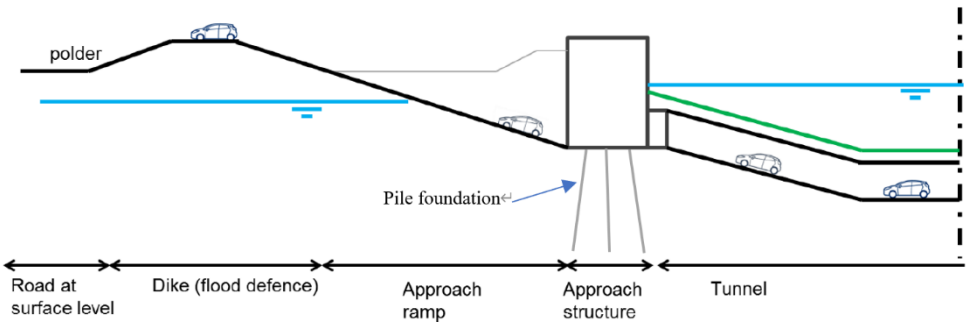

Figure 5.18: The longitudinal section of immersed tunnel and approaching structure

The movement of approaching structure is neglectable comparing with tunnel element and hence assumed as zero in the calculation process. The joint deformation is equal to the fluctuation of tunnel element 1 and 5 under tide. Hence, the result of optical fiber sensor is equal to the settlement variation along tunnel element 1 and 5.

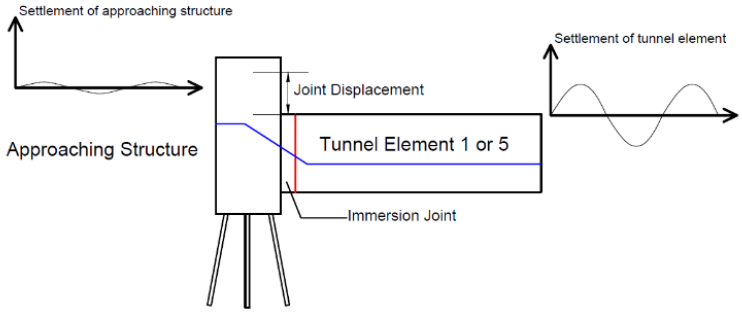

Figure 5.19: Joint displacement between approaching structure and tunnel element

The amplitude of periodic settlement result is in between 0.12 to 0.25 mm that is similar to the value obtained from optical fiber sensor. Figure 6.20 has shown the periodic response of immersion joint deformation at the tunnel ends. The tidal fluctuation is in the opposite phase as the measured and calculated joint deformation. The measured and calculated result is almost the same in Joint 1, but the difference is significant in Joint 6. The variation of observational and calculated result is about 0.2 mm in joint 6. The geological unit is assumed to be homogenous in the Plaxis model, but variability of stiffness parameter exists in field.

To figure out the impact of soil variability, a sensitivity analysis is conducted in the Chapter 8 of the thesis.

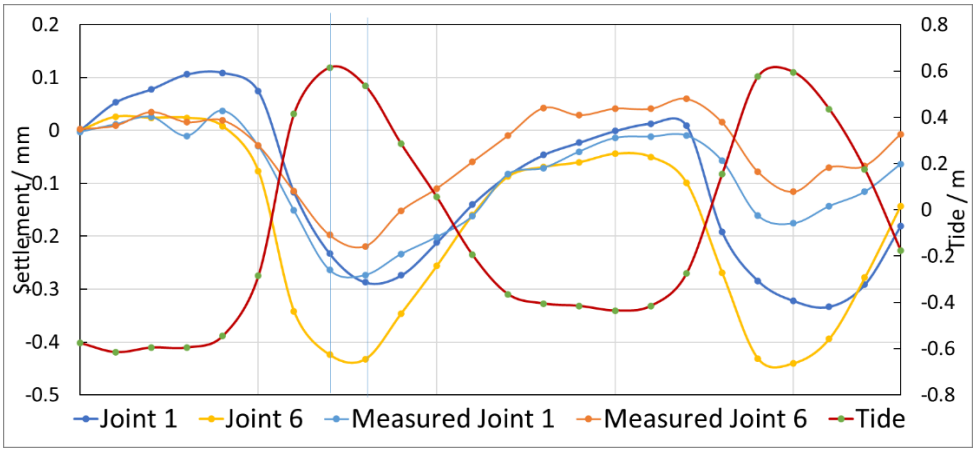

Figure 5.20: Immersion joint deformation between element and approaching structure

5.4 Limitations of the dynamic calculation in Plaxis

The main limitation of dynamic analysis is that the time step in the input function must match with calculation steps. Otherwise, Plaxis will automatically interpolate the result if those two time steps are different. This causes a source of error on the calculation results. Figure 5.23 has shown the differences between input data and output result in Plaxis.

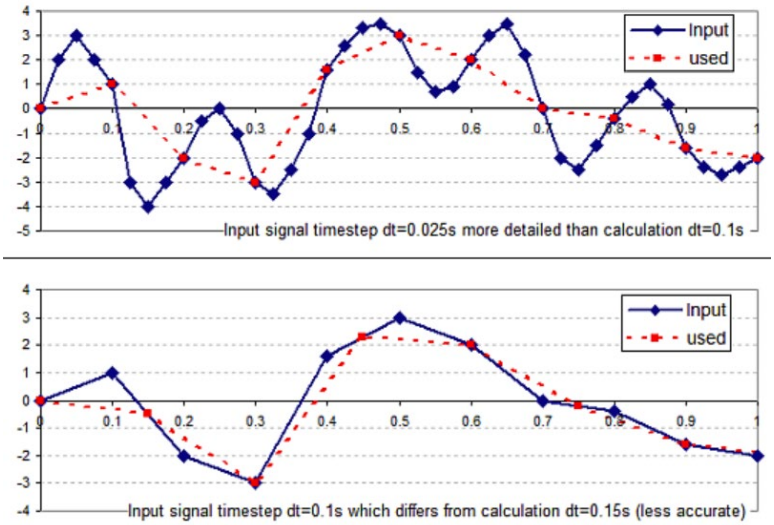

Figure 5.21: The difference between dynamic steps and input signal in Plaxis

To shorten time of calculation, Plaxis uses “line search” method to estimate the best relaxation

value in the model. The initial time step is short, but it relaxes when the calculation result is under an acceptable value. In the tidal simulation, a phase delay of excess pore water pressure and settlement occurs. The input time interval is 30 minutes which is significantly larger than the initial calculation steps. Hence, further testing on the Plaxis model is required.

A testing on the phase delay is conducted on the Plaxis model. A harmonic boundary condition is applied on the soil domain. The input time interval is 30 minutes, while the period is 0.5 days. It is expected that the settlement curve is under the period of 0.5 days and settlement value is zero under the multiple of 0.5 days. The settlement result is attached in the figure 6.22 below.

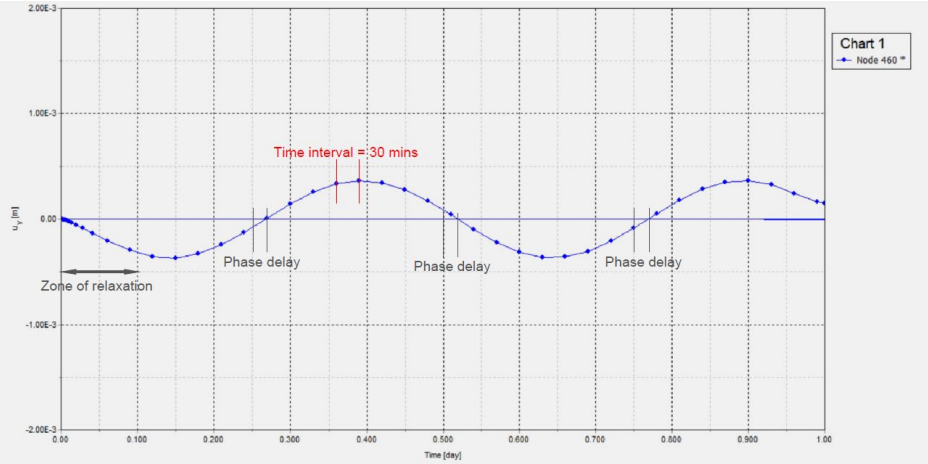

Figure 5.22: Settlement graph under the harmonic water boundary condition

The relaxation occurs in the first 0.1 day of tidal simulation. Then, the time interval become constant and is equal to the input of hydraulic boundary condition. The phase delay is found in the first half cycle and maintain constant throughout the remaining curve of settlement. Therefore, it implies that no further phase delay occurs in the Plaxis model after the relaxation phase.

Based on the above findings, the major source of error is due to the small-time steps in the relaxation phase. Plaxis has automatically interpolated some extra points from the input function to calculate the result, which can be different from the initial input function. While the coupled flow model become stables once the time interval of input is equal to time steps used in Plaxis calculation.

5.5 Summary

With the implementation of coupled flow model, the periodic settlement behavior of tunnel can be simulated under a dynamic water boundary condition. The settlement result is in the same phase of monitoring data, but at the opposite phase with tidal fluctuations. Due to the variation on geological conditions, each tunnel element settles differently under the same value of tidal load.

Considering the geological response of soil domain, time is not sufficient for water to flow into and out the clay layer. The top part of cohesive soil is under a partial drained condition. The pore pressure at bottom of cohesive soil and the sand underneath is totally independent of tidal fluctuation. When the tide rises, the compaction of soil causes settlement of tunnel. The tunnel element rebound when the tidal water level drops.

The variation exists between Finite Element result and monitoring data. Since the stiffness

parameter of soil is determined empirically, the settlement result may not reflect the condition in site. Hence, the influence of soil variability has to be verified in the Chapter 8 of the report.

Finally, the coupled flow mode of Plaxis is not perfect under the dynamic water boundary condition. Errors are encountered in the relaxation phase because the time steps taken is more than the input. Plaxis automatically interpolate more data to calculate the settlement of tunnel element, which can be a source of phase delay in the analysis stage.

Chapter 6: Settlement Analysis of Heinenoord Tunnel in Longitudinal Direction

In this chapter, the settlement of Heinenoord tunnel is calculated in the longitudinal direction. It starts with the model description of the tunnel alignment under Plaxis 2D. The choice of constitutive model, soil and concrete parameter determination are also the focus in this section. Consolidation mode is applied on tunnel construction and operation stages. The tidal response is calculated under coupled flow mode and harmonic water boundary condition. Finally, the result from finite element model is compared with monitoring data.

6.1 Input parameters in the Plaxis model

2 main objectives are discussed in this this section. They are the choice of constitutive model and the selection of strength parameter on the tunnel element, approaching structure and the geological unit.

6.1.1 Soil parameter consideration

The construction stages of Heinenoord tunnel involves trench excavation, tunnel element installation and sand backfill. Comparing with the construction of high-rise building, the load from tunnel element and sand backfill is significantly less because the impact of weight is cancelled by the buoyancy force. Hence, serviceability is a greater issue than the ultimate limit state in tunnel construction. Excessive differential settlement can cause leakage of immersion and dilation joint. It is crucial to choose a constitutive model that can precisely calculate the settlement of tunnel element.

Hardening soil model is chosen in the settlement calculation. 3 stiffness parameters (Eur, Eoed, E50) is considered which represent the stress path of unloading/reloading, odometer compaction and deviatoric loading. A more precise calculation of settlement is determined. The soil parameter is indicated as below:

Table 6.1: Soil parameter input in the Plaxis model

Type	Friction Angle	Cohesion	m	E50[kPa]	Eoed [kPa]	Eur [kPa]	Permeability constant m/d
Sand mixed with clay	25	15	0.7	$70.0x10^3$	$34x10^3$	$350.0x10^3$	$2.00x10^{-2}$
Clay Layer 1	25	10	1	$23.2x10^3$	$11.6x10^3$	$116.0x10^3$	$7.40\ x10^{-3}$
Clay Layer 2	25	10	1	$28.8x10^3$	$14.4x10^3$	$144.3x10^3$	$8.38\ x10^{-3}$
Sand	38	0	0.5	$47.3x10^3$	$47.3x10^3$	$236x10^3$	2.30

Based on the above consideration, the geological profile is shown as the figure below. The yellow, blue and purple zone refers to sand, clay and the mixed graded soil respectively.

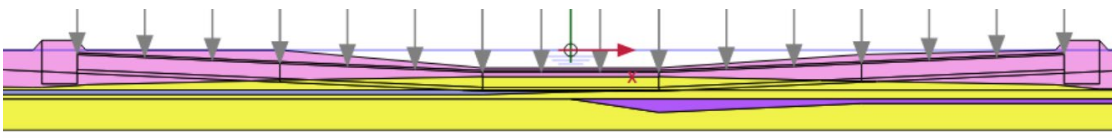

Figure 6.1: Natural ground condition in the Plaxis Model

6.1.2 Input parameter of concrete in the Plaxis model

In the traverse analysis, the concrete can be set as an impermeable layer because water flux can flow through the surrounding soil. Excess pore water pressure is dissipated under consolidation mode. When the water table changes under tide, water flow into/out of the seabed that cause a variation of the pore pressure.

In the longitudinal analysis, the passage of water is blocked when the concrete element is set as a non-porous material. Tunnel element are packed side by side that is shown as figure 6.4. Water can only flow through the approaching ramp which cannot simulate the hydraulic response of soil precisely. To solve this problem, the tunnel element is set as linear elastic, but porous material. The input permeability of tunnel element is the same as the sand backfill. The focus is the response of foundation soil rather than the structural deformation of concrete element. It is hence valid to determine the settlement of tunnel under the above circumstances.

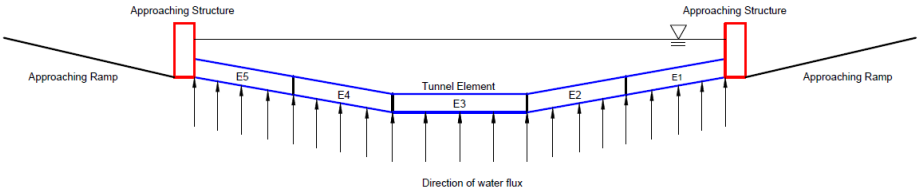

Figure 6.2: The hydralic response of Heneoord tunnel under tide

The approaching structure situates next to the ramp and tunnel element. Since Plaxis simulate the 2-D drainage response of the domain, the excess pore water pressure under the approaching structure can be dissipated through the ramp and tunnel element. The connecting structure can be determined as linear elastic and non – porous material.

Apart from the drainage condition, the unit weight of concrete is also a concern in the longitudinal analysis. The concrete element is input as a solid box rather than a hollow section in the Finite Element Model. The impact of buoyancy cannot be calculated automatically. A further adjustment on the unit weight of concrete is therefore required. To ensure the immersion of element, the total weight of tunnel element and ballast concrete is set as 1.025 of the unit weight of sea water. The installation of utilities, pavement material and finishing also induces an additional weight of tunnel element. The unit weight is risen as 12.5 kN/m^3 in the Plaxis model. The concrete parameter of approaching structure and tunnel element is indicated as table 6.4 below.

Table 6.2: Input parameter of approaching structure and tunnel element

Type	Unit Weight [kN/m^3]	Model Type	Drainage Condition	Stiffness Parameter [Gpa]	Poisson Ratio
Approaching structure	12.5	Linear Elastic	Non - porous	15	0.2
Tunnel Element	12.5	Linear Elastic	Porous	1.5	0.2

6.2 Stages of analysis along longitudinal direction

Heinenoord tunnel consists of 4 main structural components, that are construction of approaching structure, ramp and the tunnel elements. The tidal influence of Heinenoord tunnel is also included in the last stage of the analysis.

6.2.1 Summarize of the construction stages

(1) Natural soil profile in initial stage

The natural soil profile is first set up as the initial stage in the finite element software. The dimension of soil domain is 1100 m wide and 50 m depth which is sufficiently large for the calculation of immersed tunnel.

(2) Approaching structure and ramp installation

Two 280 m long and 12 m depth of ramps are first excavated that provides an access for cars to the Heinenoord tunnel. Approaching structures are built simultaneously which connect ramps with the tunnel elements. There is a significant drop of water table from river side to the entrance/exit ramps. A linear decrease of hydraulic head under the approaching structure that considered as the transition of water table between approaching ramp and river. The exact change of water table is indicated as figure 6.1 below.

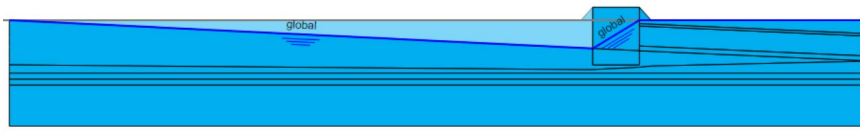

Figure 6.3: The transition of water table under ramp excavation

(3) Tunnel element installation

Before installation of immersed tunnel element, a trench is excavated along the embankment and underneath the river. 115 m wide of embankment is removed by excavator that provides adequate space for the construction of first and last tunnel element. The width of river hence widened by 230 m along the cross section.

The sand foundation is place after the trench excavation that supports the tube and the live load from vehicles. The 115m x 8.5m tunnel element is submerged alternately by flat bottom barge. The tunnel element is not a solid concrete. There is a significant portion of void for vehicles transportation, utility installation and emergency exist. Hence, a reduction of tunnel element stiffness is considered in the Finite Element analysis.

4) Daily response of Heinenoord tunnel

The harmonic water boundary condition is applied on top of the tunnel element. The impact of tide reduces drastically along the dyke and approaching structure. The water head under the approaching structure is set as constant in the flow condition. The water boundary condition is shown as figure 6.6 below.

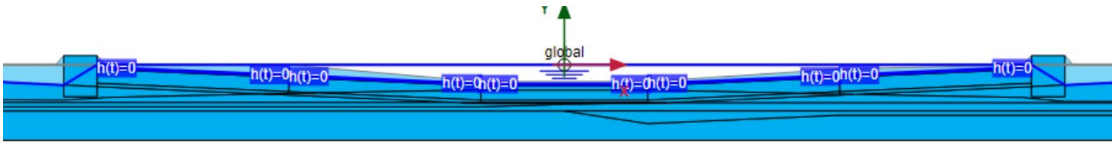

Figure 6.4: Water boundary condition of soil domain under the impact of tide

6.2.2 Calculation Steps in Plaxis

The intermediate steps of Heinenoord tunnel can be sub divided into 3 stages. They are the tunnel construction, operation and settlement analysis under tidal fluctuation. The time schedule of Plaxis is shown as the table below:

Table 6.3: Construction steps of Heinenoord tunnel

0	Ko Natural soil condition
1	Approaching structure and ramp installation (Consolidation mode)
2	Trench excavation (Consolidation mode)
3	Sand foundation installation (Consolidation mode)
4	Installation of 1st tunnel element (Consolidation mode)
5	Installation of 2nd tunnel element (Consolidation mode)
6	Installation of 3rd tunnel element (Consolidation mode)
7	Installation of 5th tunnel element (Consolidation mode)
8	Installation of 4th tunnel element (Consolidation mode)
9	Sand backfill installation (Consolidation mode)
10	Service period (Consolidation)
11	Pre-Loading of 10 kPa (Consolidation)
12	Unloading of 10 kPa (Consolidation)
13	Tidal Fluctuation Analysis (Coupled Flow Model)
Total construction process = 2.5 to 4 years	

6.3 Local result on the longitudinal analysis

Phase 1: Installation of ramps and approaching structure

The deformation of ramp is caused by the lowering of water table and the unloading of surcharge. The steady state reaches under the flow condition of Plaxis 2D. The great rebound of soil is 6.82 cm that located at connection between the ramp and approaching structure. The greatest settlement of 2.50 cm occurs along the coast of the Maas River. Although the 12.5 m depth of soil is excavated at the entrance, the value is still within 10 cm. It is because the unloading/reloading stiffness governed the settlement of tunnel element under hardening soil model. The settlement of approaching ramp is indicated as figure 6.8.

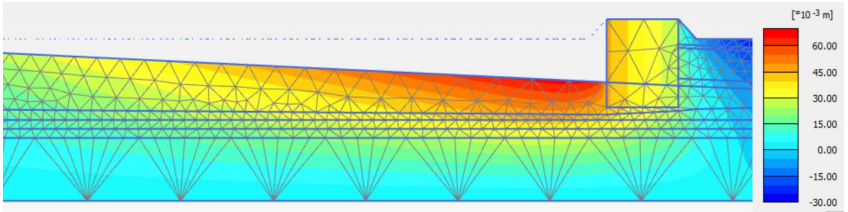

Figure 6.5: Settlement due to the excavation of approaching ramps

In the Plaxis model, positive excess pore water pressure causes the extension of soil, when soil domain reaches steady state. The negative excess pore pressure implies that compaction occurs when it is well dissipated.

The excess pore water pressure is well dissipated in the soil domain during construction. The highest value of excess pore water pressure (0.56kPa) locates at the connection between approaching structure and ramp. Further dissipation of pore water pressure does not cause significant settlement in the next calculation steps. The distribution of excess pore water pressure is shown as figure 6.9.

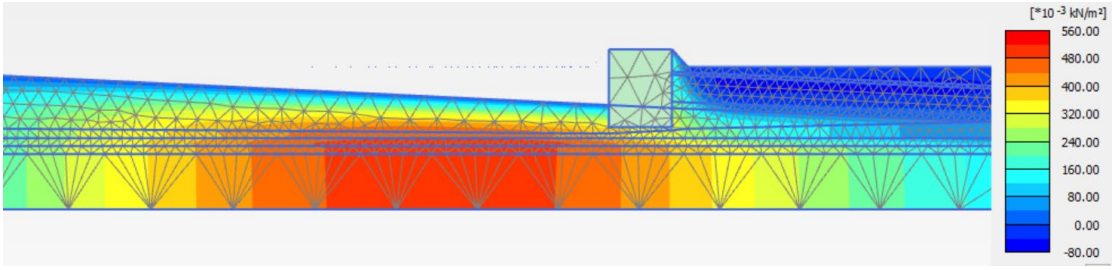

Figure 6.6: The distribution of excess pore water pressure under ramp construction

Phase 2: Trench excavation

The removal of soil induces unloading effect to the Finite Element domain. Higher rebound is found along two sides of longitudinal tunnel. The greatest value unloading displace is 5.6 cm that is 1.5 times greater than the traverse analysis. From section 6.2, the longitudinal analysis provides a more macroscopic view tunnel alignment. The difference of excavation level causes the discrepancy on the soil rebound. Figure 6.10 indicates the soil deformation from trench excavation.

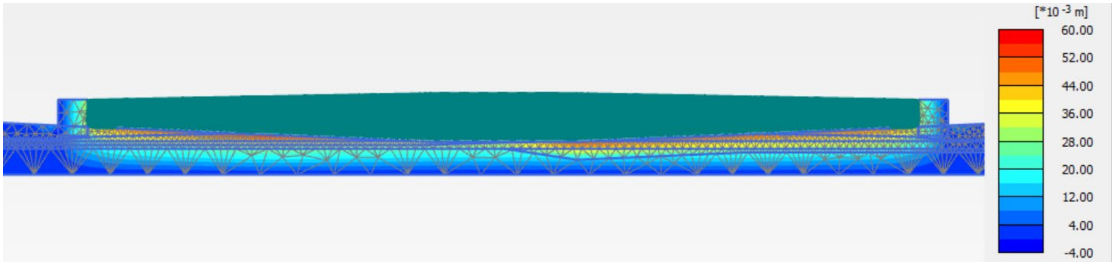

Figure 6.7: Settlement of soil rebound due to trench excavation

The seabed comprises of the mixture of silt and clay which has a high hydraulic conductivity. The excess pore water pressure drains quickly under unloading effect of trench excavation.

The greatest excess pressure of 0.5kPa is found at the clay layer and the cohesionless soil underneath. Although the sand is 100 times more permeable than clay, the flow of water is blocked by the clay layer on top. The sand layer is under a partially drained condition with the time of construction.

The soil domain is heterogenous in terms of geological unit. The variation of soil causes the non-uniform distribution of excess pore water pressure in the domain. Figure 7.10 shows the excess pore water pressure of soil under trench excavation.

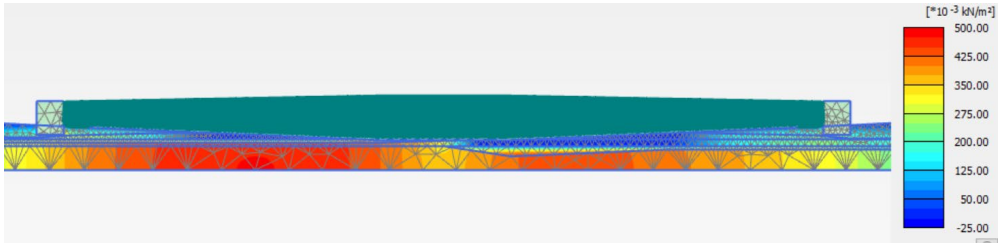

Figure 6.8: Excess pore water pressure distribution under trench excavation

Phase 3: Sand foundation installation

Before the construction of tunnel element, a sand foundation is first established at the bottom of the trench. The thickness of sand foundation is uniform and causes Ko compaction on the foundation soil. The settlement is hence the same and equal to 1.5cm along the tunnel alignment. Distribution of settlement is shown as figure 6.12 below.

The newly formed sand foundation layer contributes most to the settlement. Yielding occurs which causes both elastic and plastic strain of the foundation soil. The natural soil experienced a pre consolidation stress. The incremental load from sand foundation is not large enough to cause hardening on the natural soil. The deformation is less significant in natural soil than the sand foundation. The settlement distribution under sand foundation installation is shown as the figure 6.12 below.

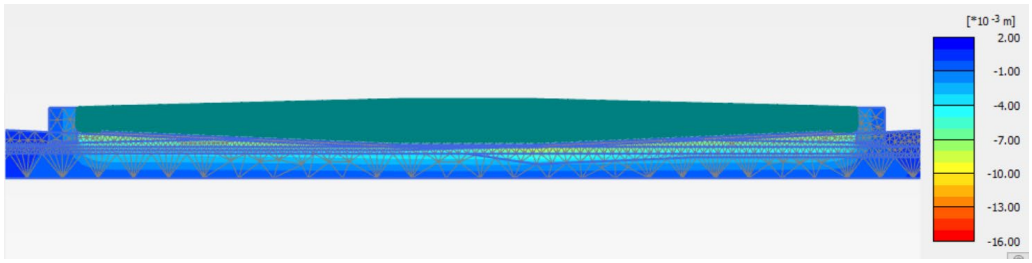

Figure 6.9: Settlement due to sand foundation installation

The loading of sand foundation induces excess pore water pressure on the entire soil domain. The duration of sand foundation installation last for 7 months which provides sufficient time for the drainage of pore pressure. The maximum value of excess pore pressure is 0.46kPa that is not influential to the Finite Element Model. The excess pore water pressure on the soil domain is shown as figure 7.12 below.

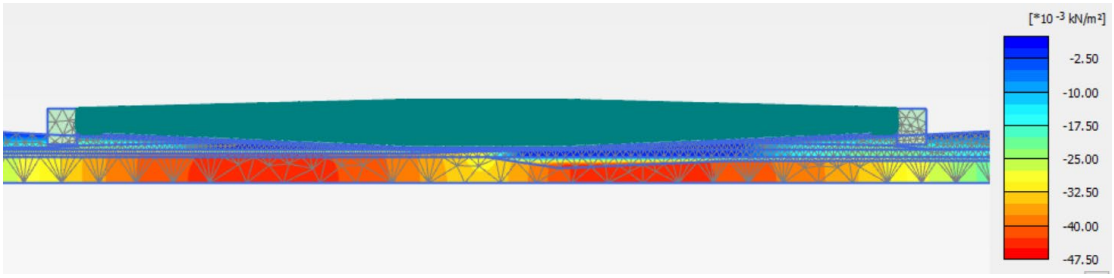

Figure 6.10: Excess pore water pressure under the loading of sand foundation

Phase 4 to 8: Installation of tunnel element

Under the influence on buoyancy force, the net force exerted on the sand foundation is significantly less than the weight of the tunnel element. The value of settlement varies between 1.10 to 1.20 cm because the thickness of cohesive soil is different. The uniformly distributed load from tunnel element

is the same. Thicker cohesive soil contributes more on the tunnel settlement.

Installation of tunnel element also causes settlement on approaching structure and other element nearby. The influence zone of tunnel element is 20m away from the construction area. The longitudinal analysis provides an additional information to the impact of surrounding structure. The first 3 tunnel elements are installed from left to right in the finite element simulation. The end element 5 is laid on the sand foundation before the intermediate 4th element Figure 6.14 to 6.18 indicate the settlement of each tunnel element due to construction.

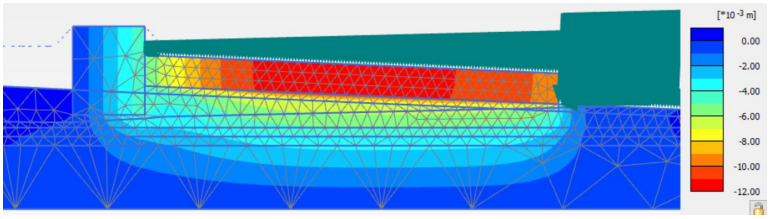

Figure 6.11: Settlement (1.16 cm) due to the installation of tunnel element 1

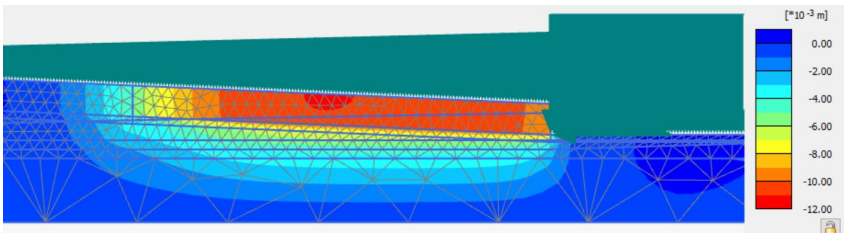

Figure 6.12: Settlement (1.102 cm) due to the installation of tunnel element 2

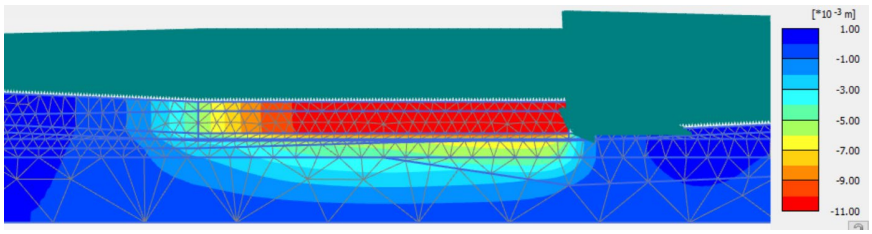

Figure 6.13: Settlement (1.101 cm) due to the installation of tunnel element 3

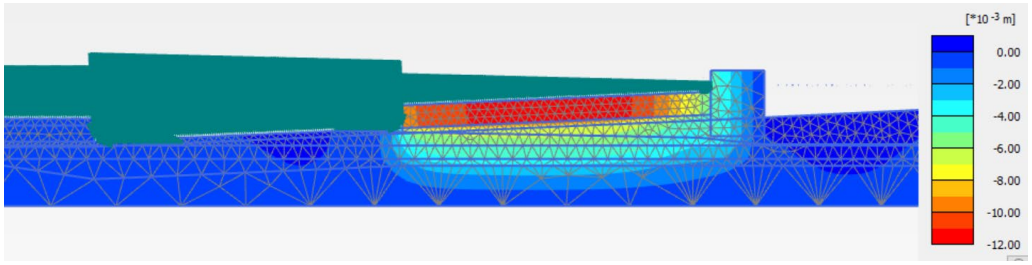

Figure 6.14: Settlement (1.172 cm) due to the installation of tunnel element 5

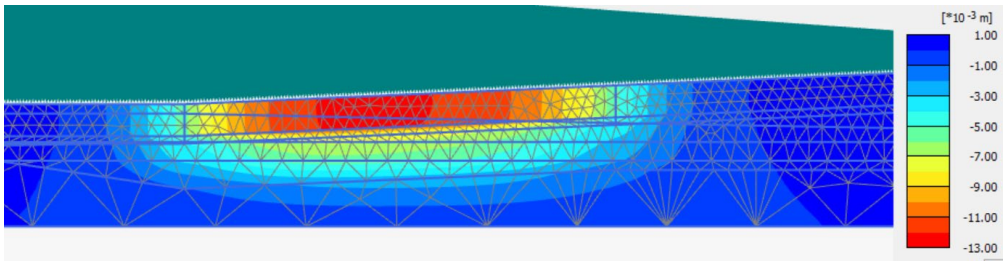

Figure 6.15: Settlement (1.122 cm) due to the installation of tunnel element 4

Apart from settlement induced by tunnel element installation, the magnitude of excess pore water pressure is a concern in the Finite Element analysis. Consolidation of soil is a time dependent behavior. Long-term settlement during the service period can be predicted from the result of excess pore water pressure. The result has shown a negative excess pore water pressure under 0.05kPa. It is expected that a long-term settlement occurs in an insignificant magnitude. Figure 6.19 to 6.23 show the distribution of excess pore pressure of the soil domain.

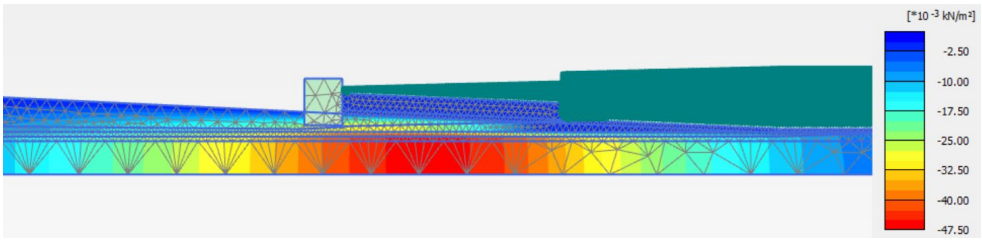

Figure 6.16: Excess pore pressure (0.047kPa) due to installation of tunnel element 1

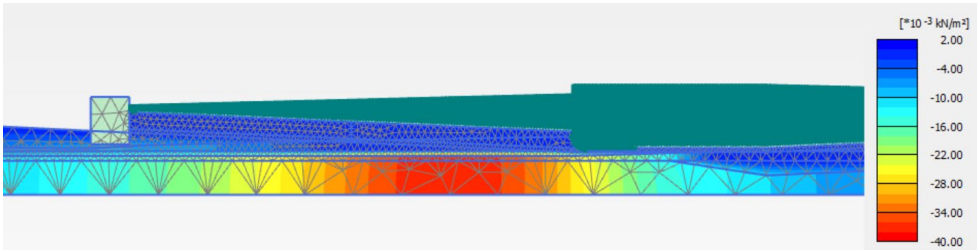

Figure 6.17: Excess pore pressure (0.038kPa) due to installation of tunnel element 2

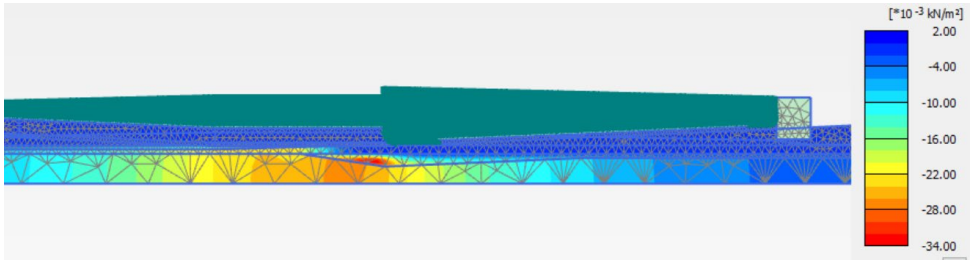

Figure 6.18: Excess pore pressure (0.033kPa) due to installation of tunnel element 3

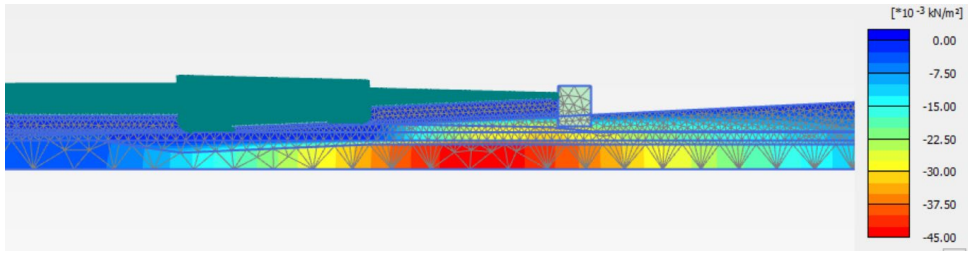

Figure 6.19: Excess pore pressure (0.044kPa) due to installation of tunnel element 5

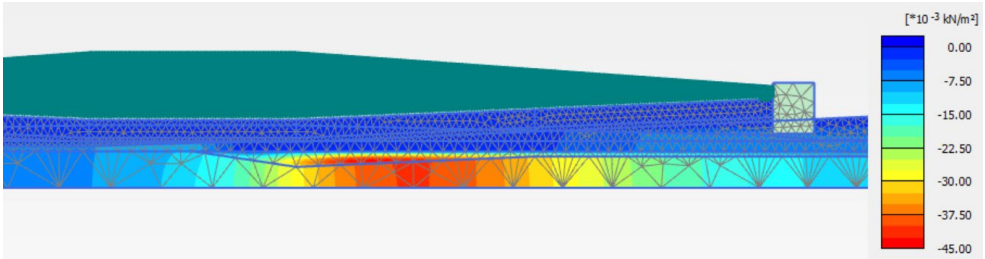

Figure 6.20: Excess pore pressure (0.044kPa) due to installation of tunnel element 4

Phase 9: Installation of sand backfill

Similar to the sand foundation installation, the construction of sand backfills applied a Ko compaction on the tunnel element and soil domain. The maximum settlement of 7.05mm occurs in the newly formed sand backfill. The settlement of tunnel element is equal to 3.1 mm along the longitudinal profile. Figure 6.24 shows the settlement of Heinenoord tunnel due to the installation of sand backfill.

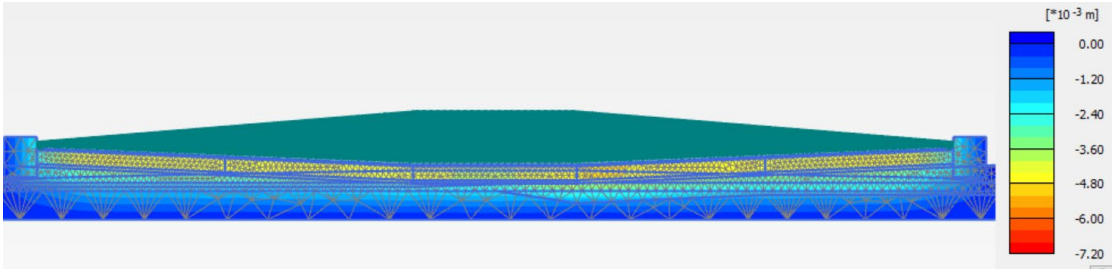

Figure 6.21: The settlement of immersed tunnel due to sand backfill

The uneven distribution of excess pore water pressure is found along the soil domain. This is caused by the heterogenous of the foundation soil. The maximum value of excess pressure is equal to 0.0317kPa that does not induce a great tunnel settlement upon service period. The distribution of excess pore water pressure is shown as figure 6.25 below.

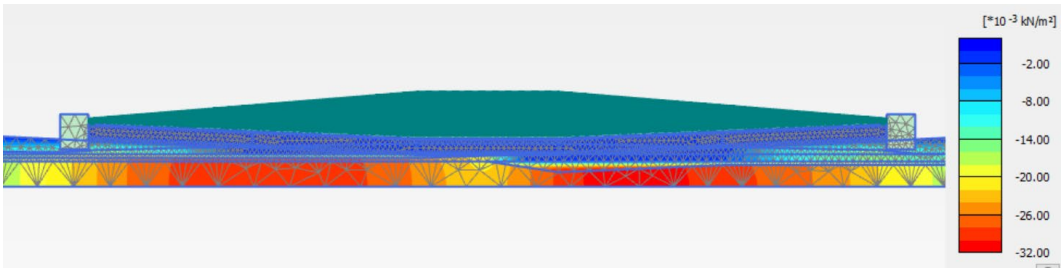

Figure 6.22: The excess pore water distribution

Phase 10: Tunnel settlement during 50 years of operation

From Chapter 5, an increasing load is applied on the Heinenoord tunnel because of the alluvial deposition and rising traffic volume. Since the load increases continuously, a better view is given when the service period is sub divided into 5 sections. A uniformly distributed load increment is added to the Finite Element Model every 10 years. The load schedule is shown as table 6.26 below.

Table 6.4: Load schedule applied to the Finite Element Model

Years of operation	10 Years	20 Years	30 Years	40Years	50 Years
Load under heavy traffic (kN/m)	33.43	36.77	48.67	53.54	58.89
Load from alluvial deposition (kN/m)	0.9	1.8	2.7	3.6	4.5
Total load applied on the tunnel	34.33	38.57	51.37	57.14	63.39

The soil domain is under Ko compaction from the traffic load and fluvial deposition. Since the geological profiles varies along the tunnel alignment, the exact value of tunnel settlement is different. The greater thickness of cohesive soil induces higher sensitivity on settlement under the same loading condition. The increase of traffic load also induce impact on the approaching structure. Figure 6.27

indicates the settlement of soil after 10 years of tunnel operation.

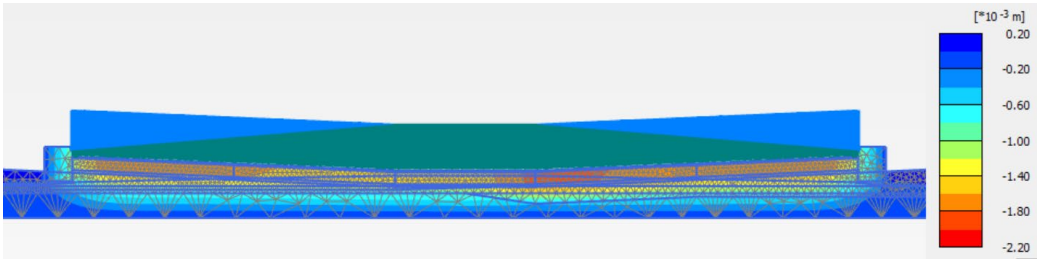

Figure 6.23: Settlement of Heinenoord tunnel after 10 years of operation

Apart from tunnel settlement of Heinenoord tunnel, the distribution of excess pore water pressure is a concern in this sub section. The consolidation mode is applied with the time interval of 10 years. The distribution of excess pore pressure is shown as figure 6.28 below. The increment of traffic load is 34.44kN/m, but the undissipated pore water pressure is in the magnitude of 10^{-3} kPa. The value of settlement converged in the first 10 years of tunnel operation. The monitoring result has shown a linear increase of settlement from 1969 to 2021. Thus, consolidation under a constant incremental load does not cause a continuous settlement of Heinenoord tunnel.

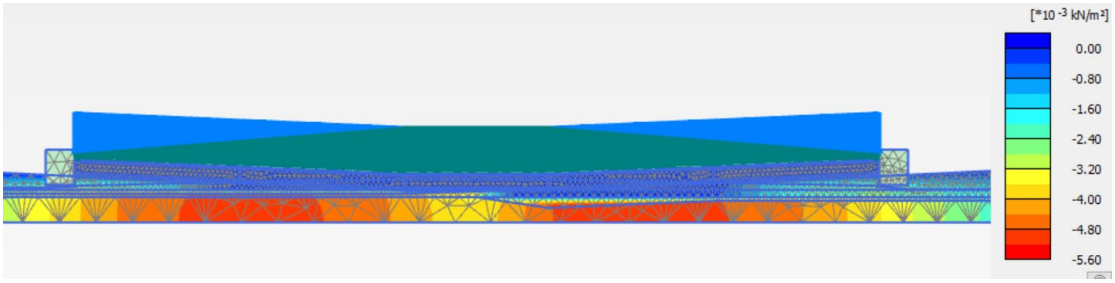

Figure 6.24: Excess pore water pressure of Heinenoord tunnel after 10 years of operation

The distribution of excess pore water pressure and settlement is the similar in the remaining sub steps. Hence, distribution graphs of the ongoing 40 years are not included in this report. To compare the settlement of tunnel element, a deformation – time graph is plot as figure 6.29 below.

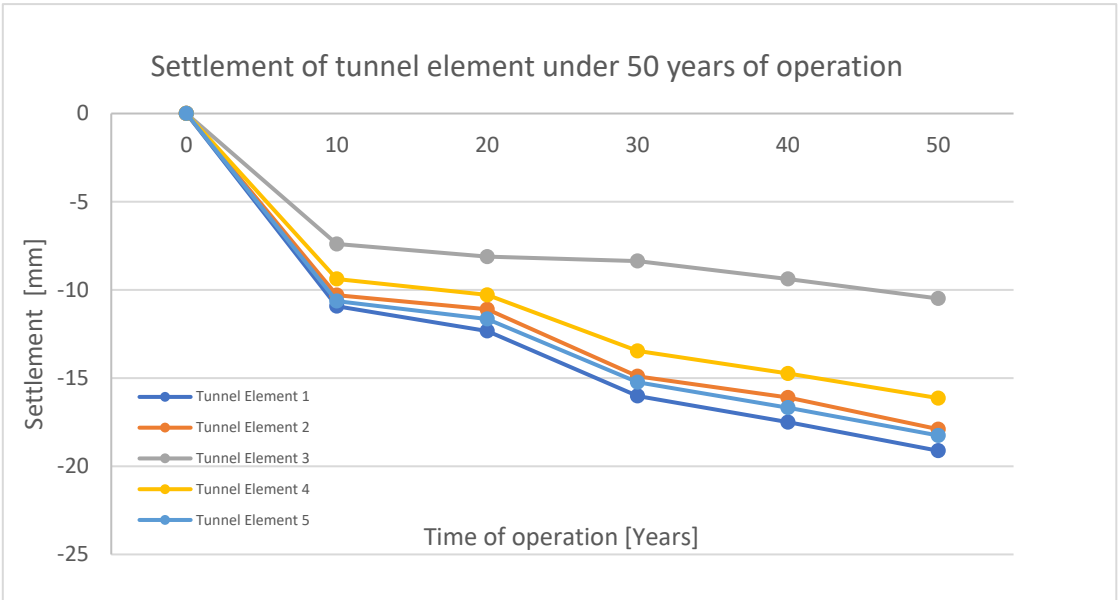

Figure 6.25: Settlement graph of tunnel element over the past 50 years of operation

The value of settlement varies between -10 to -18 mm under the 50 years of tunnel operation. The thickness of cohesive soil underneath element 3 is the smallest which is the half of element 5. Settlement of element 5 and 4 are the highest along the tunnel alignment. Although a huge variation exists between monitoring data and finite element result, the order of calculation result in different tunnel elements has matched with the data from observation method.

Various assumptions are made in both longitudinal and traverse Finite Element simulation, it is difficult to conclude which method is more precise than the others. However, the consistency of traverse and longitudinal analysis can still be verified. Both Finite Element Model has shown a linear tunnel settlement across time. The discrepancy of settlement is under 5mm in tunnel element 5, but 8mm in element 3. This is due to the high variability of geological profile under tunnel element 3. In the traverse analysis, a single bored hole is selected that cannot reflect the actual ground condition under element 3. Hence, longitudinal analysis gives more precise calculation on the settlement calculation.

Phase 11 and 12: Preloading and unloading of 10kN/m

The preloading and unloading of 10kN/m can increase the pre – overburden pressure and expand the yield contour of the soil domain. The stress path of tidal fluctuation can remain within the yield contour and cause an elastic response. The pre-loading and unloading steps do not exist in reality, but it is a necessary process to simulate an elastic tidal response on Heinenoord tunnel.

Figure 6.30 and 6.31 have shown the settlement of Heinenoord tunnel under loading and unloading of 10kN/m respectively. The maximum settlement is 3.73 mm in phase 11, while the greatest value of rebound is 3.58 mm. This indicates that only 4 percent of settlement is plastic and the yield contour expands in a trivial amount.

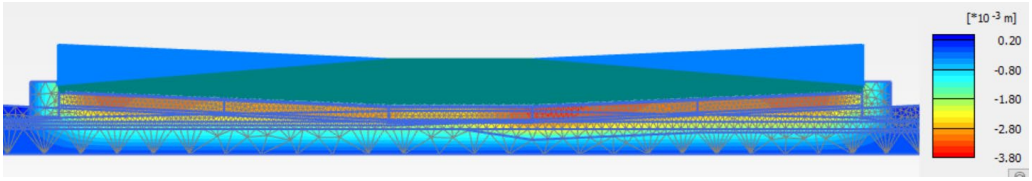

Figure 6.26: Settlement of Heinenoord t6nnel under loading of 10kN/m

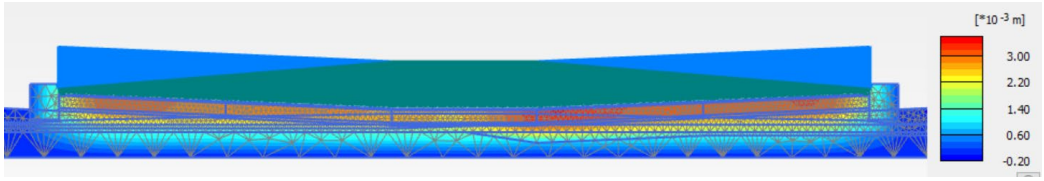

Figure 6.27: Rebound of Heinenoord tunnel under reloading of 10kN/m

To ensure the excess pore water pressure is well dissipated, the time interval is taken as 50 years under the consolidation mode. The excess pore pressure across the domain has shown as figure 7.32 below.

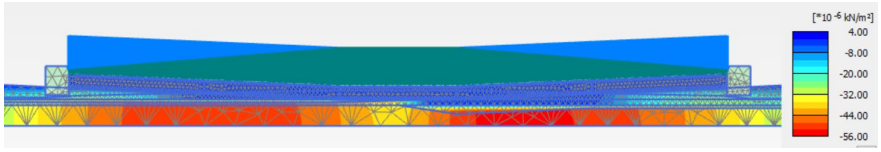

Figure 6.28: The excess pore water pressure of soil domain in phase 11

The maximum value of excess pressure is in the order of 10^{-5} kPa. The pre overburden pressure is equal to the current stress state in phase 11.

Phase 13.1: Impact of tidal fluctuation (Peak water level)

A periodic boundary condition is applied on top of the immersed tunnel element. The period of tide is 12 hours and the amplitude is 0.6m. In the high tidal events, the water head rises and the flux flows into the soil domain. The pore water pressure in cohesive soil cannot be in phase with the change of water head. The net increase of effective stress cause Ko compaction on the element 2, 3 and 4 that locate in the middle of Heinenoord tunnel.

The same hydraulic boundary condition also applied on the first and last tunnel element. However, the water level near the approaching structure and ramp is hydrostatic and constant with time. When the water table rise along the river, the soil underneath tunnel element 1 and 5 is subjected to a deviatoric stress. The deformation mechanism at the end of tunnel is different from element 2, 3 and 4.

The value of settlement under high tidal event is shown as the figure 8.33 below. The maximum settlement -0.193mm that locates at both ends of the tunnel. The greatest value of extension (0.28mm) is found at entrance of approaching structure. The settlement found in element 2, 3 and 4 varies between -0.054 to -0.032mm, because of the difference in loading stage.

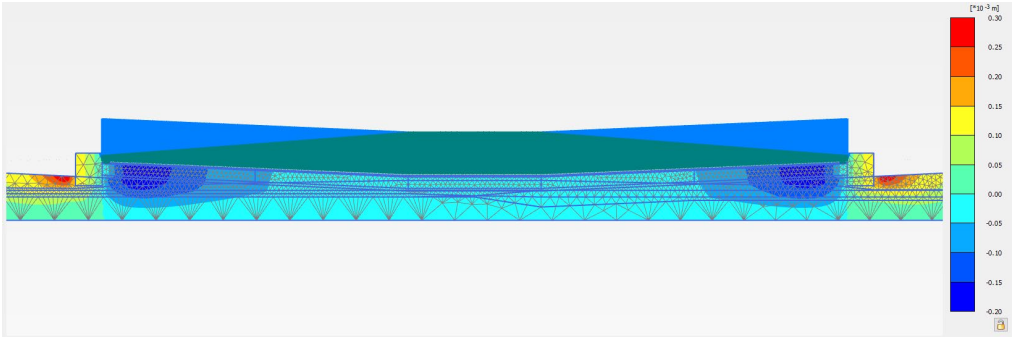

Figure 6.29: Settlement of immersed tunnel under the crest of the tide

Under the high tidal event, the sign of excess pore water pressure is with reference to the current water level. When the pore pressure of soil is less than the hydrostatic pressure, a negative sign is shown as the Plaxis model. The phase delay of water pressure in the soil underneath Heinenoord tunnel induce a negative excess pore water in the domain. Hence, it causes a compression along the longitudinal tunnel alignment.

On the other hand, the water level is kept constant on the approaching structure and ramps. The water flux flow from the river to the soil under the approaching structure. Pore pressure of soil under the ramp is higher than the hydrostatic pressure. Thus, a positive excess is found that causes an extension along the approaching ramp.

The distribution of excess pore water pressure is shown as figure 6.34 below. The greatest value of excess pressure (1.159kPa) locates at the entrance and exit of the Heinenoord tunnel. The minimum value is -0.324kPa along the tunnel element.

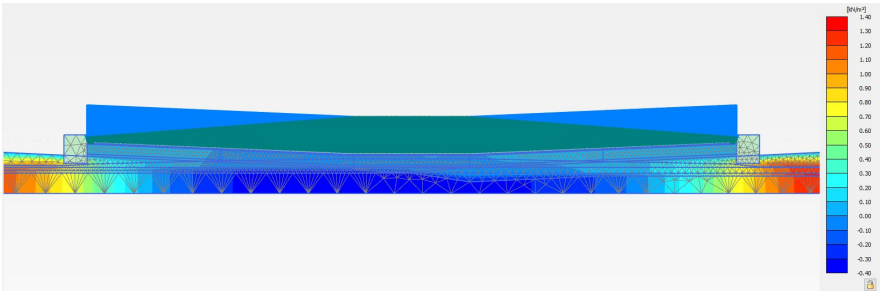

Figure 6.30: Excess pore water pressure of Heinenoord tunnel under tide

Phase 13.2: Impact of tidal fluctuation (Mean water level)

The water level reaches the average value when the time interval is input as 0.333 day in the coupled flow model. The figure 7.35 indicates the settlement of Heinenoord tunnel under the mean water level. In theory, the response of soil domain is elastic under the impact of tide. The settlement across the entire soil domain returns to zero when it reaches the mean water level. The numerical modeling result has shown a significant reduction of settlement along the tunnel alignment. The peak settlement is 4.6 $x10^{-3}$mm that locates at tunnel element 1 and 5. A localized peak extension, 16.5 $x10^{-3}$mm, is found at the entrance and exist of the Heinenoord tunnel.

Similar to the Finite Difference Method, coupled flow analysis starts with the change of water boundary condition. The variation of water level triggers the flow of water flux and causes settlement of the immersed tunnel. The Mean Water Level occurs at 0.333 days from the tidal record. The selected water level is slightly earlier than 0.3333 days that causes a delay of settlement in the Finite Element Model. Thus, settlement still exist when the time interval is chosen as the Mean Water Level in the Plaxis Model.

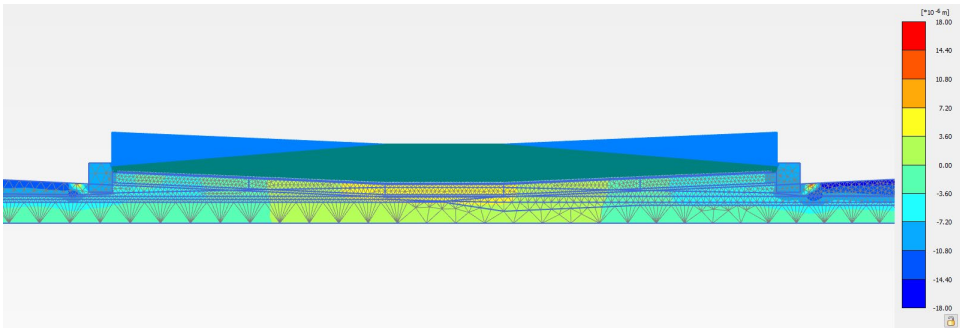

Figure 6.31: Settlement of immersed tunnel under mean water level

Apart from the settlement of immersed tunnel, the phase delay exists in the calculation of excess pore water pressure. The highest value of excess pore pressure (130$x10^{-3}$kPa) locates at the first and last of tunnel element. The minimum value of excess pore water pressure (-50$x10^{-3}$kPa) locates at the tunnel element 3. The distribution of excess pore water pressure is shown as figure 6.36 below.

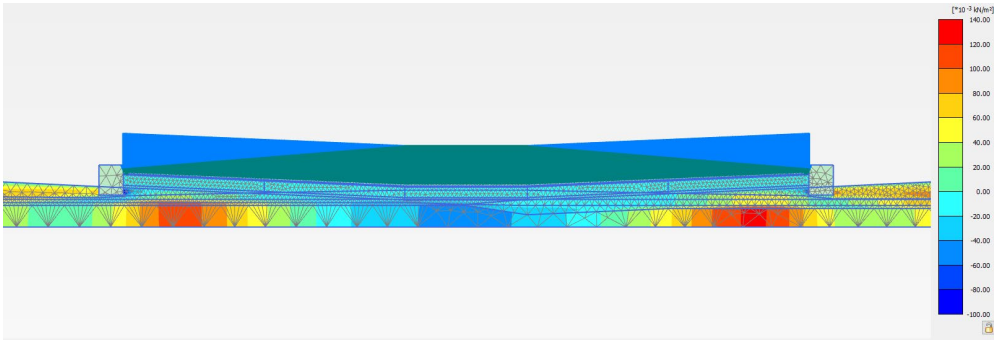

Figure 6.32: Excess pore water pressure of soil under mean water level

Phase 13.3: Impact of tidal fluctuation (Low water level)

Under the low tidal condition, the rebound of soil occurs along the longitudinal alignment of Heinenoord tunnel. The greatest value of extension is 0.135mm that locates at the first and last of the tunnel element. The swelling of soil under tunnel elements 2, 3 and 4 are in the range between 0.024mm to 0.034mm. The magnitude of soil rebound is almost equal to the settlement under high tidal condition. Hence, the settlement of tunnel element under tide is an elastic response in the numerical simulation. Figure 6.37 indicates the deformation of Heinenoord tunnel under the low tidal scenario.

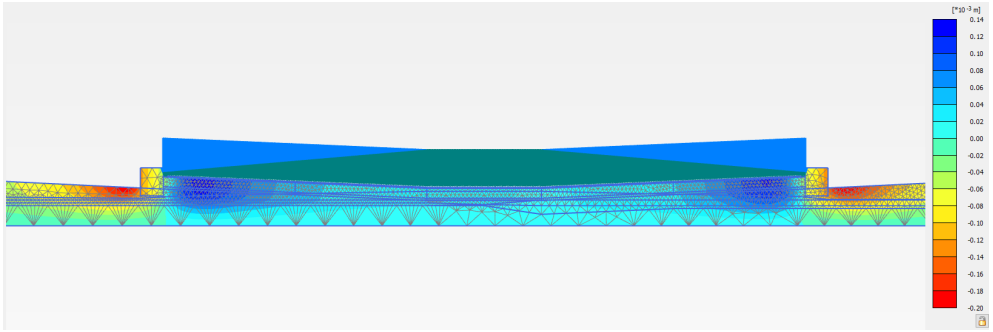

Figure 6.33: Settlement of immersed tunnel under the trough of the tide

The distribution of excess pore water pressure under the low tidal condition is shown as figure 6.38 below. The pore water pressure of soil underneath the immersed tunnel element does not synchronize with the drop of water table from tide. The positive excess pressure is found along the tunnel alignment with the maximum value of 0.2kPa.

Due to difference in hydraulic head, water flow out from the soil under the approaching ramp which causes a reduction on pore pressure. When the water pressure of soil is lower than the hydrostatic pressure, a compressive pore water pressure is found. Figure 8.38 shows that a minimum excess pore pressure occurs in the entrance and exit of the Heinenoord tunnel, with the magnitude of -0.7kPa.

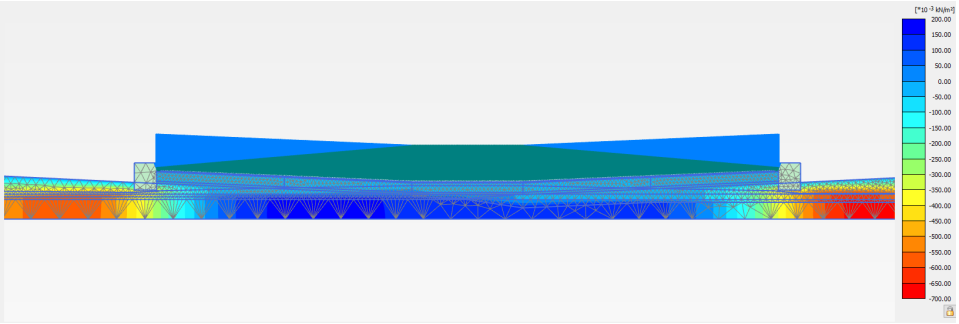

Figure 6.34: Excess pore water pressure distribution under the trough of the tide

6.4 Global response of Heinenoord tunnel under tide

6.4.1 Periodic settlement of tunnel element

The periodic settlement of tunnel element is indicated as figure 6.39 below. Both traverse and longitudinal model have shown the same qualitative response on tidal fluctuation. When the tide rises, compaction of soil occurs that causes the settlement of tunnel element. On the other hand, the drop of water level from tide induce an heaving on the tunnel element.

In terms of quantitative response, a wide variation of setttlement exist between between longitudinal and traverse model. It is because each element is analysised independently under the traverse analysis. The approaching structure does not exist and cause impact on any calculation stages of tunnel element. On a contary, the entire approaching ramp and Heinenoord tunnel is taken into account in the longitudinal mode. This causes a 0.05 mm settlement vairation in tunnel element 1 and 5 between two models.

The cyclic settlement of immersed tunnel 3, 4 and 5 are highly different between longitudinal and traverse analysis. This is caused by the simplification of geological profile in Finite Element Model. In the longitudinal analysis direction, a horizontally heterogenous clay is set along the alignment of Heinenoord tunel. The thickness of clay is significantly less than the transeverse model which shorten the drainage path under the change of water level. Water flux flow into the soil domain when the water level rises. The pore pressure under the soil is almost the same as the hydrostatic level. Hence, the change effective stress is less than a tenth of that in the traverse mode. The amipliude of settlement in Element 2, 3 and 4 under longitudinal mode is less 0.05 mm.

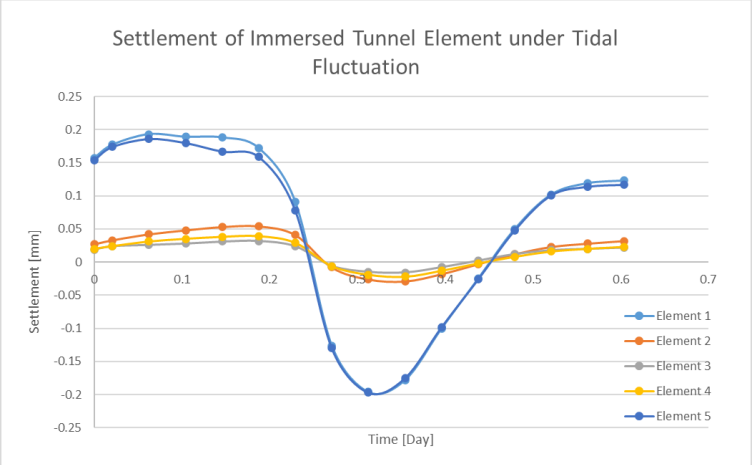

Figure 6.35: Settlement of tunnel element across time

6.4.2 Joint deformation between tunnel elements

The immersion joint deformation is equal to the differences of settlement between two tunnel elements. As mentioned in section 6.7, the simplification of geological profile causes a reduction of settlement along tunnel element 2, 3 and 4 under tide. The immersion joint deformation between intermediate elements is under 0.025 mm.

Tunnel element 1 and 5 is under deviatoric load from tide. The maximum settlement of element 1 and 5 are between 0.13 and 0.15 mm, but the settlement of elements nearby (E2, E3 and E4) is below 0.05mm. The deformation between E1-E2 and E4-E4 are much greater than rest of the immersion joint.

Comparing with the data from optical fiber sensor, the longitudinal analysis result has shown a greater discrepancy than the traverse data. One of the possible reasons is the simplification of geological profile along the longitudinal direction of Heinenoord tunnel. This causes low settlement value in the intermediate element (E2, E3 and E4) and excessive joint deformation between E1-E2 and E4-E5. The joint deformation result under tide is shown as figure 6.40 below.

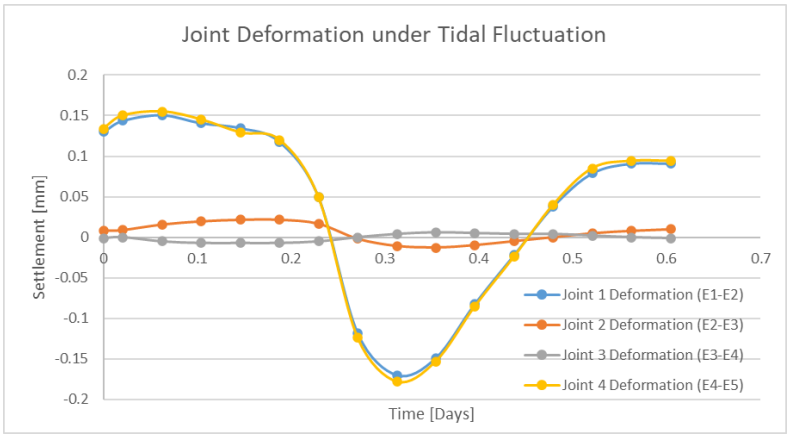

Figure 6.36: Joint deformation between tunnel element nuder tidal fluctuation

6.4.2 Joint deformation between approaching structure and element

A cyclic joint deformation between approaching structure and element is determined under longitudinal model. The approaching structure is supported by piles and the impact of tide reduces along the shores. It is hence indicated that approaching structure has a great resistance from tide. The joint deformation is solely caused by the settlement from element 1 and 5.

Figure 6.41 shows a cyclic joint deformation under tidal fluctuation. The amplitude of element – approaching structure deformation is 0.2 mm. Comparing with the traverse model, the longitudinal result is closer to the monitoring data from the optical fiber sensor.

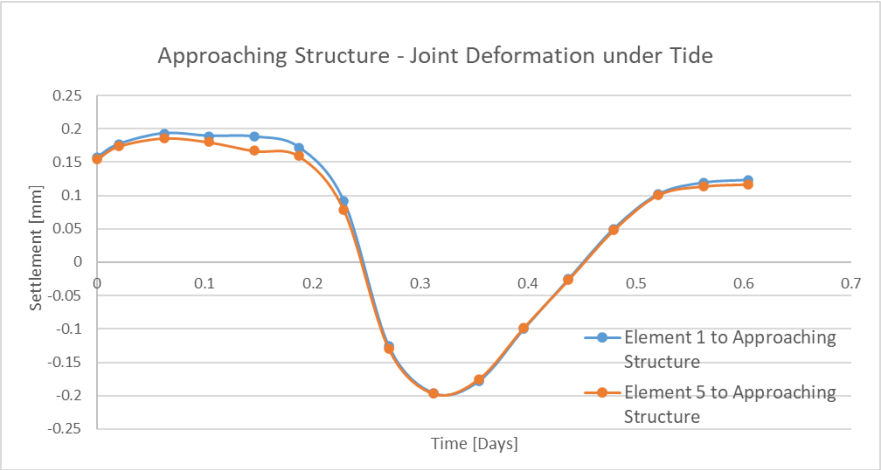

Figure 6.37: Joint deformation graph between approaching structure and element under tide

Chapter 7: Sensitivity analysis on the settlement of Heinenoordtunnel

This chapter focus on the impact of soil variability in the settlement calculation of Heinenoord tunnel. It starts with the identification of stiffness parameter under an increasing depth. The type of parameter distribution and coefficient of variance is also a concern. It is important to figure out which geological unit is the most sensitive to the tunnel settlement. By changing those soil parameters, the calculated result becomes closer to the monitoring data. It can distinguish whether importance of soil variability in the calculation result.

Soil variability is not always a single factor to the differences between observational and numerical result. Further explanation is required when the sensitivity analysis cannot sufficiently match with the surveying data of Heinenoord tunnel.

7.1 Variability of soil and tip resistance from CPT

In the Plaxis 2-D simulation, it is assumed that all geological unit is homogenous in both vertical and horizontal direction. The strength and stiffness parameters are isotropic stress dependent under hardening soil model.

Cone penetration tests are conducted along the alignment of Heinenoord tunnel. The value of odometer stiffness Eoed can be calculated from the tip resistance by the empirical formula below.

$$\text{Eoed} = 3\sim5\text{qc} \tag{7.1}$$

Where qc is the tip resistance of penetrometer, Eoed is the odometer stiffness

The remaining unloading/reloading stiffness and E50 can be further calculated from the odometer modulus. Hence, the settlement of Heinenoord tunnel is controlled by the tip resistance in the Cone Penetration Test.

The value of qc does not increase in a perfectly linear shape with depth. Variation of stiffness and error exist in the field observation. Figure 9.1 has shown a typical tip resistance across depth. The local maximum value is twice as the minimum value. In order to extract useful information from raw CPT data, the characteristic value of qc is taken as the mean the tip resistance. This is expressed as the formula below.

$$\text{qc} = az + b \tag{7.2}$$

Where z is the depth, qc is the tip resistance of penetrometer, a and b is the constant.

The average value of qc is determined by drawing the approaching line along the CPT data. The determination of average qc value is shown as figure 7.1 below.

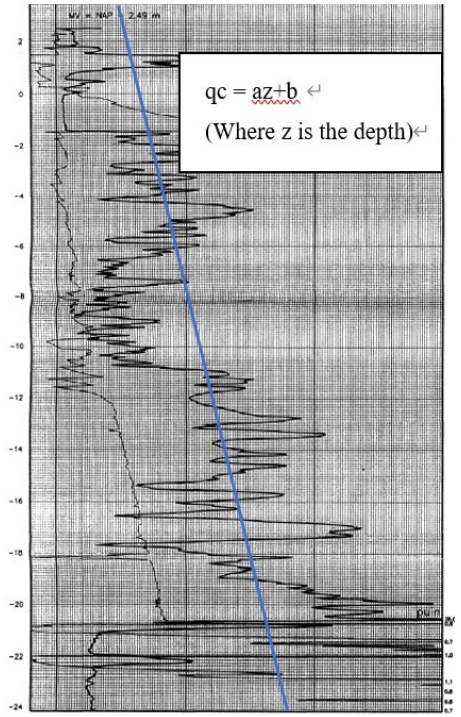

Figure 7.1: Measured and mean value of tip resistance in Cone Penetration Test (CPT)

Phoon and Kullhawy(1999) identify the value of stiffness parameter in the combination of trend parameter t(z), variance value of soil w(z) and also uncertainty from measurement error e(z) as the equation and figure 7.2 below:

$$\gamma(z) = t(z) + w(z) + e(z) \qquad (7.3)$$

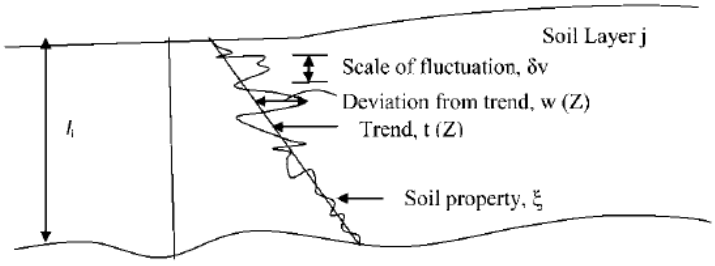

Figure 7.2: Vaiation of stiffness parameter with depth by Phoon and Kullhawy(1999)

To identify the variability of soil parameter, the determination of probability density function is required in the next stage of the report.

7.2 Statistical parameter determination

7.2.1 Distribution of stiffness parameter

The variability of soil parameter can be represented by the normal distribution. The uncertainty of stiffness parameter can be characterized with several statistical parameters. They are mean value, standard deviation and coefficient of variance. Mean refers to the trend of soil stiffness under depth. Standard deviation measures the difference between the variable and mean value. The coefficient of variance is the ratio of standard deviation and mean. In the normal distribution, 68.2 percent of sample lies between $\mu - \sigma$ and $\mu + \sigma$. The probability density function is shown as figure 7.3 below.

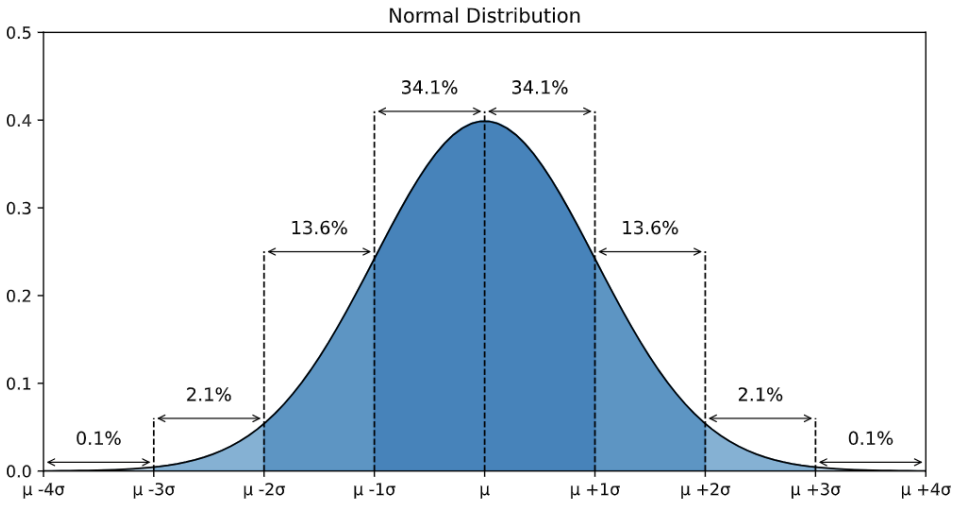

Figure 7.3: The probability density function under normal distribution

7.2.2 Determination of coefficient of variance

As mentioned in section 7.1, the mean value of tip resistance is determined graphically from the cone penetration test. It is then converted to the odometer stiffness by an empirical formula.

Comparing with the friction angle and cohesion, the stiffness parameter distributes widely and shares a high value of standard deviation. Research is done to approximate the coefficient of variance in Young's modulus of soil. Srivastava and Babu (2009) estimated that the coefficient of variance (COV) is 0.34 in clay. While Phoon and Kulhawy (2009) has made an approximation of the COV in sand between 0.2 to 0.7. To make a conservative approach, the COV of sand is taken as 0.35 in this research. By changing the parameter between $\mu - 2\sigma$ and $\mu + 2\sigma$, it can determine whether sensitivity of stiffness is a dominant factor on the variation of monitoring data and Finite Element Model (FEM) result.

7.3 Identification of sensitive geological unit

7.3.1 Identification of sensitive geological unit under operation

According to chapter 4, the surveying data of tunnel settlement is 3 to 5 times as the Finite Element Model result. The impact of soil variability is still an unknown on the calculated settlement. To figure

out the sensitivity in Plaxis 2D, the stiffness parameter of soil can be lowered by 2σ that is 2.2 percentile in the normal distribution curve.

It is not practical to lower the stiffness of the entire domain because the probability of occurrence is extremely low. However, the sensitivity analysis can be done by lowering the stiffness parameter of two to three soil layers that contribute most to the total settlement.

To identify the most sensitive geological unit, it is vital to understand the mechanism of settlement calculation in Plaxis. During 50 Years of tunnel operation, an increasing traffic load is applied to the soil domain. The soil that is closer to the tunnel element are under greater stress level. The load spread across the soil domain and the impact become insignificant. Figure 7.4 indicates the load spread mechanism under different zone in the soil domain.

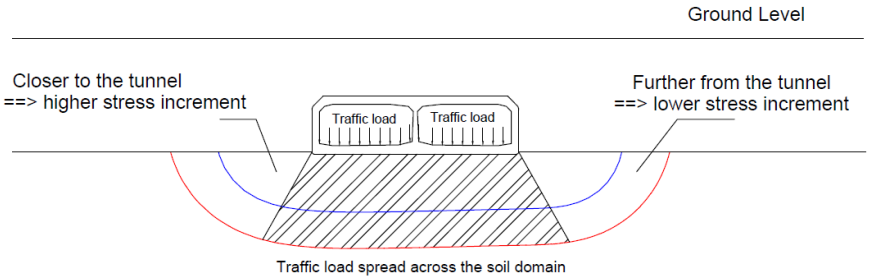

Figure 7.4: The load spread across the soil domain under different zone

Apart from load spread, several factors can be influential to the soil settlement. Lower soil stiffness causes higher sensitivity of domain under load. Also, the thickness of soil layer is directly proportional to its settlement. To identify the most sensitive geological unit, the histograms of soil settlement are plotted in the section 7.6.

7.3.2 Identification of sensitive geological unit under tide

Before conducting the sensitivity analysis, it is important to identify the most responsive geological unit under the variation of tide. In Chapter 6, the soil domain can be classified into 3 zones that behave differently under tide. They are the highly permeable zones on top, the transition zone and the undrained zone underneath. The distribution of excess pore water pressure is different. Hence, a further discussion is required to identify the response of soil domain under tidal fluctuation.

Sand backfill is highly permeable and acts as a protective layer on the tunnel element. Water flow into and out of the sand backfill quickly under the variation of water level. The change of total stress from tide is equal the change of pore water pressure in the sand backfill. The effective stress is hence constant in the sand backfill. This does not cause any settlement of Heinenoord tunnel under tidal fluctuation.

The hydraulic conductivity of cohesive soil is much lower than the sand backfills. Water flux cannot penetrate through the low permeability layer effectively under tide. The cohesive soil layer is therefore under a partial drained condition. The top part of cohesive soil is sensitive to the change of water table under tide, but the impact is insignificant to the lower part of it. The increase of effective stress occurs at the bottom of transition zone and causes cyclic settlement of tunnel element under tidal fluctuation.

The highly permeable soil underneath the transition zone contributes most to cyclic settlement.

It is because the flow of water is completely blocked by the cohesive soil layer. The pore water pressure of soil is independent of time and equal to the hydrostatic pressure under the mean water condition. The change of total pressure from tide is equal to the variation of effective stress. The change of effective stress causes the cyclic settlement of Heinenoord tunnel. Figure 7.5 has indicated the behavior of seabed under the tidal variation.

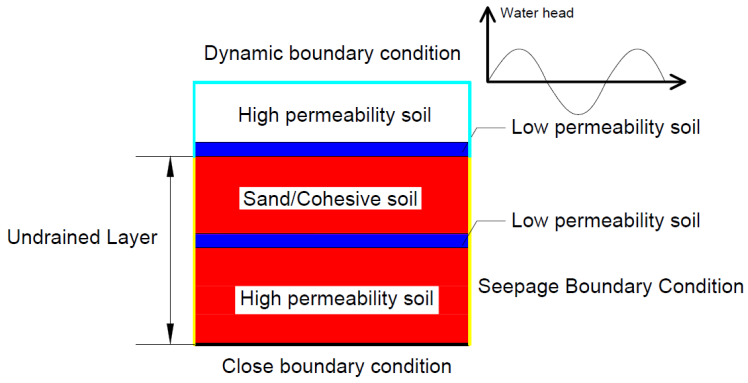

Figure 7.5: The hydraulic behavior of soil under the tidal variation

Since the composition of geological unit varies along the tunnel alignment, the location and thickness of undrained zone is not the same which causes immersion joint deformation under tide. To illustrate the differences on hydraulic behavior, figure 7.6 has shown the excess pore water pressure of tunnel element 4 and 5 under high water level of tide.

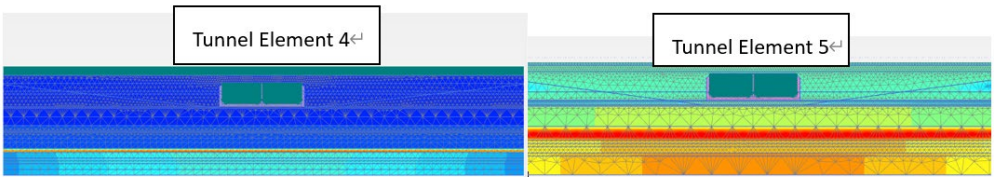

Figure 7.6: Excess pore water pressure distribution under high tidal condition

To better illustrate the zone of compaction, figure 7.7 has indicated the distribution of settlement and excess pore water pressure under high water level. The settlement and delay of pore pressure occurs under the cohesive soil, while the sand on top does not contribute to the settlement of immersed tunnel. Also, the rise of total pressure from tide is equal to the increase of effective stress on the undrained sand layer. Hence, the undrained sand layer contributes to the total settlement the most.

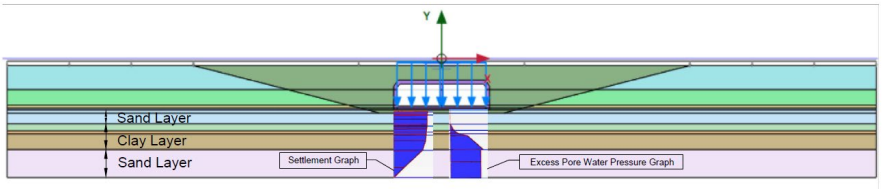

Figure 7.7: The excess pore water pressure and settlement under high tide events

7.4 Quantitative verification of the most sensitive geological unit with Plaxis

Although the sensitive zone can be identified conceptually from section 7.4 and 7.5, further verification is required under a quantitative method from Plaxis. The applied load causes compaction or extension on the soil domains. The settlement of immersed tunnel is the summation of deformation from every single geological unit. Due to the differences in stiffness modulus, soils have various response under the change of loading condition. Highly sensitive soil is more influential on the total settlement. The sensitivity of the soil material itself is governed by the deformation per unit length, ie $\frac{\Delta h}{H}$. However, the most sensitive soil may not have a significant contribution on the total settlement if the thickness is not sufficient. A better comparison is achieved by plotting the histogram of compaction every geological unit under loading condition.

Figure 8.6 has shown the value of compaction from different geological unit during the first 10 years of service period. The soil layers are selected underneath the tunnel element 5 and the name is labeled in sequential order. The greater layer number indicates that is further aways from the element. The result has shown that layer 5 and 6 has a greater influence on the total tunnel element. The sensitivity analysis can be conducted by changing the stiffness parameter of the most influential geological unit in the Finite Element Model.

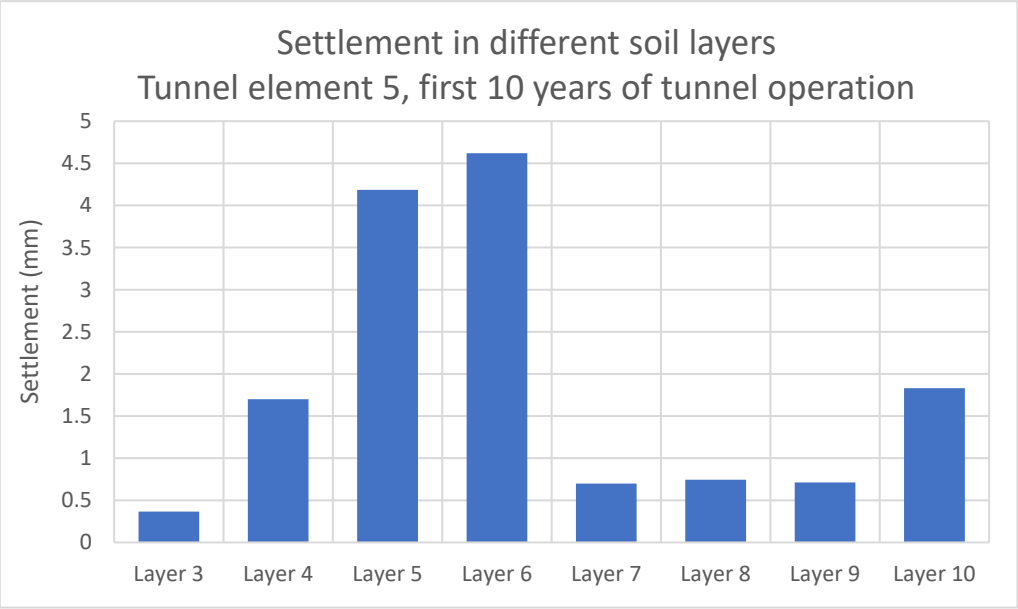

Figure 7.8: The histogram of soil settlement throughout the operational period

The calculation mechanism is totally different between tidal impact assessment and settlement history calculation. It is necessary to figure out which geological contributes most under the impact of tide. Same approach is applied on the determination of the sensitivity of geological unit and the result is shown as figure 7.7.

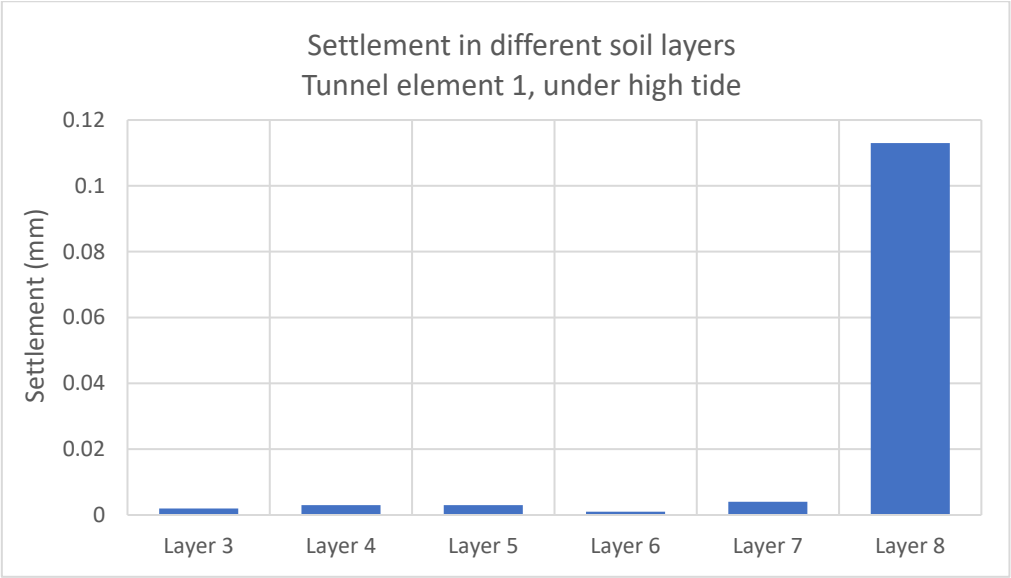

Figure 7.9: Histogram of soil settlement from tunnel element 1 under tidal fluctuation

Figure 7.7 has shown that layer 8 has a greater contribution on the total settlement of tunnel element 1. It has matched with the prediction from the section 9.5. Further sensitivity analysis can be done by changing the stiffness parameter of layer 8 under the tidal fluctuation.

7.5 Result of the sensitivity analysis in the settlement history

The stiffness parameters of sand and clay are lowered by 2σ that is about 70 percent of mean stiffness. The sensitivity analysis is conducted under an extreme traffic condition (Traffic Jam Condition), secondary compaction and sedimentation. As mentioned from Section 8.4, several factors are related to the sensitivity of soil over the operational period. It is important to plot histogram which indicate the settlement of every geological unit. Then, two most sensitive soil layers in the domain are selected in the analysis stage. Stiffness parameters Eoed, Eur and E50 are lowered by two standard deviations that is 70 percent of the average value. On the other hand, the coefficient of secondary compaction maintains the same in the sensitivity analysis. The change of settlement on different element is shown as the table 7.8 below.

Table 7.1: The change of settlement under sensitivity analysis

	Element 1	Element 2	Element 3	Element 4	Element 5
Settlement between 1979 – 2019 before parameter adjustment	-30.14	-18.27	-30.62	-28.00	-22.30
Settlement between 1979 – 2019 after parameter adjustment	-49.32	-23.80	-48.66	-46.85	-36.23
Percentage increase after adjustment	63%	30%	59%	67%	62%

Although the stiffness parameter has change by about a third, the actual proportion change is in between 30% to 67%. The sensitivity of soil domain causes a significant change of settlement in the Plaxis model. To verified impact of sensitivity, it is vital to compare the differences between monitoring and Finite Element data under the adjustment of parameter.

With the change of stiffness parameter, the differences of leveling and Finite Element result converge. Table 7.9 indicates the variation of settlement due to the adjustment of stiffness parameter.

Table 7.2: The difference between monitoring data and result of FEM in sensitivity analysis

	Element 1	Element 2	Element 3	Element 4	Element 5
Monitoring data [mm]	-63.72	-36.3	-40	-40	-65.6
Difference between monitoring data and FEM result before adjustment [mm]	-33.58	-18.03	-9.38	-12.00	-43.30
Difference between monitoring data and FEM result after adjustment [mm]	-14.4	-12.5	+8.66	-6.85	-29.37
Percentage reduction after adjustment	57%	30%	(192%)	43%	32%

The difference between observational method and Finite Element result converges by 30 to 57 percent. It implies that the variability of stiffness parameter can cause significant impact on the precision in numerical modeling. Settlement of element 3 becomes 8.66 mm greater than the monitoring data. However, it is still insufficient to claim that it is a one and only factor on the variation.

Several possible reasons contribute to this phenomenon. As mentioned in Chapter 5, hardening soil (HS) model is chosen to calculate the stress-strain relationship in the Plaxis model. HS model adopts the Mohr Coulomb failure criteria in the ultimate limit state, but the stiffness parameters are different under various loading conditions. In the operational stage, the settlement of tunnel element can be due to the elastic or elasto-plastic response of soil. If the stress path is under the yield contour, elastic deformation of soil occurs. If the yield contour expands upon loading, the elasto- plastic settlement occurs. The stiffness parameters of Eur, Eoed and E50 governs the value of settlement under traffic load. However, only a few CPT are found in the construction site. The estimation of stiffness parameters from cone resistance value is considered as “Rule of Thumb”, rather than a precise calculation. To determine a more precise value of stiffness parameter, soil sampling and tri axial test are required. Comparing the field and laboratory test result can provide a more precise judgement on the stiffness parameter.

7.6 Result of the sensitivity analysis under cyclic settlement response

To indicate the significance of soil variability, the stiffness modulus of sensitive geological unit is set as the 84th percentile of the normal distribution, i.e $\mu + \sigma$. From the section 8.3, the coefficient of variance is 0.35. All three stiffness parameters of soil increase to $\mu + \sigma$ in the Plaxis model. The change of cyclic settlement under the crest of the tide is shown as table 7.10 below.

Table 7.3: The change of settlement amplitude under sensitivity analysis ($\mu + \sigma$)

Change of cyclic settlement amplitude under sensitivity analysis					
	Element 1	Element 2	Element 3	Element 4	Element 5
Before parameter adjustment [mm]	-0.143	-0.146	-0.203	-0.156	-0.215
After parameter adjustment [mm]	-0.126	-0.125	-0.18	-0.129	-0.206
Proportion change	12%	14%	11%	17%	4%

With the increase of stiffness parameter, the peak value of cyclic settlement changes by 4 to 17 percent. A significant reduction of settlement is found under element 2 and 4. This is due to the thick undrained soil layer under the low permeability transition zone. High value of compaction occurs at the peak of tide. The optical fiber does not measure the value of cyclic settlement in tunnel element,

but the deformation of immersion joint. Hence, the settlement obtained from Finite Element Software is converted to joint deformation and compared with the monitoring result. Table 7.11 has shown the change of joint deformation due to the impact of sensitivity analysis.

Table 7.4: The amplitude of immersion joint deformation under sensitivity analysis

Amplitude of immersion joint deformation under sensitivity analysis				
	Element 1-2	Element 2-3	Element 3-4	Element 4-5
Before parameter adjustment [mm]	-0.003	-0.057	-0.047	-0.059
After parameter adjustment [mm]	-0.001	-0.055	-0.051	-0.077
Proportion change	-66%	-4%	9%	31%

After the adjustment of stiffness parameter, deformation of immersion joint is also under 0.1mm. The change of settlement is in between -66 percent to +31 percent. The negative value indicates a reduction of joint settlement, while the positive sign shows a greater joint deformation. Joint deformation is calculated as the settlement difference between two adjacent tunnel elements. Although the value of settlement reduces after parameter adjustment, the magnitude of settlement reduction can be different. It is possible to cause a greater joint deformation. The joint deformation (with the magnitude of 0.1mm) does not cause leakage or serviceability issue on the immersed tunnel. Hence, the impact of tide under soil variability is not a significant factor on tunnel stability.

In the section 6.9, it mentioned that approaching structure has a stronger resistance to tidal fluctuation because of pile support. The settlement of approaching structure is significantly less than element 1 and 5. The optical fiber sensors in Joint 1 and 6 measure the cyclic settlement of first and last tunnel element under tide. Table 7.12 indicates the immersion joint deformation between approaching structure and the element 1 and 5.

Table 7.5: The immersion joint deformation at end of Heinenoord tunnel

Cyclic joint deformation under sensitivity analysis		
	Element 1 to approaching structure	Element 5 to approaching structure
Before parameter adjustment [mm]	-0.143	-0.215
After parameter adjustment [mm]	-0.126	-0.206
Monitoring Data [mm]	-0.15	-0.14
Proportion change between monitoring data and Finite Element Result	11%	-6%

Based on the above data, the change of 35 percent in stiffness parameter causes 6 to11 percent differences in tunnel settlement. Comparing with tidal response in on tunnel element, the long- term differential settlement has a greater threat to the water tightness in Heinenoord tunnel.

Chapter 8: Conclusion and Recommendation

The goal of this research is providing a reasonable explanation on the long term- and daily settlement behavior of Heinenoordtunnel, an immersed tunnel in Netherlands.

The entire research can be sub divided into 3 parts: the simulation of long-term settlement of immersed tunnel, determination of daily response of tunnel under tide and sensitivity analysis of soil parameter on the Finite Element result. The conclusions are listed on those three sub sections.

(1) Long Term Settlement over the Operational Period

The tunnel settlement is simulated by 2D PLAXIS which considered the impact of construction load throughout the operation period. When a constant traffic load is applied on the Heinenoordtunnel, the excess pore water pressure is almost fully dissipated in first 10 years of tunnel operation. The settlement converges and is equal to 2 mm under the remaining period of operation. However, the leveling result shows a consistent increase of settlement over the 50 years of service period. The highest settlement is 65 mm which locates at tunnel element 5, while the lowest settlement is 35 mm in element 2. Finite Element result does not provide a sound explanation to leveling data under the constant loading condition. Therefore, 3 addition factors are suggested and investigated in the long-term settlement analysis.

To begin with, the increasing traffic load is considered in PLAXIS to investigate the long term response of Heinenoordtunnel. Two scenarios are considered: the first one is the traffic load in the peak hour and the second is under the normal traffic condition. The numerical result shows that the tunnel settlement increases linearly over the service period. The tunnel settlement under peak-hour traffic condition is closer to the monitoring data than the normal traffic condition. In tunnel element 3, for example, the calculated result increases by 20 mm under the peak traffic. However, the simulation result is still lower than the monitoring result. For example, the settlement simulated at tunnel element 3 is still 15 mm lower than field monitoring result. The increasing traffic volume alone is still insufficient to explain the long-term settlement response of Heinenoordtunnel.

Apart from the increase in traffic volume, the fluvial deposition also induces a rising load on the Heinenoordtunnel. Based on the previous research, the thickness of sedimentation is assumed as 9 mm per year and considered in model. PLAXIS 2D estimated that fluvial deposition contributes 15mm of total settlement over the service period, but the total settlement is still lower than the field measurement. In tunnel element 3, for example, the difference between monitoring data and finite element result is greater than 35 mm. Therefore, the fluvial deposition alone cannot explain the high long-term settlement on Heinenoordtunnel.

The impact of secondary compaction is also considered. It is estimated that the secondary compaction contributes 20 mm of the total settlement throughout the 50 years of tunnel operation. Although some simplifications on the geological profile are made, the empirical result can shows the trend of long term settlement under secondary compaction.

The increasing of traffic load, fluvial deposition and secondary compaction are not the isolated events. Instead, all three factors can be added up and simulated with PLAXIS 2D. The total settlement

of Heinenoordtunnel is in between 18.27 to 30.62 mm, that is greater than the constant loading condition. However, the difference between Finite Element result and monitoring data is still significant. A difference of 43.3 mm is found in tunnel element 4. Further explanation on the long term settlement is required.

One of the possible reasons is the poor workmanship throughout the foundation bed construction process. The Heinenoordtunnel was constructed in the 1960s. The construction technology was less advance than today. Siltation could be formed between sand foundation and significantly lowered its stiffness. Also, the sand foundation was under the loose state and sensitive to the applied load. Therefore, the construction of backfill and tunnel element can cause long term settlement on Heinenoordtunnel.

Another possible reason is the accumulation of plastic strain under the influence of tide. A repeated loading and unloading occurs along the impermeable soil under tidal water level fluctuation. Although only a small value of plastic settlement is generated from each cycle, the plastic settlement accumulates when time passes. Over the past 50 years of tunnel operation, more than 30 thousand of cycles are applied to the tunnel element. Further investigation on the accumulation of plastic settlement is required to understand the impact of tide in a greater depth.

(2) Settlement of Immersed Tunnel under Tidal Fluctuation

PLAXIS 2D simulates cyclic settlement of Heinenoordtunnel under tide in both longitudinal and traversed direction. PLAXIS 2D solves the coupled governing equation which determine the settlement and excess pore water pressure of soil. The result has shown that PLAXIS 2D is capable to simulate the periodic response of Heinenoordtunnel under coupled flow mode. In general, the calculated settlement is in phase with the monitoring data and opposite phase with the tidal fluctuation. The monitoring data is higher than numerical result in PLAXIS 2D. Therefore, the sensitivity analysis is conducted to determine the influence of soil variability on the daily settlement of Heinenoordtunnel element.

In the traverse section analysis, tunnel sections are calculated separately under the coupled flow and deformation mode. The immersion joints deformation is classified into two types: The first type is joint deformation between tunnel elements, while the second type is joint deformation between tunnel and approaching structures. Since the geological profile varies along the tunnel alignment, tunnel element settles with different magnitudes under tide. The calculated tunnel settlement is in between 0.143 to 0.215 mm. Considering the first type of joint deformation, the relative uneven joint settlement is calculated as different vertical displacement between consecutive tunnel elements. The calculated value of joint deformation is in between 0.005 to 0.059 mm and match with the measured data by Distributed Optical Fiber Sensors (DOFS). Therefore, the coupled flow model can simulate immersion joint deformation between tunnel elements well under the change of water boundary condition.

Considering the second type of joint deformation, the both the monitoring and calculation result have shown a larger deformation than the first type. It is because the approaching structure is supported by piles that has greater resistance on tide. The measured end joint deformation is equal to the settlement variation of the first and last tunnel element. The amplitude of calculated joint

deformation at joint 1 and 6 is equal to 0.215mm that is about 2 times greater than the inter-element joint deformation. It is because all the five tunnel elements are moving up and down in the same phase under tide. The DOFS is basically measured the relative displacement between tunnel elements rather than the settlement itself. Also, the calculated deformation of joint 1 has matched with monitoring data, but the difference is greater than 0.1mm in joint 6. Hence, further investigation on the soil variability is required in the final stage of the report.

In the longitudinal analysis, the entire tunnel alignment is considered in the Finite Element calculation. The ramps and approaching structures are influential to the settlement of the tunnel element. The dynamic water boundary condition is applied on tunnel element along the longitudinal direction, but water head of the onshore soil is under hydrostatic condition. The result shows that the deformation of immersion joint 1 and 6 is equal to 0.2 mm under tide. While the magnitude of deformation is below 0.03mm in joint 2, 3, 4 and 5. The simplification of geological profile can be an accountable factor on the low value of tunnel settlement in between element 2, 3 and 4. The end joint deformation matches with monitoring data from optical fiber sensor.

Apart from the settlement of immersed tunnel, the hydro-mechanical response on geological profile under tide is also the main concern. The period of tide is not sufficient for water to flow into the cohesive soil and develop any changes on pore water pressure. PLAXIS coupled flow results indicated that clay layer is under partial drained or even undrain condition. The pore water pressure of clay and soil underneath is independent of tidal level fluctuation under a sufficient depth. When the tide level rises, the increase of effective stress occurs in the low permeability clay layer and the soil below. On the other hand, the decrease of effective stress occurs in the cohesive soil layer when water level drops. Compaction and extension of soil occurs alternately under tidal fluctuation. This causes the periodic settlement response of Heinenoordtunnel.

(3) Sensitivity Analysis on the Long Term and Cyclic Settlement of Heinenoord Tunnel

To investigate the effects of soil variability, a sensitivity analysis is conducted in the Finite Element Analysis. To simulate the tunnel behavior realistically, the most sensitive zone from the soil domain is selected in the sensitivity analysis. The stiffness parameter was amended by the increment of the standard deviation. Then, the impact of soil variability on the settlement result is determined.

In the long-term settlement analysis, the two most sensitive soil layer (layer 5: an organic normally consolidated clay, layer 6: a 6.5 m thick moderate dense sand) are selected in the sensitivity analysis. The stiffness parameter increased by twice of the standard deviation 2σ, that is 2 percentiles in normal distribution. Settlement increases between 30% and 67% after parameter adjustment. However, the differences between monitoring data and Finite Element result are still significant. Tunnel element 5, for example, 29.37 mm of difference is found when the stiffness parameters are reduced by 2σ. Therefore, even considering the soil variability, the difference between simulation results and measured results are significantly large. Hence, it is logical to conclude that the variability of soil is not a solid reason on the high value of long-term settlement.

The variability of soil has a significant influence on the cyclic settlement response under tide. The most sensitive geological unit locates below the cohesive soil layer. The pore water pressure of this soil layer is independent with tide. This causes the variation of effective stress and periodic compaction and rebound across the day. The stiffness parameter is modified by one standard deviation that is 15.8 percentiles under the normal distribution curve. The change of stiffness parameter contributes up to the 17% change of the cyclic settlement. The difference between calculation and monitoring result becomes neglectable after the modification. Therefore, it can be concluded that the variability of soil is a valid reason on the difference between the DOFS data and Finite Element results.

(4) Recommendations

To perform a precise simulation on soil variability, 3D PLAXIS model can be built and the result is compared with 2-D Finite Element Model. Comparing with two-dimension model, PLAXIS 3D can more effectively capture the heterogeneity of soil. The differential settlement of tunnel element can be simulated under a 2 - dimensional plane rather than a strip with infinite length. Also, the immersion joint deformation is under three axis which shows more information in the serviceability analysis.

Capturing the 3D geological profile often requires more bored holes than usual. However, the bore hole information cannot simulate a continuous geological profile, because it requires interpolation of geological unit. One of the possible alternatives is the geophysical survey.

Previous analysis indicates that the compaction of loosen sand-bed foundation can be a possible reason to the long-term settlement. However, the magnitude of settlement has not been analyzed quantitatively. Further laboratory research can be done to determine the stiffness loose sand. Due to the poor-quality assurance in the 1960s, silty sediments is likely mixed with sand bed in Heinenoordtunnel construction. Thus, the consolidation coefficient of loose silty sand should be determined from falling head test and odometer test. The long term settlement of Heinenoordtunnel can be modified with the new parameters of sand bed.

In the tidal impact assessment, PLAXIS 2D calculate the settlement of immersed tunnel and the excess pore pressure throughout the entire period. A phase delay of excess pore water pressure is calculated, but no field measurement is found along Heinenoordtunnel. To verify the calculation result, the piezometer can be installed along the soil profile. The back analysis of settlement can be achieved by setting the distribution of pore water pressure and current water level in PLAXIS.

Apart from the geological response, the structural deformation of Heinenoordtunnel should also be considered under tidal fluctuation. The rise and fall of water table causes unloading/reloading on the Heinenoordtunnel. The stress increment causes bending on the concrete elements and deformation on joints. PLAXIS 2D is an all-round geotechnical Finite Element software, but it is not sophisticated enough to simulate the structural response of Heinenoordtunnel under temperature and load. Hence, structural analysis software, for example COMSOL, should be used to determine the deformation of tunnel element under the change of tidal fluctuation.

The result has shown that the increasing traffic volume and secondary compaction causes a significant impact on the total settlement. However, those two impacts are often neglected in the standard design procedures. An estimation on future traffic volume can make a more precise simulation on tunnel settlement over the operational period. Also, the secondary compaction is a

crucial factor when the normally consolidated clay is found under the tunnel alignment.

Also, the impact of tide on immersed tunnel is not neglectable in some geological conditions. In this research, the calculated tidal settlement does not cause serviceability issue on the Heinenoord tunnel. However, the effect of tide is significant under a thick cohesive soil layer. Liefkenshoek tunnel, for example, a thick bloom clay is found underneath the tunnel alignment. More than 2 cm of tunnel settlement is measured under the variation of tide. This causes serviceability issue on tunnel segments and joints. Therefore, geological investigation is an essential phase in the tunnel design process. Tidal impact should be considered when a thick layer of highly compressive clay is found under the tunnel alignment.

References

Biot, M.A. (1940) “General Theory of Three-Dimensional Consolidation” Journal of Applied Physics 12, 155 – 164

Bogaert, P. (2009). “Recent and future railway tunnels in Belgium.” Proc., ITA-AITES World Tunnel Congress 2009: Safe Tunnelling for the City and for the Environment, P. Kocsonya, ed., Hungarian Tunnelling Association, Budapest, Hungary, 689–690.

Bogaert, P., and Vereerstraeten, J. (2005). “Antwerp North-South railway link for a new urban development tunnelling and underground techniques.” Receuil du Congrès International de l’AFTES Les Tunnels Clé d’une Europe Durable, A.A. Balkema, Chambéry, France, 279–286.

Çelik (2017) “Comparison of Mohr-Coulomb and Hardening Soil Models Numerical Estimation of Ground Surface Settlement Caused by Tunneling” Iğdır Univ. J. Inst. Sci. & Tech. 7(4): 95-102,

Delahaye, C. and Alonso, E. E. (2002). “Soil heterogeneity and preferential paths for gas migration.” Engineering Geology, 64: 251-271.

Fu., B.Y, Chen, W.L., Xu, G.P., Song S.Y. and F. Y. Xia (2019). “Summary of the Development of New Technologies for Submarine Immersed Tunnel Foundation Reinforcement and Settlement Control” IOP Conference Series: Materials Science and Engineering

Gang, W., Lu S.J., Wang Z., and Huang X (2017) “A Theoretical Model for the Circumferential Strain of Immersed Tunnel Elements Under Tidal Load” Geotech Geol Eng

Gatmiri, B. (1990). “A simplified Finite-element analysis of wave-induced elective stresses and pore pressures in permeable seabed” Geotechnique 15-30.

Glerum, A. “Developments in immersed tunnelling in Holland.” Tunnelling and Underground Space Technology, 1995, 10(4): 455–462

Gokce, A., Koyama, F., Tsuchiya, M. and Gencoglu, T. (2009)“Challenges involved in concrete works of Marmaray immersed tunnel with service life beyond 100 years,” Tunnelling and Underground Space Technology, vol. 24, no. 5, pp. 592–601

Grantz, W. C. (2001). “Immersed tunnel settlements. Part 1: Nature of settlements.” Tunnelling and Underground Space Technology, 16(3): 195–201

Grantz, W. C. (2001). “Immersed tunnel settlements: Part 2: Case histories.” Tunnelling and Underground Space Technology, 16(3): 203–210

Gursoy, A.,1995. Immersed steel tube tunnels: An American experience. Tunnelling and Underground Space Technology, 10 (4): 439-453.

He, H.T., Lin, Y.G., Li, J.Y. and Zhang, N. (2018). “Foundation of an immersed tunnel on marine clay improved by cement deep mixing and sand compaction piles” Marine Geo-resources & Geotechnology VOL. 36, NO. 2, 218–226

Hu, Z,. Xie, Y. and Wang J. “Challenges and strategies involved in designing and constructing a 6 km immersed tunnel: A case study of the Hong Kong-Zhuhai-Macao Bridge.” Tunnelling and Under-ground Space Technology, 2015, 50: 171–177

Hu, Z.N., Xie, Y.L., Xu, G.P., Bin, S.L., Liu, H.Z. and J.X. Lai. (2018). “Advantages and potential challenges of applying semi-rigid elements in an immersed tunnel: A case study of the Hong Kong-Zhuhai-Macao Bridge” Tunnelling and Underground Space Technology (79), 143-149

Janssen, W., de Haas, P. and Yoon, Y. H. (2006) “Busan-Geoje Link: Immersed tunnel opening new horizons.” Tunnelling and Underground Space Technology, 21(3): 332–340

Jardine, R., Overy, R. F., and Cho, F. C. (1998). “Axial capacity of offshore piles in Dense North Sea Sands” Journal Of Geotechnical and Geo-environmental Engineering 171-178

Kasper, T., Steenfelt, J. S., Pedersen, L. M., Jackson, P. G. and R. W. M. G. Heijmans, “Stability of an immersed tunnel in offshore conditions under deep water wave impact,” Coastal Engineering, vol. 55, no. 9, pp. 753–760

López-Higuera, José Miguel, Luis Rodriguez Cobo, Antonio Quintela Incera, and Adolfo Cobo, 2011. Fiber optic sensors in structural health monitoring. *Journal of lightwave technology,* 29, no. 4, 587-608.

Lai, J.X., Wang, K.Y., Qiu, J.L., Niu, F., Wang, J. and Chen, J. (2016). “Vibration response characteristics of the cross tunnel structure,” Shock and Vibration, 16 pages.

Lai, Y. P., Bergado, D. T., Lorenzo, G. A., and Duangchan, T. (2006). “Full scale reinforced embankment on deep jet mixing improved ground.” Proc. Inst. Civ. Eng. Ground Improv., 10(4), 153–164.

Lee, J. S. (2012). “The Gravel bedding for a foundation of the Busan-Geoje Immersed Tunnel” Innovative Infrastructures - Toward Human Urbanism 18TH CONGRESS OF IABSE, SEOUL

Liu, X., Jiang, W., De Schutter, G., Yuan, Y and Su, Q.K. (2014). “Early-age behaviour of precast concrete immersed tunnel based on degree of hydration concept” Verlag für Architektur und technische Wissenschaften GmbH & Co. KG, Berlin · Structural Concrete 15, No. 1

Liyanapathirana, D.S. (2012). “Implementation of an elasto-plastic constitutive model for cement stabilized clay in a non-linear finite element analysis” Engineering Computations Vol. 30, Issue 1, 74 – 96

Łotysz, S. (2010) “Immersed Tunnel Technology: A Brief History Of Its Development” Civil And Environmental Engineering Reports

Lunniss, R. and J. Baber (2013). Immersed tunnels, CRC Press.

Madsen, O. S. (1978). “Wave-induced pore pressures and elective stresses in a porous bed”. Geotechnique (28) 377-393.

Marshall., C (1999) “The Oresund Tunnel - Making a Success of Design and Build” Tunnelling and Underground space Technology, Vol 14, No3, 355-365

Motil, A., Bergman, A. and Tur, M., 2016. State of the Art of Brillouin Fiber-Optic Distributed Sensing. Optics & Laser Technology, 78, 81-103.

Nie, X.X., Wei, X.B., Li, X.C. and Lu, C. (2018). “Heat treatment and ventilation optimization in a deep mine,” Advances in Civil Engineering,, 12 pages

Nishanthan, R., Liyanapathirana, D. S. and C. J. Leo “Deep Cement Mixed Walls with Steel Inclusions for Excavation Support”

Okusa, S. (1985). “Wave-induced stresses in unsaturated submarine sediments”. Geotechnique (35) 517-532.

Olsen., T, Kasper, T, de. Wit., J. (2022). “Immersed tunnels in soft soil conditions experience from the last 20 years” Tunnelling and Underground Space Technology incorporating Trenchless Technology Research 121

Pedersen, S. K. and Brøndum, S. (2018) “Fehmarnbelt fixed link: The world’s longest road and rail immersed tunnel.” Civil Engineering, 171(5): 17–23

Qiu, J.L., Liu, H.Q. and Lai, J.X. (2018). “Investigating the long-term settlement of a tunnel built over improved foundation soil using jet grouting technique,” Journal of Performance of Constructed Facilities, vol. 32, no. 5

Rasmussen, N. S. and Grantz, W. C. (1997). “Catalog of Immersed Tunnels International Tunnelling Association Immersed and Floating Tunnels” Working Group: State of the Art Report.

Rijkswaterstaat. 2008. Report-Lekkage-in-tunnels-dilatatievoegen-beton. Seehttps://www.cob.nl/document/lekkage-in-tunnels-dilatatievoegen-beton/(lateast accessed April 2022)

Rijkswaterstaat GPO. 2016. Report-Deformatiemeting-37H-312-01.

Schotte, K., Nuttens, T., De Wulf, A., Van Bogaert, P., and De Backer, H. (2016) “Monitoring the Structural Response of the Liefkenshoek Rail Tunnel to Tidal Level Fluctuations” Journal of Performance of Constructed Facilities 30(5)

Shi, P.X., Zhang, D.L., Pan, J.L. and Liu, W. (2016). “Geological investigation and tunnel excavation aspects of the weakness zones of Xiang’an subsea tunnels in China,” Rock Mechanics and Rock Engineering, vol. 49, no. 12, pp. 4853–4867

Smink, M. (2003). "A new approach to the foundation of concrete tunnel elements.” In: Proceedings of the ITA World Tunneling Congress 2003. Amsterdam: A. A. Belkema Publishers, 287–289

Teo, P.L. & Wong, K.S. (2012) “Application of the Hardening Soil model in deep excavation analysis” The IES Journal Part A: Civil & Structural Engineering Vol. 5, No. 3, 152–165

Tsai, C.P., and Lee, T.L. (1995). “Standing wave induced pore pressures in a porous seabed. Ocean Engineering”, 505-517.

Tsai, C. P., Lee, T. L., and Hsu, J. R. C. (2000). “Effect of wave non-linearity on the standing-wave-induced seabed response”

Van Tongeren, I. H. (1978) “The foundation of immersed tunnels. In: Proceedings of Delta Tunneling Symposium.” Amsterdam, 1978,

Wang, S. C., Zhang, X. H. and Yun, B. (2020). “Comparative study on foundation treatment methods of immersed tunnels in China” Frontiers of Structural and Civil Engineering Vol 14, No 1, 82-93

Wang, Z., Xie, Y. and Liu, H. (2018). “Analysis on deformation and structural safety of a novel concrete-filled steel tube support system in loess tunnel,” European Journal of Environmental and Civil Engineering.

Wang, Z.F., Wang, Y.Q. and Cheng, W.C. (2018). “Investigation into geohazards during urbanization process of Xi’an, China,”Natural Hazards, Vol. 92, No. 3.

Xie, X., Wang, P., Li, Y., Niu, J. and Qin, H. (2014). “Monitoring data and finite element analysis of long term settlement of Yongjiang immersed tunnel.” Rock and Soil Mechanics, 35(8): 2314–2324 (in Chinese)

Yan, Q.X., Chen, H., Chen, W.Y., Zhang, J., Ma, S. and Huang, X. (2018).“Dynamic characteristic and fatigue accumulative damage of a cross shield tunnel structure under vibration load,” Shock and Vibration, vol. 2018, 14 pages, 2018.

Yang, G.C., Wang, X.H. and Wang, X.G. et al., “Analyses of seepage problems in a subsea tunnel considering effects of grouting and lining structure,” Marine Georesources and Geotechnology, vol. 34, no. 1, pp. 65–70,

Yapage, N. N. S., Liyanapathirana, D. S., Kelly, R. B., Poulos, H. G., and Leo, C. J. (2014). “Numerical Modeling of an Embankment over Soft Ground Improved with Deep Cement Mixed Columns: Case History” Journal of Geotechnical and Geo-environmental Engineering 140

Yue, X.B., Xie, Y. and Xie, Y.L. “The Deformation Characteristics of Weak Foundation with High Back Siltation in the Immersed Tunnel” Advances in Materials Science and Engineering Vol 2018

Zhang, Q., Draper, S., Cheng, L. and H. An, (2016). “Effect of limited sediment supply on sedimentation and the onset of tunnel scour below subsea pipelines, Coastal Engineering, vol. 116, pp. 103–117

Zhang, X. and Broere, W., 2022. Design of a Distributed Optic Fiber Sensor System for Measuring Immersed Tunnel Joint Deformations, Tunnelling and Underground Space Technology. (Revised submitted)

Zhou, H.Z., Wang, L.C., Jiang, B.S., and Wang, Y.N. (2021). “Improved vertical displacement calculation model for immersed tube tunnel considering tidal load” Marine Geo-resources & Geotechnology September